

**Deutsches Zentrum
für Luft- und Raumfahrt**

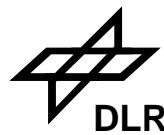
Forschungsbericht 98-08

**Microscopic Modeling of Traffic Flow:
Investigation of Collision Free Vehicle Dynamics**

Stefan Krauß

Hauptabteilung Mobilität und Systemtechnik
Köln

115 Seiten
50 Abbildungen
83 Referenzen



Manuskript eingereicht am 6. April 1998

Microscopic Modeling of Traffic Flow: Investigation of Collision Free Vehicle Dynamics

Inaugural-Dissertation
zur
Erlangung des Doktorgrades der
Mathematisch-Naturwissenschaftlichen Fakultät
der Universität zu Köln

vorgelegt von
Stefan Krauß
aus Recklinghausen

Köln, April 1998

Deutsches Zentrum für Luft- und Raumfahrt
Hauptabteilung Mobilität und Systemtechnik
Hauptabteilungsleiter: Dr.-Ing. H.-G. Nüßer

Berichterstatter: Prof. Dr. D. Stauffer
 Prof. Dr. R. Schrader

Tag der mündlichen Prüfung: 12. Februar 1998

Traffic Simulation, Car-Following Model, Jamming Transition, Phase Transitions

Microscopic Modeling of Traffic Flow: Investigation of Collision Free Vehicle Dynamics

The continuous growth of road traffic volumes leads to significant environmental and economical problems. For this reason there have been efforts for more than four decades to understand the dynamics of traffic flow in order to find ways to optimize traffic with respect to a reduction of environmental impacts and economical losses due to congestion.

In this work a microscopic model of traffic flow is proposed that adds to the understanding of the different types of congestion that are found in traffic flow. The main assumption the model is based on is the fact that in general vehicles move without colliding. From this property of vehicle motion a model can be derived that shows a rich dynamics and proves to be in good agreement with empirical data.

The model is mainly characterized by the parameters describing typical acceleration and deceleration capabilities of the vehicles. It closely resembles other well-known models for certain choices of these parameters. By varying acceleration and deceleration capabilities a thorough understanding of the dynamics of the model and the previously known special cases is gained.

Verkehrssimulation, Fahrzeugfolgemodelle, Staubbildung, Phasenübergänge

Mikroskopische Modellierung des Verkehrsflusses: Untersuchung einer kollisionsfreien Fahrdynamik

Das anhaltende Wachstum des Straßenverkehrsvolumens führt in wirtschaftlicher und umweltpolitischer Hinsicht zu spürbaren Problemen. Aus diesem Grund gibt es seit mehr als vier Jahrzehnten Bemühungen, ein Verständnis für die Dynamik des Verkehrsflusses zu gewinnen, um hierauf aufbauend Wege zu einer Optimierung des Verkehrs im Hinblick auf die Reduktion von Umweltbelastungen und wirtschaftlichen Verlusten aufgrund von Überlastungsscheinungen zu finden.

In dieser Arbeit wird ein mikroskopisches Modell des Verkehrsflusses entwickelt, das zu einem tieferen Verständnis der verschiedenen Überlastungszustände im Straßenverkehr beiträgt. Die grundlegende Annahme, auf der das Modell beruht, besteht in der Tatsache, daß Fahrzeuge sich in der Regel kollisionsfrei bewegen. Aus dieser Eigenschaft der Fahrzeugbewegung kann ein Modell abgeleitet werden, das eine reichhaltige Dynamik aufweist und sich in guter Übereinstimmung mit empirischen Daten befindet.

Das Modell wird hauptsächlich durch die Parameter charakterisiert, die typische Beschleunigungs- und Verzögerungsfähigkeiten der Fahrzeuge beschreiben. Für spezielle Werte dieser Parameter wird das Modell anderen, bereits bekannten, Modell-

len sehr ähnlich. Indem Beschleunigungs- und Verzögerungsfähigkeiten variiert werden, lässt sich ein sehr gutes Verständnis für die Dynamik des Modells und seiner bereits früher bekannten Spezialfälle erlangen.

Contents

1	Introduction	1
1.1	The problem of growing traffic demand	1
1.2	About this work	2
2	Empirical properties of traffic flow	5
2.1	The fundamental diagram	5
2.2	Traffic jams	6
2.3	Synchronized flow	8
3	Known model approaches	11
3.1	Introduction	11
3.2	Microscopic models	12
3.2.1	Car-following	12
3.2.2	Lane changes	16
3.3	Macroscopic models	16
3.4	Mesoscopic models	18
4	Model formulation	19
4.1	The general approach	19
4.2	Modeling of interactions	20

4.2.1	Time continuous description	20
4.2.2	Discrete time steps	22
4.3	The model equations	23
5	The Gipps–Family	25
5.1	Introduction	25
5.2	The role of acceleration and deceleration	27
5.3	The limit of high acceleration	28
5.3.1	Approximate model equations	28
5.3.2	Mean–field–approximation	29
5.3.3	Simulation results	31
5.4	The high–deceleration–low–acceleration–limit	34
5.4.1	Introduction	34
5.4.2	The jammed state	35
5.4.3	The mechanism of microscopic jam formation	40
5.4.4	Evolution of jams	43
5.4.5	The outflow from jams	45
5.4.6	Finite size effects	46
5.5	Low–acceleration–low–deceleration–models	48
5.5.1	Phase separation	48
5.5.2	Metastability	50
5.5.3	The outflow from jams and jamming dynamics	51
5.6	The role of noise	54
5.6.1	Introduction	54
5.6.2	The jamming point	54
5.6.3	The outflow from jams	54

5.6.4	The homogeneous flow	56
5.7	Model classes in the Gipps–family	57
5.7.1	Introduction	57
5.7.2	The existence of jams	59
5.7.3	Stability of the outflow from jams	61
5.7.4	Model classes	62
5.8	Concluding remarks	63
6	Discrete space coordinates	65
6.1	Spatial discretization of the model	65
6.2	The effects of discretization	66
7	Deterministic jamming	71
7.1	Introduction	71
7.2	The effective desired gap	72
7.3	Deterministic car following and escaping from jams	73
7.4	A deterministic model of jamming	75
7.5	Outflow from jams	76
8	Multilane traffic	79
8.1	The distribution of maximum velocities	79
8.2	Generalization of the model	80
8.3	Comparison to empirical data	84
8.3.1	Clustering	84
8.3.2	Quantitative comparison	86
8.4	Modeling of synchronized flow	87

9 Concluding remarks	91
9.1 Summary	91
9.2 Conclusion and Outlook	93
A Remarks on the model	95
A.1 Update rules	95
A.1.1 Single lane traffic	95
A.1.2 Twolane traffic	96
A.2 Computational performance	99
B A car-following experiment	101

Chapter 1

Introduction

1.1 The problem of growing traffic demand

“The volume of vehicular traffic in the past several years has rapidly outstripped the capacities of the nation’s highways. It has become increasingly necessary to understand the dynamics of traffic flow and obtain a mathematical description of the process.” These words, that could have been drawn from a recent work, actually originate from a classical article by Greenberg [27], published in 1959. Since 1959, the amount of traffic has increased continuously, and the problem of limited road capacity has been growing worse ever since.

The increasing traffic volume and congestion effects in the road network have become a severe environmental and economical problem. In Germany approximately 58% of the CO-emissions, 18% of the CO₂-emissions, and 46% of the NO_x-emissions are caused by road traffic. A significant fraction of this can be traced back to traffic jams, where vehicles pollute the air without moving. Economically, enormous costs have to be attributed to the delay times caused by traffic jams. It is quite obvious that measures have to be taken to reduce the burden of an uncontrolled growth of traffic.

Unlike in 1959, environmental problems do not allow a further extension of the road network to solve the ubiquitous capacity problems. Instead, more intelligent solutions, that do not put any higher burden on the environment, have to be found.

A natural point to start out from is the notion that there are three types of traffic, namely necessary traffic, unnecessary traffic and inefficient traffic. An optimization of necessary traffic with respect to environmental aspects can only take place by reducing fuel consumption and exhaust of vehicles and by supporting the use of public transport facilities. Unnecessary traffic can be reduced by optimizing logistics using fleet manage-

ment systems and applying methods of combinatorial optimization as well as by designing urban planning in such a way that the need for transportation is minimized.

Inefficient traffic is the topic that is mainly addressed by this work. The benefit that each individual can draw from a transportation network often deteriorates before the true capacity of a network or a road segment is reached. It can be expected that increasing efficiency at the same time improves the “level of service” of a network and reduces environmental impacts of traffic. Numerous approaches have been proposed to address this subject, examples of which are advanced traveler information systems, variable message signs, and variable speed limits. In all approaches detailed information about the state of the network or a road segment, as well as precise knowledge about the way the system responds to traffic management measures, is of central importance. For this reason a thorough knowledge of the dynamics of traffic in a network is necessary for an optimal utilization of traffic management measures.

The prediction of the way a network responds to an operation before it is actually employed is just as important a prerequisite for optimized traffic management as the on-line short-term-prediction of traffic loads. In both cases the modeling of traffic flow and simulation techniques play a key role. This already has been seen by Greenberg in 1959 and continues to be true.

1.2 About this work

The field of traffic simulation has a long tradition. The first articles on this topic were published in the nineteen-fifties [7, 24, 27, 31, 52]. Ever since, the field has been drawing growing attention, and numerous approaches to the modeling of traffic flow have been proposed. Today, there are many different modeling techniques that are in use.

There are two main problems about the large number of modeling approaches that are available. Firstly, each model has got its specific range of application, for which it has been designed, but little is generally known about the actual range of validity that a model has. Secondly, the way that different models are interrelated is only known in very few cases. These two facts are highly unsatisfactory from a theoretical, as well as from a practical point of view. Despite the impressive number of traffic flow models it has to be conceded that there is no such thing as a widely accepted theory of traffic flow yet. Instead there are different “schools” that exist independently. For the practitioner this has the consequence that it is very difficult to decide what model to use for a certain application and what computational effort is actually necessary to acquire reliable results.

The main reasons responsible for this situation are quite obvious. Firstly, many approaches, especially the microscopic ones, are derived from more specific assumptions

about the processes that take place in traffic flow than may be absolutely necessary. These models are generally quite complex and contain a large number of free parameters, which makes it difficult to attribute specific properties of a model's behavior to specific properties of the model's design. Secondly, the validation of the models is generally performed only by comparing certain quantities of traffic flow in specific situations, as found from the model, to those found in reality and choosing the free parameters in such a way that the mean deviation is minimized. Typical examples of the quantities considered for this kind of calibration are the average flow–density–relation or the gap between vehicles in car following experiments. The problem about this is that strictly quantitative considerations often do not lead to a qualitative understanding of the phenomena found in traffic flow. Very often it cannot be distinguished clearly in this way, whether a model actually captures the essentials of traffic flow correctly or if it is merely the sufficient number of free parameters that allows to obtain a seemingly satisfactory result for a specific situation. In addition, it can happen easily that a model is calibrated to reproduce quantities that are of minor importance to the qualitative performance of the model.

This work tries to perform a step towards overcoming the problems noted above. Here a model approach will be proposed that is still simple enough to allow attributing model properties to properties of the model's design, but that captures essential qualitative properties of traffic flow correctly. The influence that the different free parameters have on the model performance will be studied systematically. The main focus of these investigations will be the qualitative behavior of the model. It will be seen that quantitative agreement with reality is achieved easily after the qualitative aspects of traffic flow have been understood.

Therefore the work will start by giving a short overview over the most important phenomena found in traffic flow experimentally. It will be seen that, besides quantitative properties of traffic flow, like the numerical value of a road's capacity, there are certain qualitative features of traffic flow that will help to judge the phenomena found in different models quite easily. In this way a sound basis for a thorough understanding of the different traffic flow models is gained.

After that, one chapter is devoted to a short overview over traditional and more recent approaches in traffic flow modeling.

Following this, a family of stochastic traffic flow models for single lane traffic will be proposed, from which all models used in this work are derived.

A specific member of that model family will be considered after that. This model is mainly characterized by three free parameters that describe acceleration and deceleration capabilities of the vehicles as well as a stochastic element, introduced to model imperfections in driving. Since quite different types of behavior are found, depending on how the free parameters are chosen, this model will itself be referred to as a “model

family” again, the members of which are characterized by the free parameters. The role that these parameters play will be elucidated systematically by describing and comparing the phenomena found for different choices of these parameters. It will be found that three classes of models exist in this model family that show qualitatively different types of macroscopic behavior. In the first class the formation of traffic jams corresponds to a phase transition in the sense of physics, whereas the second class displays structure formation, but rigorously no phase transition. The third class describes only unstructured flow. Some remarks on the role that stochasticity plays in the model family will be made. It will be seen that the properties of the model depend on the stochastic model element in an undesirably strong way. The knowledge about the qualitative properties of traffic flow will allow a clear judgment of the different classes of the model family concerning their ability to describe traffic.

The models that will be discussed up to that point use continuous space coordinates and are discrete only with respect to time. Very often it is computationally more efficient, to use integer coordinates only, so a cellular automaton model is obtained. Therefore the cellular automaton models corresponding to the continuous models discussed so far will be introduced. The effects of discretization will be discussed and it will be shown that discretizing the systems can lead to a loss of important phenomena.

The strong dependence of all model properties on the introduction of an artificial noise term will be the motivation for a simple approach to a deterministic model of jamming in traffic flow. It will be shown that most model properties found in the stochastic case can be resumed without the existence of a stochastic element in the model.

Before quantitative comparisons to real traffic flow data can be made, the model has to be generalized to multilane traffic. This will be done while keeping the model still as simple as possible. It will be seen that excellent qualitative and quantitative agreement between the model and reality is obtained. Finally, the phenomenon of synchronized flow will be discussed.

Chapter 2

Empirical properties of traffic flow

2.1 The fundamental diagram

Road traffic is a complex system consisting of a large number of individual agents, that interact with each other. As an agent we want to adopt the “compound” subject made of a driver and his or her car. In this work this subject will frequently be referred to simply as “driver” or “car”. The way the agents move in traffic is determined by the complex processes of human perception and decision making, by the way driver and car interact, as well as technical restrictions imposed by the car the driver uses.

It is rather obvious that modeling traffic flow directly on the basis of the microscopic details governing the motion of individual vehicles is impossible. However, there are certain properties of traffic flow that do not depend on the details of the underlying processes. One property of this kind is the fact that interactions between vehicles are generally motivated by the intention not to collide with one another. It is very plausible and has been confirmed by many empirical investigations [10, 27, 28] that this requires the average velocity V in a locally homogeneous traffic flow to decrease with increasing vehicle density ρ . If averages are taken, one may expect to find some functional relation between V and ρ , for which we expect

$$\frac{dV(\rho)}{d\rho} < 0 . \quad (2.1)$$

For very small traffic densities the average velocity V approaches some finite value v_{\max} , whereas for the maximum density ρ_{\max} , when all vehicles are found bumper to bumper, no motion is possible.

$$\begin{aligned} V(0) &= v_{\max} , \\ V(\rho_{\max}) &= 0 . \end{aligned} \quad (2.2)$$

The corresponding average flux of vehicles $Q(\rho) = \rho V(\rho)$, which is the average number of vehicles passing a given cross section per unit time, is a function that vanishes at $\rho = 0$ and $\rho = \rho_{\max}$ and has a maximum at some intermediate density. The slope of this function for small densities is given by v_{\max} . The function $Q(\rho)$ is usually referred to as the fundamental diagram.

Besides the velocity in the free flow and the maximum density the fundamental diagram is characterized by the maximum flow q_{\max} . Different fundamental diagrams will already look alike at a first glance if only these three parameters coincide. If the fundamental diagram of a model is compared to that of real traffic, the parameters ρ_{\max} and v_{\max} only prescribe the natural length- and time scale of the system. The only quantity that is governed by the interactions is the maximum flow q_{\max} . Generally, models have one or more free parameters to adjust this quantity, so it is rather obvious that virtually all microscopic models that describe collision free motion of vehicles seem to be able to reproduce the fundamental diagram quite well at first sight.

The important conclusion, that has to be drawn from this, is the fact that these three characteristic quantities of the fundamental diagram alone do not give much information about the properties of traffic flow, neither are they sufficient to judge the validity of a model.

In order to understand the validity of the dynamic properties of a traffic flow model, dynamical phenomena of traffic flow will have to be compared to the corresponding dynamical phenomena of the traffic flow model. Looking at the averaged fundamental diagram can only give a first hint in this respect.

In the following two sections empirical findings by Kerner and Rehborn [38, 39, 40] about traffic flow, that go far beyond the measurement of a fundamental diagram, will be reported. The main empirical result is the fact that traffic flow can be found in three qualitatively different states, that are denoted as free flow, synchronized flow, and jams. The transitions the system performs between these states can be interpreted as first order phase transitions [40]. Now a brief overview over the properties of the two congested states, synchronized flow, and jams will be given.

2.2 Traffic jams

The most prominent structures known in traffic flow are traffic jams. In a traffic jam the vehicle density is considerably higher than in the free flow. Correspondingly the velocity and the flow in a traffic jam are very small, although usually non-vanishing.

The first important empirical result is that even under “pure” conditions, i.e. in the absence of ramps, road construction or other obstacles, a jam can develop and exist for a

considerable period of time. For instance, Kerner and Rehborn tracked a jam for about 50 minutes. This means that the boundaries of jams show no tendency to flatten out by any kind of “diffusion process”.

Jams move in upstream direction at a velocity that is determined by flow and density upstream, downstream, and inside the jam. If these flows and densities are denoted by ρ_{in} , q_{in} , ρ_{out} , q_{out} , ρ_{jam} , and q_{jam} , the velocity of the upstream and downstream front are given by

$$\begin{aligned} v_{\text{up}} &= -\frac{q_{\text{in}}-q_{\text{jam}}}{\rho_{\text{jam}}-\rho_{\text{in}}} , \\ v_{\text{down}} &= -\frac{q_{\text{out}}-q_{\text{jam}}}{\rho_{\text{jam}}-\rho_{\text{out}}} \end{aligned} \quad (2.3)$$

respectively. The velocity of the upstream front v_{up} depends strongly on the inflow into the jam, whereas the velocity of the downstream front v_{down} has been found to be independent of the inflow conditions and is typically close to -15 km/h .

If inflow and outflow are equal, the jam does not change its size. Therefore situations have been found empirically where jams moved more than 10 km in backward direction without changing their size or shape significantly [38].

The flux out of the jam q_{out} is an intrinsic property of the jam and does not depend on the inflow conditions. Under similar road conditions, different jams have been found to have almost the same outflows, even if the inflow conditions were substantially different. So the downstream front of a jam always organizes to the same state, independent of whether the jam is stationary or not. Sometimes sequences of moving jams are found on a road. Since in this situation the inflow to all jams downstream of the first one is the outflow of some other jam upstream, the downstream jams remain stationary (i.e. they do not change size) for a long time. If multi-lane traffic is considered, the flux out of the jam is different on different lanes. Typically the leftmost lane yields the highest, the rightmost lane the lowest flux.

The maximum flux in free traffic q_{max} can be considerably higher than the outflow from jams q_{out} . Typical values for the passing lane are $q_{\text{out}} \approx 1800 \text{ veh./h}$ and $q_{\text{max}} \approx 2700 \text{ veh./h}$. So $q_{\text{max}}/q_{\text{out}} \approx 1.5$. The fact that the outflow from jams is considerably lower than the maximum flow is often referred to as the capacity drop.

The flux out of a jam can be interpreted as a boundary flux of the existence of jams. If the inflow is lower than this boundary flux, any jam will dissolve again, since under these conditions the outflow from the jam would be higher than the inflow. If the inflow to an existing jam is higher than this boundary flux, the jam grows. So systems that display a laminar flow at densities above ρ_{out} are obviously metastable, because on the one hand they may continue to be laminar and on the other hand a sufficient perturbation (a small jam) would grow inevitably.

Fig. (2.1) displays free flow and a jam in the flow–density plane, as measured using

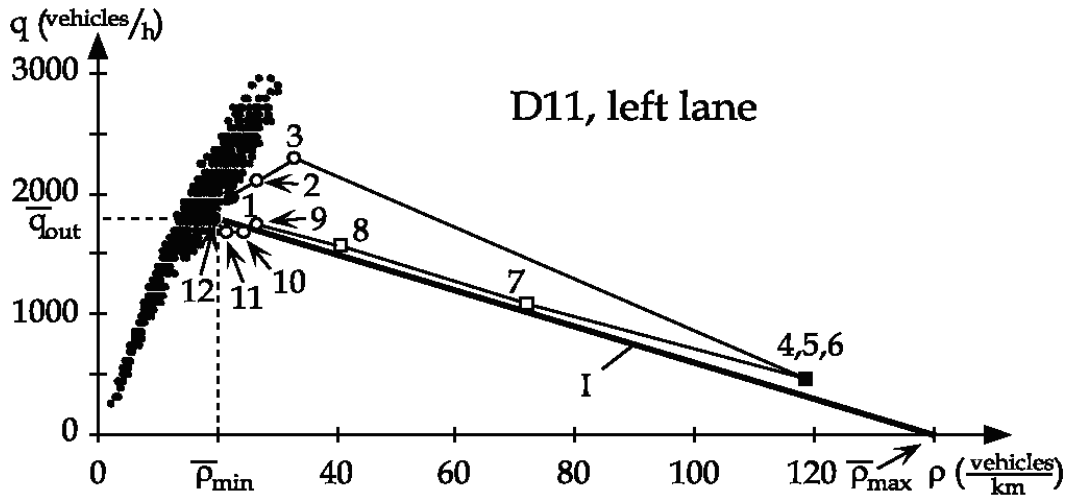


Figure 2.1: Free flow and a jam in the flow–density–plane. The picture has been supplied by B.S. Kerner.

an induction loop. The figure has been taken from [39] with friendly support of the authors. Points that correspond to the jam have been numbered according to the time when they were measured, where consecutive points have been connected by a line. Points 4,5, and 6 correspond to an average that has been taken over three minutes, to obtain a good estimate of the density, even at a low flux. The line “I”, found in the figure, represents the average path to which the downstream front of a jam organizes.

Obviously the empirical properties of traffic jams that are known go far beyond the notion that some kind of clustering is found in traffic flow. In fact, it will be seen, when the modeling approaches are discussed, that not all clustering phenomena are compatible with the empirical properties of traffic jams.

2.3 Synchronized flow

Although jamming is the phenomenon possessing the greatest impact on the performance of a road or a network, there are more properties that have to be considered. In [39, 40] it has been shown that besides the well known states of “free flow” and “jammed flow” there is a third class of states, denoted as “synchronized flow”. In synchronized flow traffic is found under congested conditions, where interactions between vehicles are significant, lane changes are rare and the velocities on both lanes are approximately equal. The average velocity in synchronized flow is considerably lower than the velocity in the free flow.

If traffic is looked at in the (ρ, q) –plane, the free flow at low density shows a very simple

behavior. In this regime the flow clearly is an increasing function of vehicle density. In contrast to this, synchronized flow is very complex. If a time series of measurements of ρ and q in synchronized flow is looked at, the system performs random translations in the (ρ, q) -plane. In this state an increase of vehicle density can be accompanied by an increase as well as a decrease of the flux. Obviously in the state of synchronized flow disturbances can travel in downstream as well as in upstream direction. That means there is a constant change between seemingly free and influenced motion of the vehicles.

Note that this sort of congestion is substantially different from jamming, where traffic flow has the strong tendency to organize in essentially the same way all the time.

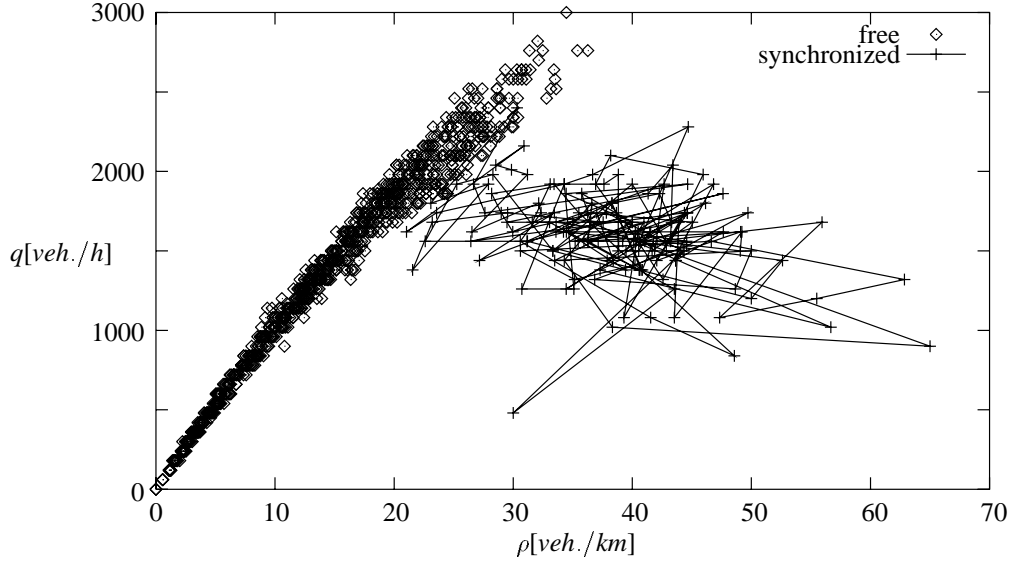


Figure 2.2: Free and synchronized traffic on the Autobahn A 43 near Bochum. There is one transition from free to synchronized flow and one transition back.

Fig. (2.2) shows free and synchronized flow in the (ρ, q) -plane for data gathered from the Autobahn A43 near Bochum. In the synchronized regime consecutive points (with respect to time) are connected by lines. Each point corresponds to an average taken over one minute. The same type of measurement has first been performed near Frankfurt in [39].

Chapter 3

Known model approaches

3.1 Introduction

Modeling traffic flow allows a great variety of different model approaches for two reasons. First, the details of traffic flow can be resolved to different extents, ranging from the dynamics of averaged quantities down to individual vehicle motion. Secondly, no first principles of traffic flow are known, from which models of different resolution could be derived, so the field of traffic flow dynamics leaves room for a lot of substantially different ideas. Classifying existing models with respect to the latter, i.e. the essentials of the traffic flow theory underlying a specific model is a quite difficult task that can only be performed in parts within this work.

Nevertheless, the classification of the models with respect to their resolution is quite straightforward and unequivocal. In general, microscopic models, which address the subject by describing individual vehicle dynamics, and macroscopic models, which are based on equations for averaged quantities like vehicle density and average flux, are distinguished. There is a third class of models, often referred to as mesoscopic models, that describes the vehicles using a mixture of macroscopic and microscopic dynamics. In these models individual vehicle dynamics are governed by field quantities, like average vehicle density in the region where the vehicle moves, so every vehicle moves in the “mean field” created by all the other vehicles.

Now a short overview over these model classes will be given.

3.2 Microscopic models

3.2.1 Car-following

The idea of microscopic modeling of traffic flow is to describe the dynamics of each individual vehicle as a function of the positions and velocities of the neighboring vehicles. In general, the two dynamical processes of car-following and lane-changing have to be considered. Since there are much more sophisticated methods for describing car-following than lane changes, we will start with a description of car-following models, assuming a road with only one lane. Positions and velocities of all vehicles are denoted by x_i and v_i respectively, where the index i rises in downstream direction.

Deriving a car following theory can obviously always start from the quite reasonable assumption that a change of the velocity is only performed, if the momentary velocity does not coincide with some desired velocity V_{des} , which is determined by safety considerations, legal restrictions and so on. The simplest dynamics that describes how a driver tries to approach the desired velocity is that of a relaxation on some time scale τ :

$$\frac{dv_i(t)}{dt} = \frac{V_{\text{des}} - v_i}{\tau} \quad (3.1)$$

Virtually all car following theories can be traced back to this simple idea. Usually, however, this dynamical relation is not interpreted as a relaxation process, but as a stimulus-response-ansatz. In this case the reciprocal of τ is usually referred to as the “sensitivity”. The models that will be discussed now only differ in the choice of V_{des} and τ .

Classical car-following-models

Almost all car following theories are based on the assumption that the motion of vehicle i is governed exclusively by the motion of the preceding vehicle $i + 1$. Since a steady state obviously requires the velocity of all vehicles to be equal (otherwise they would collide), it seems natural to assume that the desired velocity of a car is equal to the velocity of the car it is following, which would mean

$$\frac{dv_i(t)}{dt} = \frac{v_{i+1}(t) - v_i(t)}{\tau} . \quad (3.2)$$

This dynamical equation was first proposed by Pipes [66]. It should be noted, however, that Pipes derived this equation by stating that the spacing between the vehicles should increase linearly with speed and differentiating the resulting relation. Solving this equation one immediately arrives at the conclusion that the steady state solution, where all vehicles move at the same speed, is always stable so no clustering effects are described.

The steady state can be destabilized by introducing a finite reaction time Δt , as done by Chandler, Hermann, and Montroll [7], leading to a delay differential equation:

$$\frac{dv_i(t)}{dt} = \frac{v_{i+1} - v_i}{\tau} \Big|_{t-\Delta t}. \quad (3.3)$$

It is a well known fact that delay times tend to destabilize initially stable systems, so it is not surprising that the steady state in this model becomes unstable, if $\Delta t/\tau$ is large enough. The detailed analysis shows that the limit of stability is reached for $\Delta t/\tau = 1/2$. Although spontaneous clustering is modeled in this way, the applicability of the model is greatly restricted by the fact that the dynamics is independent of the distances between the vehicles. From this fact two things follow directly. The first consequence is that the vehicles collide in this model, the second is that there is no density dependence of the vehicle dynamics, so the speed-density relation cannot be derived from the model.

This problem was overcome by Gazis, Herman, and Potts [24] who introduced a dependence of the relaxation time or, as they put it, the sensitivity, on the distance between the vehicles.

$$\frac{dv_i(t)}{dt} = \alpha \frac{v_{i+1} - v_i}{x_{i+1} - x_i} \Big|_{t-\Delta t}. \quad (3.4)$$

Since the right hand side is the time derivative of $\alpha \ln(x_{i+1} - x_i)$, the model equations can be integrated and the density-dependent homogeneous steady state solution is found to be

$$v \propto \ln \left(\frac{\rho_{\text{jam}}}{\rho} \right), \quad (3.5)$$

where ρ_{jam} is the jam density, for which the velocity vanishes. This result is in accordance with Greenberg's macroscopic theory [27]. Unfortunately, the velocity of the homogeneous solution diverges as the vehicle density vanishes. However, since the divergence is only logarithmic, the flux $q = \rho v$ vanishes for vanishing density. So a qualitatively correct fundamental diagram is obtained.

Edie [16] proposed that the sensitivity also depends on the momentary velocity of a vehicle. He supposed that the sensitivity towards velocity again is inversely proportional to spacing, leading to the dynamical equation

$$\frac{dv_i(t)}{dt} = \alpha' v_i(t) \frac{v_{i+1} - v_i}{(x_{i+1} - x_i)^2} \Big|_{t-\Delta t}. \quad (3.6)$$

The most important point about Edie's work however is that he was the first to suspect that there is a discontinuity in the fundamental diagram, which led him to the idea to differentiate between two different "modes of operation", namely free flow and congested flow, corresponding to two different values for the sensitivity α' .

Gazis, Herman, and Rothery [23] formally unified and generalized all the above approaches by allowing the sensitivity to depend on arbitrary powers of spacing and velocity:

$$\frac{dv_i(t)}{dt} = \alpha' v_i(t)^m \frac{v_{i+1} - v_i}{(x_{i+1} - x_i)^l} \Big|_{t-\Delta t}. \quad (3.7)$$

Here the exponents l and m are free parameters. However, determining these exponents from empirical data proved to be difficult [23]. The dynamical equations can be integrated directly to yield the speed–density–relation of a homogeneous flow. For $m = 0$ and $l = 2$, for example, a linear dependence between speed and density is found, which coincides with the results of Greenshields [28].

The optimal velocity model

Of course, there can be choices of the desired velocity other than the velocity of the leading car. Bando et al. [2, 3] assumed that the desired velocity is a function of the distance between the vehicles under consideration:

$$\frac{dv_i(t)}{dt} = \frac{V_{\text{des}}(x_{i+1} - x_i) - v_i}{\tau} \Big|_t. \quad (3.8)$$

The function $V_{\text{des}}(\Delta x)$ has to vanish for $\Delta x \rightarrow 0$ and has to be bounded for $\Delta x \rightarrow \infty$. Bando et al. chose the desired velocity to be $V_{\text{des}}(\Delta x) = \tanh(\Delta x)$ and τ to be a constant. In this approach the speed–density–relation cannot be calculated from the model equations, but has to be prescribed through V_{des} .

Note that no explicit delay time has been introduced into this model. Still the model describes spontaneous clustering of vehicles. It has been shown on a phenomenological basis [42] that the qualitative dynamical properties of this model are almost exactly the same as those of the macroscopic Kerner–Konhäuser–model [36, 37] and furthermore compare very well with empirical observations.

Coupled map modeling and cellular automata

Instead of solving a differential equation for the velocities of the vehicles it is also possible to update the velocity in discrete time steps directly. This means that the velocity of car i at time step t is calculated from the conditions ahead at time $t - \Delta t$:

$$v_i(t) = f(v_i(t - \Delta t), v_{i+1}(t - \Delta t), x_{i+1}(t - \Delta t) - x_i(t - \Delta t), \dots). \quad (3.9)$$

An example of such a coupled map model is that of Yukawa et al. [82, 83]. The model is deterministic, but the function f is chosen in such a way that the dynamics of the individual vehicles is chaotic.

Another example of this model type is the model proposed by Gipps [25], who started from considering braking distances of the vehicles and derived a safe (that means collision free) update scheme for the vehicle velocities from this. Under the assumption that drivers underestimate the braking capabilities of the car they are following, the Gipps–model can describe overreacting of drivers and correspondingly the existence of instabilities in traffic flow.

The great advantage about this kind of modeling approach is the fact that it is computationally quite efficient, because no differential equation has to be solved. An even faster model is obtained, if the model is discretized not only with respect to time, but also with respect to the space coordinates. In this case a cellular automaton model of traffic flow is obtained and the whole dynamics can be simulated using only integer operations or even single bit coding. The first models of this kind were proposed by Cremer and Ludwig [11] and Schütt [76].

The most prominent representative of this class of models, however, is the Nagel–Schreckenberg–model [1, 57, 58, 62, 73, 75]. In this model the road is discretized into cells corresponding to segments of about 7.5 meters length. A cell can either be empty or be occupied by a vehicle. The velocity of a vehicle is an integer number, namely the number of cells that the vehicle jumps per time step. Contrasting to most other models discussed so far, the Nagel–Schreckenberg–model is a stochastic model that incorporates imperfections of driving using a noise term in the update rules. The model reproduces the empirical speed–density–relation and spontaneous clustering quite well. The mechanisms governing the dynamics of this model will be discussed further in this work.

The cellular automaton models are the first microscopic models that are computationally efficient enough to be used in large road networks, even for real–time applications.

Subsequently there have been efforts to build a bridge between cellular automata and space–continuous models and to perform other refinements to obtain quantitative agreement with empirical data [5, 18, 19, 20, 44].

Modeling of human behavior

All models discussed so far are based on extremely simplified ideas about the way humans behave in traffic. In fact it may be suspected that some details of the model design like the model of Gazis, Herman, and Potts can be traced back to considerations about analytical tractability of the model rather than realism of the assumptions that are made about human behavior.

For this reason other approaches to traffic flow have been proposed, that treat the “driver–vehicle–system” in greater detail. For instance, the concept of perception thresholds

was introduced by Michaels [55]. Based on the idea that drivers only react, if certain perception thresholds are exceeded, Todosiev [78] formulated the so called action-point-model. In the same line the model proposed by Wiedemann [80] can be seen. In this model different modes of operation are distinguished, for which different dynamical equations are proposed. The Wiedemann approach has been developed further to yield high fidelity models of individual driver behavior [53].

A completely different approach is that proposed by Rekersbrink [68], who modeled the driver–vehicle system using fuzzy controllers.

Unfortunately, all models of this kind have in common that they are computationally expensive and consequently are not applicable to large network problems. Rekersbrink, for example reports that about 25 vehicles can be simulated in real–time using his model.

3.2.2 Lane changes

The topic of lane changes has been addressed much less in the literature than that of car-following. Sparmann [77] performed a partly empirical and partly theoretical analysis of lane changing on two–lane–freeways, while Leutzbach and Busch [51] performed this kind of analysis for three–lane freeways. A model for the structure of lane–changing decisions in urban driving situations, where traffic signals, obstructions and heavy vehicles all exert an influence, has been developed by Gipps [26].

The generalization of the minimalistic rules used in cellular automaton models to multi-lane traffic was done by Latour [50], Rickert et al. [71], Wagner et al. [79], and Chowdhury et al. [9].

3.3 Macroscopic models

In macroscopic approaches it is not the dynamics of individual vehicles that is considered, but the dynamics of quantities that only have a macroscopic meaning. In general, the vehicle density $\rho(x, t)$ and average velocity $v(x, t)$ are considered, which are both functions of space x and time t . These quantities are obtained by averaging over a region of sufficiently large spatial extent. Since the number of vehicles in a road segment can only change by vehicles entering or leaving the segment, an equation of continuity holds for ρ and v :

$$\frac{\partial \rho}{\partial t} + \frac{\partial}{\partial x}(\rho v) = 0 . \quad (3.10)$$

The model equations are closed assuming one more relationship between density and velocity. The simplest model of this kind was proposed by Lighthill and Whitham [52],

where the velocity is assumed to be a function $V(\rho)$ of the density, leading to the model equation

$$\frac{\partial \rho}{\partial t} + c(\rho) \frac{\partial \rho}{\partial x} = 0, \quad \text{where} \quad (3.11)$$

$$c(\rho) = \frac{d}{d\rho} (\rho V(\rho)).$$

The model equation describes kinematic waves. The characteristics $x(\rho)$, i.e. the places where some prescribed density ρ is found, travel at the constant velocity $c(\rho)$. This model has been used very much in the last few decades. However, as pointed out by Kerner [42], it is not capable of describing the properties of clusters in traffic flow correctly. Nevertheless, still other models for kinematic waves have been proposed [12, 13, 14, 63, 64, 65].

The main problem about the Lighthill–Whitham approach is that it assumes local equilibrium. In general, one will have to replace the static relation $v(x, t) = V(\rho(x, t))$ by a dynamic equation that describes the way vehicles accelerate. After works by Greenberg [27] and Franklin [21], Payne formulated the dynamic equation for the velocity in the way that is in use today. The idea is that the acceleration of a vehicle, which is the total time derivative of the velocity field $v(x, t)$, is described by a relaxation towards a local equilibrium velocity and an anticipation term, which can be identified with the pressure term in fluid dynamics. The idea that the pressure term describes anticipation is motivated by the fact that this term can be derived by assuming that a driver at point x adjusts to the conditions ahead at the point $x + 1/\rho$, where the preceding car is found. The resulting equation is

$$\frac{\partial v}{\partial t} + v \frac{\partial v}{\partial x} = \frac{V(\rho) - v}{\tau} - \frac{c_0^2}{\rho} \frac{\partial \rho}{\partial x}. \quad (3.12)$$

The left hand side of this equation is the total time derivative of the velocity, the first term on the right hand side describes relaxation, the second term anticipation. Unfortunately this model shows difficulties in the treatment of shock waves, because it develops solutions that are discontinuous in space. Different approaches were proposed to solve this problem [10, 72]. The most straightforward solution was given by Kühne, who introduced an additional viscous term that prevents the formation of discontinuities [47, 48, 49], the dynamical equation being

$$\frac{\partial v}{\partial t} + v \frac{\partial v}{\partial x} = \frac{V(\rho) - v}{\tau} - \frac{c_0^2}{\rho} \frac{\partial \rho}{\partial x} + \frac{1}{\rho} \frac{\partial}{\partial x} \left(\mu \frac{\partial v}{\partial x} \right). \quad (3.13)$$

Kerner and Konhäuser [36, 37] used structurally the same model as Kühne, and investigated the nonlinear dynamics of cluster formation thoroughly. A recent work by Helbing [29] extends the Kerner–Konhäuser–theory by an equation for the velocity variance and takes into account that vehicles occupy a nonvanishing amount of space.

Similar models have also been formulated using discrete space coordinates right away [10, 32], leading to coupled ordinary differential equations or even coupled maps (if a forward discretization in time is used).

Finally, kinetic theories of vehicular traffic [67] should be mentioned, in which macroscopic equations are derived from assumptions about the microscopic mechanisms of interaction between vehicles.

3.4 Mesoscopic models

Apart from microscopic and macroscopic models it is also possible to use “mixed” dynamics, where individual vehicles are moved according to dynamic laws that are governed by macroscopic quantities [35, 81]. These models combine the computational efficiency of macroscopic models with the opportunity to derive properties that refer to individual vehicles, like emissions, probability distributions for accelerations, individual travel times and so on.

Chapter 4

Model formulation

4.1 The general approach

In this work a modeling approach will be used that is not based on a model of human perception and decision making, but rather addresses the subject by only using assumptions about very general properties of traffic flow. The idea behind this is, that there are certain very general properties of traffic flow that govern the behavior of individuals participating in traffic and that it is not the details of individual behavior from which the macroscopic properties of traffic emerge.

If traffic flow is to be modeled on a microscopic scale, two types of motion of vehicles have to be considered. The first type is the free motion of a vehicle, the second is the motion of a vehicle while interaction with another vehicle takes place. Corresponding to this, two main assumptions can be made. The main property of free motion is, that the velocity at which a vehicle moves is bounded by some maximum velocity v_{\max} :

$$v \leq v_{\max} . \quad (4.1)$$

The maximum velocity can be interpreted as the desired velocity of the driver under consideration.

The reason why vehicles interact at all, is the fact, that drivers have the intention not to collide with any other car. So the second assumption we want to make is that, no matter how interaction actually takes place on the level of perception and decision making, it always turns out in such a way that the system remains free of collisions. So we assume that a driver always chooses a velocity that is no higher than the maximum safe velocity v_{safe} :

$$v \leq v_{\text{safe}} . \quad (4.2)$$

The way the maximum safe velocity is determined specifies the way vehicles interact and will be considered in the next section.

It is possible to formulate models on the basis of these two assumptions alone. However, it is quite reasonable to assume that positive and negative accelerations are bounded, too:

$$\begin{aligned} -b \leq \frac{dv}{dt} \leq a, \\ a, b > 0. \end{aligned} \quad (4.3)$$

It will be shown later on that this is in fact an essential ingredient, if the complexity of traffic flow is to be described correctly.

In this work only models that are updated in discrete time steps Δt will be considered. For such models the above restrictions can be formulated as

$$v(t + \Delta t) \leq \min[v_{\max}, v(t) + a\Delta t, v_{\text{safe}}], \quad (4.4)$$

where v_{safe} is calculated under the restriction

$$v(t + \Delta t) \geq v(t) - b\Delta t. \quad (4.5)$$

The complete information about how the individual vehicles interact is contained in the way v_{safe} is calculated. Once v_{safe} is determined, inequality (4.4) constitutes an update scheme for a traffic flow model, if the velocities of the vehicles are always chosen to be the highest velocities compatible with the above restrictions.

4.2 Modeling of interactions

4.2.1 Time continuous description

To complete the traffic flow model, the interactions have to be modeled. We look at a pair of cars, a leader at position x_l with velocity v_l and a follower at position x_f with velocity v_f . If the vehicle length is l , the gap g between the vehicles is given by

$$g = x_l - x_f - l. \quad (4.6)$$

As mentioned before, the reason for interaction is the intention of drivers to move without colliding with any other car. That means the gap g always has to be nonnegative. Unlike most modeling approaches, this work will not start with some assumption about how a car's acceleration can be calculated from the conditions in front of it, because collision freeness is not fulfilled automatically in these approaches and is sometimes hard to prove.

Instead, we start by noting that in a time continuous model interacting vehicles certainly do not collide if the gap g between the leading and the following vehicle is larger than some nonnegative desired gap g_{des} once and obeys the dynamical inequality

$$\frac{dg}{dt} \geq \frac{g_{\text{des}} - g}{\tau_{\text{des}}} . \quad (4.7)$$

The desired relaxation time τ_{des} and the desired gap g_{des} may be functions of the gap between the vehicles and their velocities. Specific expressions for these quantities will be derived in the next section. The fact that collisions cannot occur in this model is obvious, because for $g = 0$ the time derivative of g is always nonnegative if g_{des} is. All the models considered in this work will be described by dynamical relations of this kind.

However, the above inequality will not be used as an ad hoc assumption, but be derived from a simple argument now. Consider the case of a leader and a follower with a gap g between them at velocities v_l and v_f , respectively. The follower travels at a safe velocity, if the driver can, under any circumstances, bring the car to a complete stop before colliding with the preceding vehicle. That means, if the follower has a reaction time τ and the braking distance of the vehicles from velocity v is given by the function $d(v)$, the situation is safe, if

$$d(v_f) + v_f \tau \leq d(v_l) + g . \quad (4.8)$$

Note that $d(v)$ is not necessarily the minimal physically possible braking distance, which would be quadratic in v , but can be some other function that emerges from personal ideas that drivers have about comfortable driving. The same holds for the reaction time, which is not necessarily equal to the physiologically determined minimal reaction time.

Inverting this inequality with respect to v_f would lead to a safe update rule for the velocity of the follower. However, we will not do this directly for two reasons: Firstly, the inversion would require the specification of $d(v)$, which we will see is unnecessary. Secondly it seems unreasonable and is definitely computationally inefficient to use a driving strategy that requires anticipating the unlikely event of having to brake to a complete stop at every time step. Therefore a Taylor series expansion of the braking distance $d(v)$ around the average velocity of the leader and the follower $\bar{v} = (v_l + v_f)/2$ is performed in the inequality. Obviously the even orders of the series cancel out from the inequality and dropping only the third and higher order terms we get

$$d'(\bar{v})v_f + \tau v_f \leq d'(\bar{v})v_l + g . \quad (4.9)$$

An interpretation of the derivative $d'(v)$ can be given easily. Looking at a car decelerating from velocity v to velocity 0 at some (not necessarily constant) rate $\dot{v} = -b(v)$, $b(v) > 0$ it can be seen that

$$\begin{aligned} d'(v) &= -\frac{d}{dv} \int_v^0 \frac{v'}{b(v')} dv' \\ &= \frac{v}{b(v)} . \end{aligned} \quad (4.10)$$

Now the safety condition can be restated as

$$v_l - v_f \geq \frac{v_l \tau - g}{\frac{\bar{v}}{b(\bar{v})} + \tau} . \quad (4.11)$$

Note that

$$\frac{dg}{dt} = v_l - v_f. \quad (4.12)$$

So inequality (4.11) takes exactly the form of inequality (4.7) with the desired gap $g_{des} = v_l \tau$ and desired relaxation time $\tau_{des} = \tau_b + \tau$, where $\tau_b = \bar{v}/b(\bar{v})$ is determined by the typical decelerations b that a driver is willing to use. Note that by deriving inequality (4.11) considering nonvanishing braking distances, the effect of negative accelerations being bounded by $-b$ has been incorporated.

4.2.2 Discrete time steps

The inequalities derived so far have to be modified slightly to provide a scheme for updates of the vehicles' velocities in discrete time steps. The use of discrete time steps also provides a crude model for effects of finite reaction time.

The most natural way to construct an update scheme from the safety condition is to interpret the velocity v_f in the expression for $\dot{g}(t) = v_l(t) - v_f(t)$ as the velocity of time step $t + \Delta t$ leading to

$$v_f(t + \Delta t) \leq v_l(t) + \frac{g(t) - g_{des}(t)}{\tau_{des}(t)}. \quad (4.13)$$

The vehicles in the models considered in this work will obey this rule. The space coordinate x of the cars will be updated according to

$$x(t + \Delta t) = x(t) + v(t + \Delta t) \Delta t. \quad (4.14)$$

We know that for $\Delta t \rightarrow 0$ and $g_{des} \geq 0$ this rule guarantees safety. For finite Δt safety has to be checked again, however.

Having a gap $g(t)$ between a pair of vehicles at time t , the gap at time $t + \Delta t$ is given by

$$g(t + \Delta t) = g(t) + \Delta t (v_l(t + \Delta t) - v_f(t + \Delta t)). \quad (4.15)$$

Inserting inequality (4.13) yields

$$\begin{aligned} \xi(t + \Delta t) &\geq \xi(t) \left(1 - \frac{\Delta t}{\tau_b + \tau}\right) + \Delta t \frac{g_{des}(t) - v_l(t)\Delta t}{\tau_b + \tau}, \\ \text{where} \end{aligned} \quad (4.16)$$

$$\xi(t) = g(t) - v_l(t)\Delta t.$$

So safety ($g \geq 0$) is guaranteed, if $\xi(t=0) \geq 0$ and

$$\begin{aligned} \Delta t &\leq \tau \\ \text{and} \\ g_{\text{des}} &\geq v_l \Delta t \end{aligned} \tag{4.17}$$

for $t > 0$. This, of course, is exactly the result that had to be expected. It only states that the update rule is safe, if the true reaction time (i.e. the length of one time step) is smaller than or equal to the reaction time that each driver assumes, when choosing a driving strategy.

Before the model is finally formulated, we want to look at one more quantity, namely

$$\hat{\xi}(t) = g(t) - g_{\text{des}}(t) . \tag{4.18}$$

The time evolution of $\hat{\xi}$ is described by

$$\begin{aligned} \hat{\xi}(t + \Delta t) &\geq \hat{\xi}(t) \left(1 - \frac{\Delta t}{\tau_b + \tau}\right) + \delta , \\ \text{where} \end{aligned} \tag{4.19}$$

$$\delta = g_{\text{des}}(t) - g_{\text{des}}(t + \Delta t) + \Delta t(v_l(t + \Delta t) - v_l(t)) .$$

$\hat{\xi}$ can become negative, if δ becomes negative. Assuming g_{des} to be a function of v_l and performing a Taylor series expansion of g_{des} around $v_l(t)$ yields

$$\delta = \left(\Delta t - \frac{g'_{\text{des}}(v_l)}{v_l} \right) (v_l(t + \Delta t) - v_l(t)) . \tag{4.20}$$

So δ becomes negative if the leading car accelerates and $g'_{\text{des}}(v_l)$ is sufficiently large or if the leading car slows down and $g'_{\text{des}}(v_l)$ is sufficiently small. It will be shown later that the latter is of importance for a deterministic theory of clustering in traffic flow.

We will call models, for which $\hat{\xi}(0) > 0$ implies $\hat{\xi}(t) \geq 0$ for any $t > 0$, strictly free of collisions, because in these models the gap can never become smaller than the desired gap.

4.3 The model equations

So far only car following and free motion on a single lane have been considered. Lane changes on multilane roads have not been covered and will be treated in the chapter “Multilane traffic”. At the moment the model will be restricted to single lane traffic.

It will be assumed that, apart from random fluctuations, every vehicle moves at the highest velocity compatible with the restrictions stated above. In this way the model can be formulated immediately, giving

$$\begin{aligned}
 v_{\text{safe}}(t) &= v_l(t) + \frac{g(t)-g_{\text{des}}(t)}{\tau_b+\tau} , \\
 v_{\text{des}}(t) &= \min[v_{\max}, v(t) + a(v)\Delta t, v_{\text{safe}}(t)] , \\
 v(t + \Delta t) &= \max[0, v_{\text{des}}(t) - \eta] , \\
 x(t + \Delta t) &= x(t) + v\Delta t .
 \end{aligned} \tag{4.21}$$

The desired gap g_{des} can be chosen in different ways. This work will start out with a model family, where the desired gap is chosen to be $g_{\text{des}} = \tau v_l$ and τ is the reaction time of the drivers. The time scale τ_b is defined as $\tau_b = \bar{v}/b$. Here the random perturbation $\eta > 0$ has been introduced to allow for deviations from optimal driving. This perturbation is assumed to be δ -correlated in time. The choice of Δt and g_{des} is subject to the restrictions (4.17). Every model considered in this work will be of the form (4.21).

For all simulations performed in this work the vehicles will be updated in parallel. If not notified differently, periodic boundary conditions will be used.

Chapter 5

The Gipps–Family

5.1 Introduction

In [25] Gipps proposed a car following model that is based on the safety condition that can be derived from considering the braking distances of individual cars (inequality (4.8)). The update rule proposed by Gipps is slightly different from the one used here. Gipps assumed the braking distances $d(v)$ to be quadratic in v and solved the resulting inequality for the velocity v_l of the follower using the solution as the maximum safe velocity for the next update.

Although the Gipps–model is in certain respects different from the approach presented here, it parallels this approach in the respect that interactions are derived from considering braking distances. Therefore the models derived from inequality (4.8) will from now on be referred to as the Gipps–family.

As shown before, interaction in these models is described using the maximum safe velocity v_{safe} defined by

$$v_{\text{safe}} = v_l(t) + \frac{g(t) - v_l(t)\tau}{\frac{\bar{v}}{b(\bar{v})} + \tau} . \quad (5.1)$$

For the models that will be discussed now, some specializations will be made. The maximum acceleration a and deceleration b will be assumed to be constant (i.e. independent of the velocity), the time step Δt will be assumed to be equal to the reaction time τ . The unit of time will be the reaction time τ , the unit of the space coordinates will be the length of one car l , so $\tau = l = 1$. Here the “length” of a car is not its true physical length, but rather the space that a car typically occupies in a dense jam, which is a slightly larger quantity.

Note that all models of this kind are strictly collision free, since $g_{\text{des}} = v_l$.

In the randomization step, each car will be slowed down by a random amount η that is uniformly distributed between 0 and ϵa , where ϵ is a parameter between 0 and 1. So the update rules of the model are

$$\begin{aligned} v_{\text{des}} &\leftarrow \min[v_{\max}, v + a, v_{\text{safe}}], \\ v &\leftarrow \max[0, \text{rand}[v_{\text{des}} - \epsilon a, v_{\text{des}}]], \\ x &\leftarrow x + v, \end{aligned} \tag{5.2}$$

where v_{safe} is calculated from equation (5.1) and $\text{rand}[x_1, x_2]$ denotes a random number between x_1 and x_2 .

There are four free parameters in this model: the maximum velocity v_{\max} , the maximum acceleration a , the maximum deceleration b , and the noise parameter ϵ .

To get an idea of what size these parameters should typically have, we use the following estimates for typical values of the parameters in SI-units:

$$\begin{aligned} \tau &\approx 1s, \\ l &\approx 7.5m, \\ v_{\max} &\approx 36m s^{-1}, \\ a &\approx 0.8m s^{-2}, \\ b &\approx 4.5m s^{-2}. \end{aligned} \tag{5.3}$$

These values have been drawn from data gathered in a car-following experiment that will be discussed in the appendix. They only provide crude estimates of what values of the free parameters should be expected and are not to be understood as results of a serious parameter estimation procedure.

In the dimensionless form of the model ($\tau = l = 1$) the estimates correspond to

$$\begin{aligned} v_{\max} &\approx 5, \\ a &\approx 0.1, \\ b &\approx 0.6. \end{aligned} \tag{5.4}$$

Our main interest will be focused on the qualitative macroscopic properties of the model proposed here, because one cannot really expect to be able to capture the microscopic details of vehicle motion correctly with a model of this simple structure. Acceleration and deceleration of individual cars, however, are clearly a microscopic property of traffic flow. Therefore the estimates of a and b , as presented so far, do not really mean very much for the model immediately. This means that setting specific values for a and b can only be justified from looking at the macroscopic properties of the model, even if finding the parameters to be in the expected range surely would make the modeler feel a lot more comfortable. For this reason the whole possible range of these parameters will be looked at.

In contrast to this, the maximum velocity is a property with an obvious macroscopic meaning. For example the slope of the fundamental diagram for low vehicle density, when every vehicle moves at its desired velocity, is given by v_{\max} . Therefore this parameter will not be considered a “free” parameter in the analysis of the model properties.

Now the role that the free parameters a , b , and ϵ play, will be discussed systematically. For this end the next sections are devoted to an investigation of the different types of phenomena that are found, when the parameters a and b are varied in the ranges $(0, v_{\max}]$ and $(0, \infty)$ respectively. Three different representatives from the model family will be considered, which display three qualitatively different types of behavior. The three representatives are the high acceleration limit ($a = v_{\max}$), the high-deceleration-limit ($b \rightarrow \infty$) and low-acceleration-low-deceleration-models ($a \ll v_{\max}$, $b \ll v_{\max}$).

After that, the role of the randomization parameter ϵ will be explained. In a few concluding remarks the results are finally interpreted using a very simple, but very powerful phenomenological picture of traffic flow.

5.2 The role of acceleration and deceleration

Before the features of the models are discussed, some remarks on the role that acceleration and deceleration play with respect to interaction between the vehicles should be made.

The parameters a and b determine typical acceleration and deceleration capabilities in the model. Note, however, that due to the discreteness of the model in time the true maximum deceleration \hat{b} is not equal to b itself, but some increasing function of b where $\hat{b}(b=0) = 0$ and $\hat{b}(b \rightarrow \infty) = v_{\max}$.

The ratio between typical accelerations and typical decelerations governs the complex interplay between interaction and free motion. This can be seen by rewriting the safety condition as

$$g(t) \geq v_l(t) + [v_f(t+1) - v_l(t)] \left(\frac{\bar{v}}{b} + 1 \right). \quad (5.5)$$

This conditions restricts vehicle motion. In other words a car interacts, i.e. it is hindered by its predecessor, if the velocity it can reach in the next time step is high enough, to violate this condition, i.e. if

$$g(t) \leq v_f(t) + a + (v_f(t) + a - v_l(t)) \frac{\bar{v}}{b}. \quad (5.6)$$

The right hand side of inequality 5.6 can be interpreted as the range of interaction, which is governed by the two parameters a and b . If b is small compared to \bar{v} , which means if the time it takes a car to come to a complete stop from \bar{v} is much larger than 1

second, the last term typically dominates, so the interaction is long ranged. If b becomes sufficiently large, the second term becomes small and only a “hard core” interaction of range $v_f(t) + a$ remains. The sign of the second term is governed by the parameter a . If a is larger than typical velocity differences between successive vehicles, the cars will almost always interact.

Consider the case of $a \ll \hat{b}$. In this case an interaction can slow a vehicle down far enough that it loses contact to the leading vehicle and another interaction cannot take place for a while. For models of this kind a rather complex behavior may be expected, because a complex interplay between free motion and interaction will be found.

If, on the other hand, $a \gg \hat{b}$, the fact that acceleration is bounded does not restrict vehicle motion significantly. If we assume that traffic is dense enough so vehicles cannot move at their maximum speed, the only restriction that is put on the motion of the vehicles is due to interactions and the vehicles can be assumed to be interacting constantly.

5.3 The limit of high acceleration

5.3.1 Approximate model equations

If the vehicles’ motion is only restricted by interactions and the vehicles can be assumed to be interacting constantly, the equations of motion take a rather simple form:

$$\begin{aligned} v(t+1) &= v_l(t) + \frac{g(t)-v_l(t)}{\tau_b(t)+1} - \eta(t), \\ x(t+1) &= x(t) + v(t+1). \end{aligned} \tag{5.7}$$

For ease of notation it will be assumed implicitly that $\eta(t)$ is chosen in such a way that no vehicle is slowed down to negative velocities, so η is always smaller or equal to the other terms on the right hand side of the update rule.

As mentioned before, the equations can be rewritten in a more suggestive form using the quantity $\xi = g - v_l$:

$$\begin{aligned} v(t+1) &= v_l(t) + \frac{\xi(t)}{\tau_b(t)+1} + \eta(t) \\ \xi(t+1) &= -\frac{\tau_b}{\tau_b+1} \xi(t) + \eta(t). \end{aligned} \tag{5.8}$$

These equations describe two processes that take place on different time scales. The first process, described by the second equation, is a colored noise process on the time scale $\tau_b + \tau$, which typically corresponds to a few seconds in flowing highway traffic. The first equation then describes the backward motion of the remaining disturbances, which are gradually flattened out by a diffusion process, originating from the noise. So

it is very plausible and confirmed by simulations that the equilibrium state of the system is always homogeneous.

The velocity of the traveling waves and the average vehicle velocity can be calculated now using a mean field type approximation.

5.3.2 Mean-field-approximation

The equilibrium value of ξ is calculated by averaging the second equation from (5.8) with respect to time. If correlations between ξ and $\tau_b/(\tau_b + 1)$ are neglected, averaging yields

$$\langle \xi \rangle = \frac{\langle \eta \rangle}{1 - \langle \alpha \rangle},$$

where

(5.9)

$$\alpha = \frac{\tau_b}{\tau_b + 1}.$$

Note that α is a function of the average velocity \bar{v} of two successive vehicles. To get an estimate of the effect that fluctuations $\delta\bar{v}$ of \bar{v} have, α will be expanded around $\langle v \rangle$, yielding

$$\langle \alpha \rangle = \frac{\frac{\langle v \rangle}{b}}{\frac{\langle v \rangle}{b} + 1} - \frac{1}{\left(\frac{\langle v \rangle}{b} + 1\right)^3} \langle \left(\frac{\delta\bar{v}}{b}\right)^2 \rangle + \dots .$$
(5.10)

Now it will be assumed that the solution $\langle v \rangle$ can be expanded in powers of the fluctuations $\delta\bar{v}$, so the zeroth order of this expansion will be the mean field solution. Inserting the definition of ξ into equation (5.9) and solving for $\langle v \rangle$ yields

$$\langle v \rangle = \frac{\langle g \rangle - \langle \eta \rangle}{1 + \frac{\langle \eta \rangle}{b}} + \frac{\langle \eta \rangle}{b(\langle g \rangle + b)} \langle \delta\bar{v}^2 \rangle + \dots .$$
(5.11)

Neglecting fluctuations obviously leads to an underestimation of the velocity. The error will become the more significant the smaller b is.

In the mean field approximation small disturbances of long wavelength, that are slow enough to allow the system to relax locally, travel in backward direction through the system at the velocity

$$\begin{aligned} c &= \frac{d}{d\rho}(v\rho) \\ &= -\frac{1 + \langle \eta \rangle}{1 + \frac{\langle \eta \rangle}{b}}, \end{aligned}$$
(5.12)

where $\rho = 1/(\langle g \rangle + 1)$ is the density of the vehicles.

The approximation is expected to be valid as long as chances for vehicles to reach velocity 0 or v_{\max} are slim. For low densities the cars do not interact and travel at the mean

speed

$$\langle v \rangle = v_{\max} - \langle \eta \rangle . \quad (5.13)$$

The mean gap $\langle g \rangle_c$ at which the transition from free flow to flow governed by interactions is expected to take place is estimated equating the velocity in the free flow and the mean-field solution, giving

$$\langle g \rangle_c = v_{\max} \left(1 + \frac{\langle \eta \rangle}{b} \right) - \frac{\langle \eta \rangle^2}{b} . \quad (5.14)$$

Since velocities were assumed to be nonvanishing, the approximation is also expected to break down for high densities, when $\langle v \rangle < \langle \eta \rangle$. One may apply the mean field approach to the limit of high density by noting that the noise $\langle \eta \rangle$ becomes a function of the mean velocity, because a car cannot be slowed down to negative velocities. Now the average perturbation for vanishing density will be denoted by $\langle \eta_0 \rangle$, so $\langle \eta_0 \rangle \geq \langle \eta \rangle$.

In quite straightforward calculations it can be shown that for $\langle g \rangle < 2\langle \eta_0 \rangle + \frac{\eta_0^2}{b}$ equation (5.11) has to be replaced by

$$\langle g \rangle = 2 \left(\frac{\langle v \rangle}{b} + 1 \right) \sqrt{\langle \eta_0 \rangle \langle v \rangle} - \frac{\langle v \rangle^2}{b} , \quad (5.15)$$

to avoid negative velocities. Note, however, that fluctuations can no longer be neglected in that case because \bar{v} and $\delta\bar{v}$ are of the same order of magnitude. So the mean field approximation is not valid there.

The first term of an asymptotic expansion for high densities can be given anyway. For high densities the mean velocity and therefore τ_b approach zero. So the update rule to leading order in τ_b and g simplifies to

$$v(t+1) = g(t) - \eta(t) . \quad (5.16)$$

Now η is not independent of g any more, because no car may be slowed down to negative velocities. For those cars having a gap g in front of them the mean velocity after the update is therefore given by

$$\langle v \rangle_{\text{gap}=g} = \frac{g^2}{4\langle \eta_0 \rangle} , \quad (5.17)$$

For very high densities it is plausible and confirmed by simulations that the gap distribution becomes exponential, so $\langle g^2 \rangle = 2\langle g \rangle^2$. At this point the mean-field approach is wrong. This finally yields the asymptotic expression for the average velocity:

$$\langle v \rangle = \frac{\langle g \rangle^2}{2\langle \eta_0 \rangle} . \quad (5.18)$$

Terms of the order \bar{v}/b have been dropped in (5.16), so the quality of the approximation becomes better with increasing b . Note also that this asymptotic expression differs from the asymptotics of the mean-field result by a factor of two, due to the fact that fluctuations have now been included.

5.3.3 Simulation results

To check the quality of the approximation, the mean–field result will be compared to simulations.

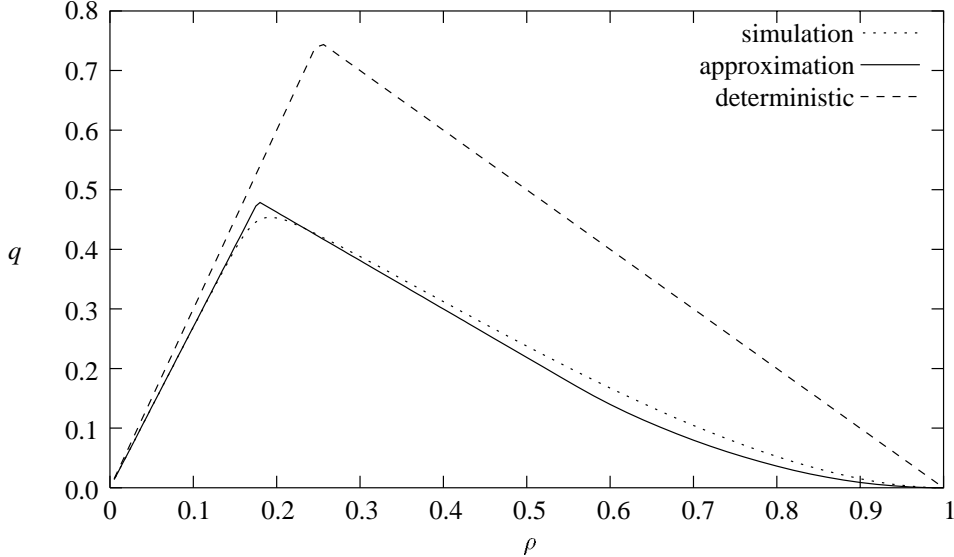


Figure 5.1: Comparison of the mean field approximation of the high acceleration limit with the simulation for $a = v_{\max} = 3$, $b = 0.5$, $\langle \eta_0 \rangle = 0.3$.

Fig. (5.1) shows the fundamental diagram, i.e. the flow q as a function of the density ρ , for a model of the high acceleration limit, once as obtained from the mean–field–approximation and once as obtained from simulations. The agreement is surprisingly good. To show that the effects of the random perturbations are not small, but have been captured correctly, the deterministic limit $\langle \eta_0 \rangle \rightarrow 0$ has been included in the figure.

To get an idea of for what ratios of a to b the approximation is valid, we define a measure for the error of the approximate solution:

$$\delta(a, b) = 2 \frac{q_m - q_s}{q_m + q_s}, \quad (5.19)$$

where q_m and q_s are the flows in the mean–field–approximation and in the simulation, respectively. The flows are measured for a fixed global density that is on the one hand high enough to get considerable interactions in the system and on the other hand low enough to keep the number of stopped vehicles small. The sign of the error is kept to show, whether the approximation underestimates or overestimates the true flow.

Fig. (5.2) shows the relative error of the mean field approximation $\delta(a, b)$ for $a = 1$ and $\langle \eta_0 \rangle = 0.5$, while (5.3) displays the corresponding proportion of interacting vehicles as a function of b . Note that, since $a = 1$ was chosen, the model does no longer correspond to the high–acceleration–limit. Three regimes can clearly be distinguished. For

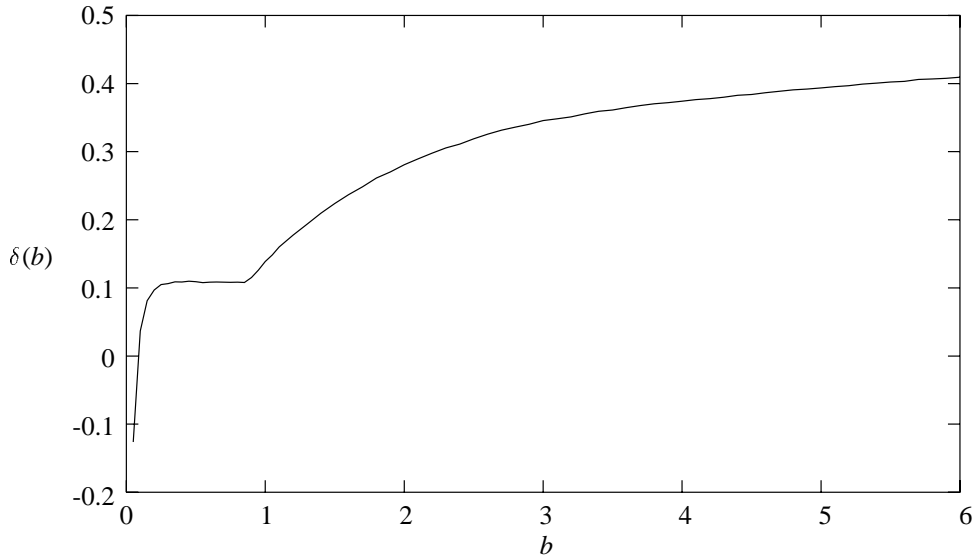


Figure 5.2: The relative deviation of the mean field solution of the high acceleration limit from simulation results for $\langle g \rangle = 4$, $a = 1$, $v_{\max} = 3$, $\langle \eta \rangle = 0.5$.

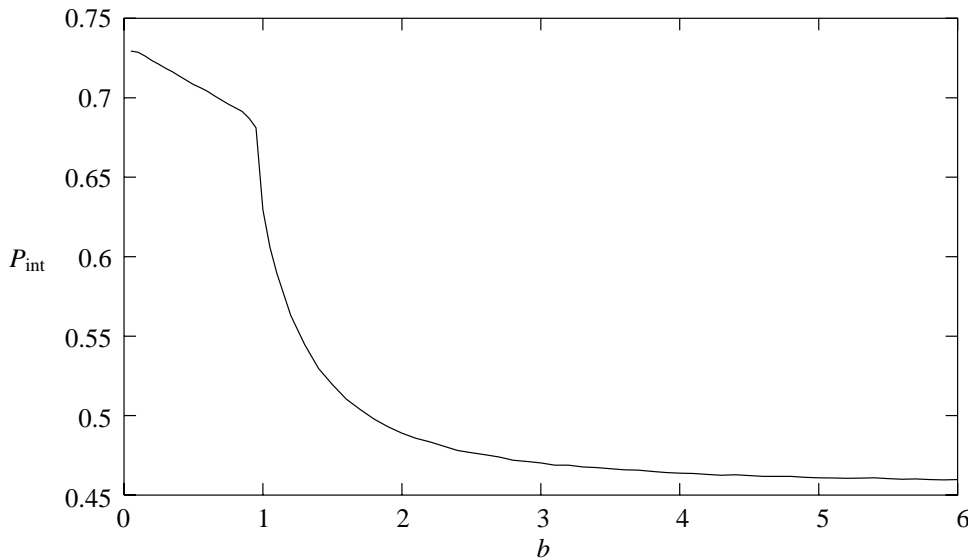


Figure 5.3: The proportion of interacting cars for $\langle g \rangle = 4$, $a = 1$, $\langle \eta_0 \rangle = 0.5$.

For $b \leq 1$ the assumption that every vehicle interacts is expected to hold approximately. In this range there is a region, where the approximation overestimates the true flow by about ten percent. This error can be traced back to the fact that not all vehicles actually do interact. For very small b the error becomes negative. As stated above, this is a consequence of the fact that fluctuations have been neglected in the approximation.

For $b > 1$ a strong increase of the error is encountered. At the same time the proportion

of interacting vehicles drops dramatically. As will be seen later, this effect is a consequence of the formation of traffic jams. It has been noted before, that the formation of jams is not possible in the Gipps-family, if a sufficiently high proportion of the cars do interact ($a = v_{\max}$). So the phenomenon of structure formation obviously depends on a balance between interaction and free motion. Note that the transition shown here does not always take place at $b = 1$, but at a point that depends on the other model parameters.

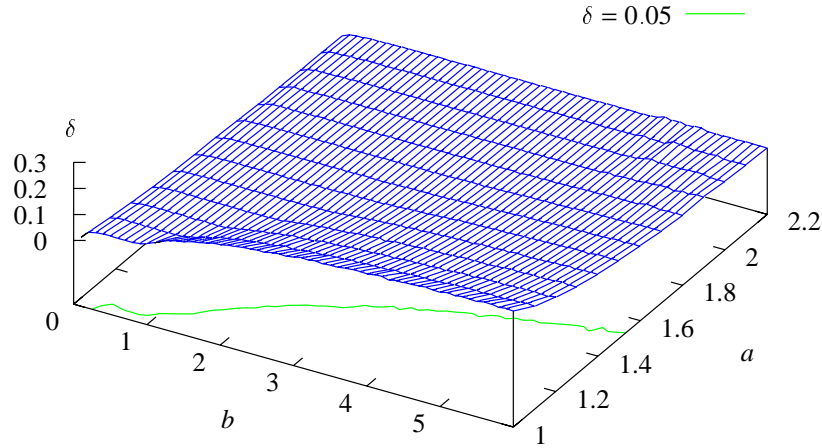


Figure 5.4: The error of the mean field approximation of the high acceleration limit.

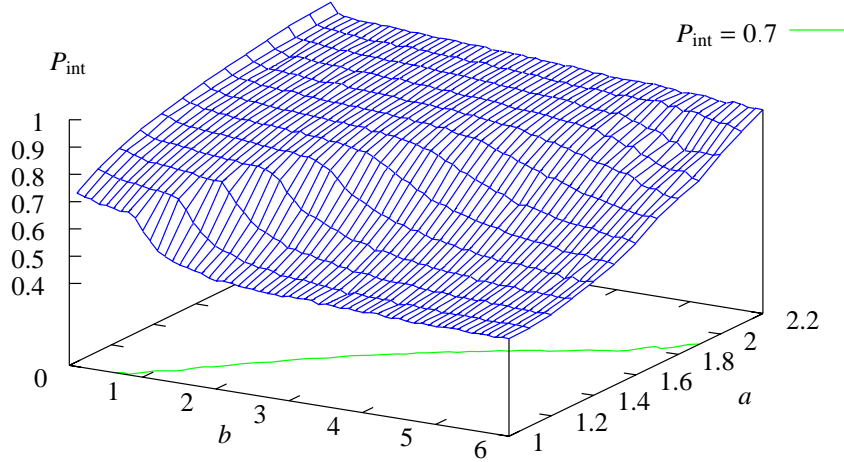


Figure 5.5: The proportion of interacting cars in a state above the density of maximum flow.

Fig. (5.4) displays the error $\delta(a, b)$ and Fig. (5.5) the corresponding proportion of interacting cars as functions of a and b . Substantial errors are only found, if b is large and a is sufficiently small. The decrease of the number of interacting vehicles due to jamming can again be seen clearly.

5.4 The high-deceleration-low-acceleration-limit

5.4.1 Introduction

The next limit that will be looked at is the limit $b \rightarrow \infty$, the limit that allows arbitrarily high decelerations.

In this limit the safety condition reduces to

$$v(t+1) \leq g(t). \quad (5.20)$$

This condition is the well-known safety condition of the Nagel–Schreckenberg cellular automaton model of traffic flow. In fact, apart from the discreteness of the space coordinates the Nagel–Schreckenberg–model is exactly identical to this limiting case of the Gipps–family. The role that the discreteness of the space coordinate plays in the Nagel–Schreckenberg–model will be clarified in the chapter on a cellular automaton version of the model discussed here.

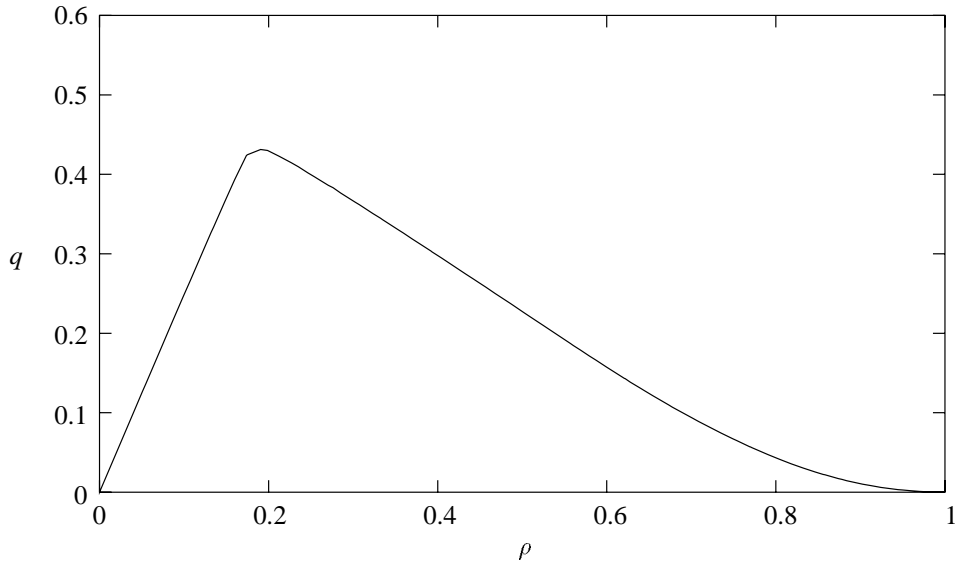


Figure 5.6: The fundamental diagram of the high deceleration limit for $v_{\max} = 3$, $a = \epsilon = 1$.

Now the parameters a and ϵ will be chosen in such a way that the approximation of constantly interacting cars does no longer hold. As shown in the last section, $a = 1$ and $\epsilon = 1$ are suitable for that purpose. The maximum velocity v_{\max} is set to 3. Fig. (5.6) shows the fundamental diagram of that model after averaging over the whole system.

Fig. (5.7) shows a space–time–plot of the model for a density above the density of maximum flow. The system is started in an initially homogeneous state. It can be seen

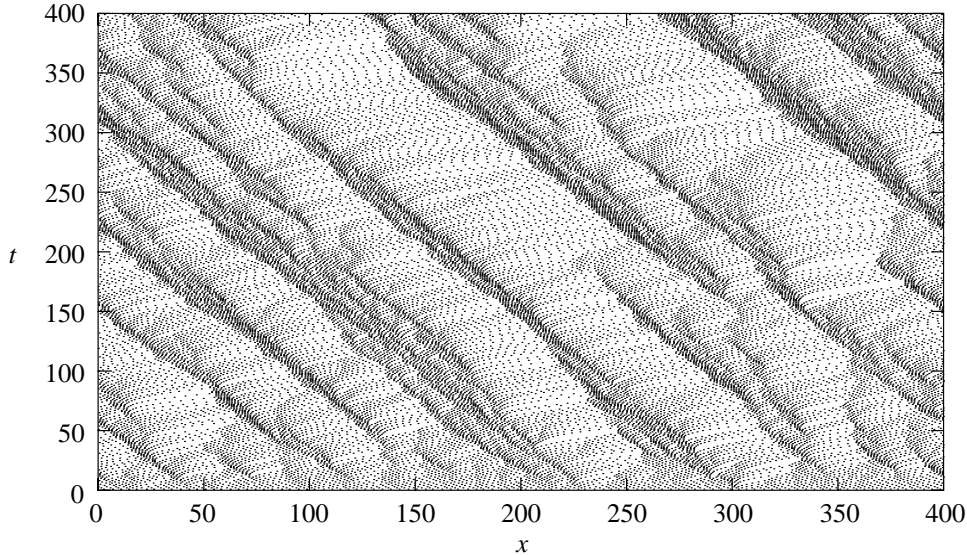


Figure 5.7: Space–time–plot of a model started at an initially homogeneous configuration.

clearly that the system separates spontaneously into regions of high density and regions of low density. The regions of high density correspond to traffic jams, those of low density to free flow. The jams travel in backward direction at an approximately constant velocity.

The formation of jams is a prominent feature of this model and will therefore be described in greater detail now.

5.4.2 The jammed state

To characterize the jammed state quantitatively, the probability distribution of the gaps between the vehicles will be looked at first. Fig. (5.8) shows this distribution for different densities at which the system displays macroscopic inhomogeneities. The distribution clearly is bimodal. The two maxima of the distribution are located at the same densities for the cases considered, only the relative height of the maxima varies.

This fact suggests that the cars can be found in two different states whose statistical properties only vary slowly with global density. Assume that the global state can be described as a combination of vehicles in a “free” and vehicles in a “jammed” state. If, for a given density ρ , a proportion $n(\rho)$ of the cars is found in the jammed state and a proportion $1 - n(\rho)$ in the free state, any probability distribution P of the system can be written as a linear combination of the corresponding distributions for the jammed state, P_j , and the free state, P_f :

$$P = n(\rho)P_j + (1 - n(\rho))P_f , \quad (5.21)$$

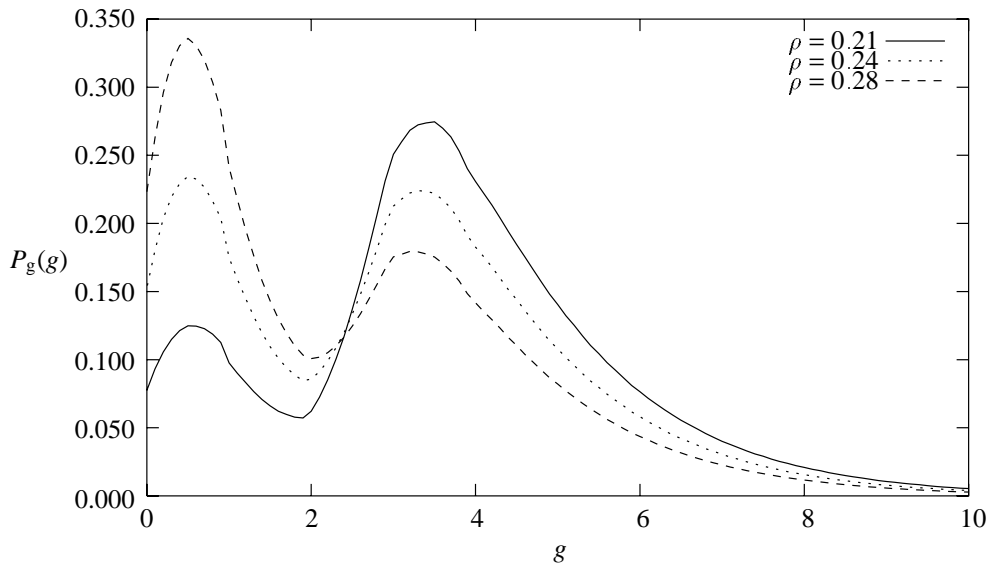


Figure 5.8: The bimodal gap distribution in the presence of jams.

where P_j and P_f are independent of ρ . The overlap of these distributions is not necessarily vanishing. Now assume that the gap distribution P_g can be written in the form of eq. (5.21).

After acquiring a series of gap distributions P_k , $k = 1, \dots, N$ from N simulations with densities ρ_k , the ansatz (5.21) can be used to calculate the gap distributions P_j and P_f of the jammed and the free regions respectively. For this end a cost function

$$C(P_j, P_f) = \sum_k \int dx (P_k(x) - n_k P_j(x) - (1 - n_k) P_f(x))^2 \quad (5.22)$$

is defined, where n_k is the proportion of jammed cars given by

$$n_k = \frac{\langle x \rangle_f - \frac{1}{\rho_k} + 1}{\langle x \rangle_f - \langle x \rangle_j} . \quad (5.23)$$

Here $\langle \dots \rangle_f$ and $\langle \dots \rangle_j$ denote averages taken with respect to P_f and P_j respectively.

The distributions P_j and P_f are then chosen in such a way that the cost function is minimized under the restrictions

$$\begin{aligned} P_f &\geq 0, \quad P_j \geq 0 , \\ \int P_j dx &= \int P_f dx = 1 . \end{aligned} \quad (5.24)$$

This approach has first been proposed in [44]. Apart from this the distributions P_j and P_f can also be estimated using a microscopic criterion. For example, we may attribute cars to a jam, if their velocity is lower than half of the maximum velocity.

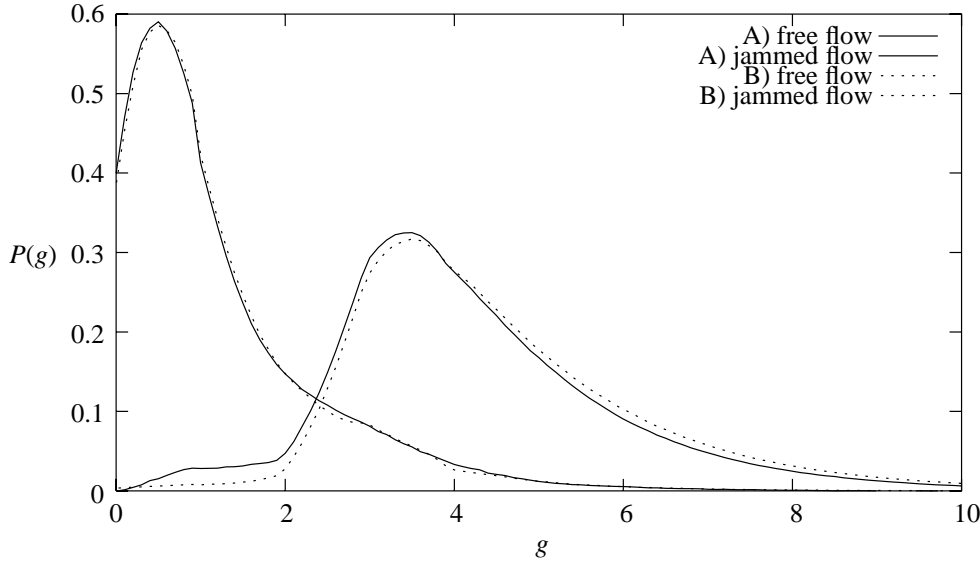


Figure 5.9: The gap distributions for the jammed and the free regions. A) macroscopic criterion, B) microscopic criterion

Fig. (5.9) shows the gap distributions acquired from the optimization process described above as well as the distributions acquired using the simple microscopic criterion $v < v_{\max}/2$. The two methods yield similar results.

The distributions P_f and P_j are worth a closer look. First, what may be a little unexpected, is the fact that the gap distribution of the free state assumes nonvanishing values down to gaps of size zero. In this respect the “free” state is substantially different from really free conditions at very low densities, where there is a sharp cutoff at nonvanishing values for the gap size. The small gaps originate from interactions between cars that do not suffice to finally cause a jam. Clearly the number of such events in the system is proportional to the number of cars in the free state as long as the density of the free state does not change significantly. So it is not surprising that the ansatz (5.21) attributes these events to the free state. From this the very important conclusion can be drawn that the assumption that the system decomposes into two different states leads directly to the conclusion that there are small gaps and consequently slow cars in the free flow. This is a quite peculiar result, which will be supported by other observations later.

Next the gap distribution for the jammed state P_j will be looked at. The distribution exhibits a strange behavior near gaps of size $v_{\max} = 3$, where more events are counted than expected. One would normally expect an exponential tail for the gap distribution, however, there are additional events that originate from the outflow regions of the jams. Since the number of such events is proportional to the number of jammed cars as long as the length distribution of the jams does not change too much, the ansatz attributes them to the jammed state.

From this, another important conclusion can be drawn. It is quite tempting to suspect that the system decomposes into macroscopic phases that correspond to the jammed and the free state. The idea that phase separation might occur in traffic flow already has been expressed elsewhere [61]. However, if actually macroscopic phases existed in this model, the “surface” effects at the downstream fronts of the jams should become less pronounced with growing system size. This, however, is not the case here. So apparently there is no such thing as macroscopic phases in this model.

This idea will be supported further by looking at the probability distributions $P_n(n, t)$ of the lengths of the jams, where n denotes the number of vehicles that a jam contains. If macroscopic phases exist, the typical length scale of the jams should become arbitrarily large in sufficiently large systems after sufficiently long periods of time.

For these calculations the following definition of a jam will be adopted. A connected structure of vehicles, traveling at a velocity below a given threshold v_{thresh} will be called a jam, if this structure contains at least one stopped vehicle. The condition that at least one stopped vehicle should be found in a jam is important to exclude small disturbances in the free flow from the definition of jams. Without this condition a large number of jams of size one would be found, that would dominate the length distribution. The threshold velocity again is chosen to be $v_{\max}/2$.

In the following simulations the system is started in a perfectly homogeneous state. The simulations show that the length distributions $P_n(n, t)$ for $t \rightarrow \infty$ and for large n is approximately proportional to the function $n \exp(-n/n_0)$, where n_0 characterizes the typical size of the jams (Fig. (5.10)).

Two quantities that can be used to characterize the typical length of jams are the average length of jams $\langle n \rangle$ and $n_0(t)$. Since it is numerically more stable, the average jam length $\langle n \rangle$ will be used here.

Fig. (5.11) displays this quantity for a system of length $L = 10000$, containing 2500 vehicles. The function has been calculated averaging over 25 independent systems. It can be seen that $\langle n \rangle$ does not grow arbitrarily, but approaches a finite value n_∞ . The difference $n_\infty - \langle n \rangle(t)$ shows a power law behavior. To eliminate finite size effects, n_∞ has been calculated for different system sizes, allowing the system to relax for different periods of time. Fig. (5.12) displays $\langle n \rangle$ as a function of the number of vehicles in the system. The quantity $\langle n \rangle$ has been calculated averaging over T time steps after the system had been allowed to relax for T time steps, where T ranged from 10^3 to 10^6 .

From the above calculations it can be concluded that no separation into macroscopic phases is found for the models of the high-deceleration limit, although the system can contain clusters of arbitrary size. Instead, there is a typical length of clusters, which approaches a finite value for $t \rightarrow \infty$.

Consequently it has to be concluded that the so called jamming transition is not a real

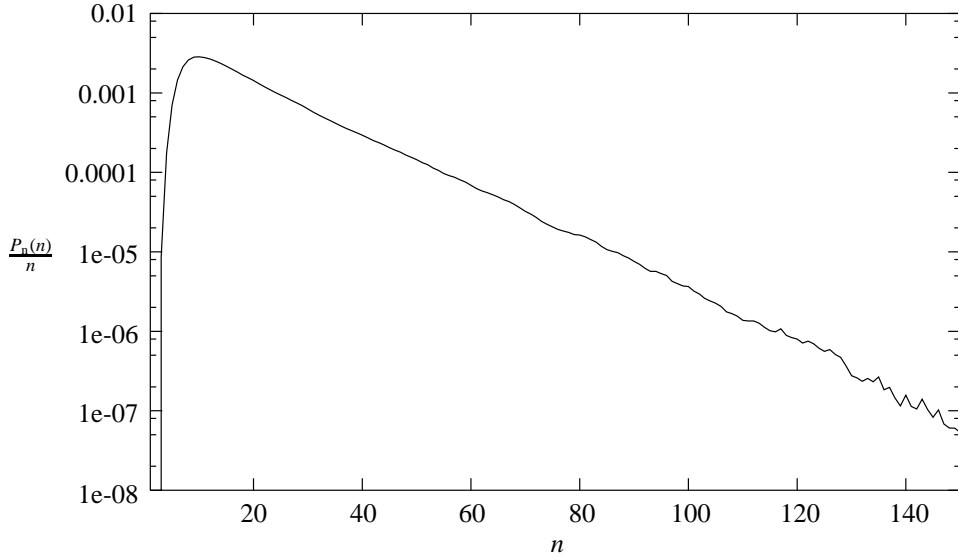


Figure 5.10: The length distribution of the jams for $v_{\max} = 3$, $a = \epsilon = 1$, $\rho = 0.25$ in the high deceleration limit. The slope of $\ln(P_n(n)/n)$ describes the typical length scale of the jams.

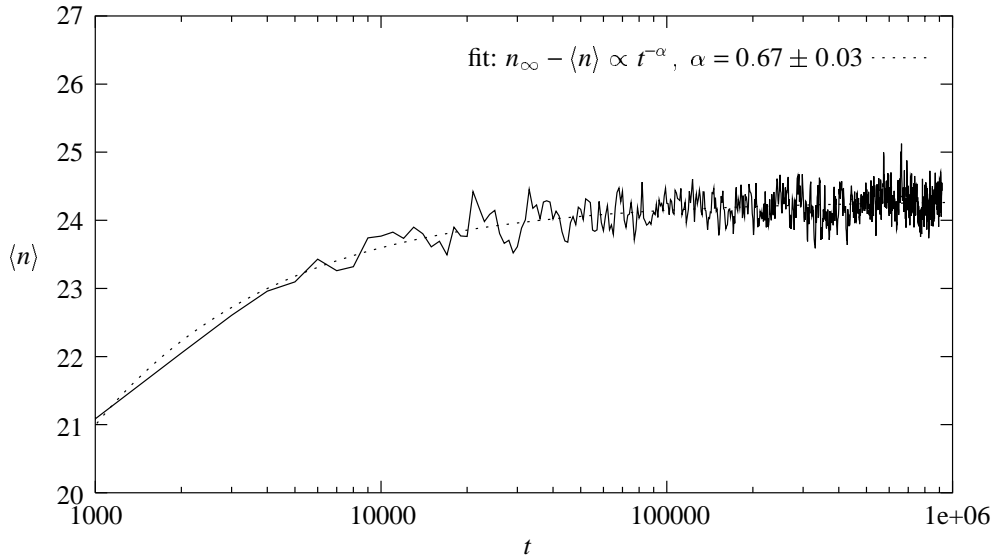


Figure 5.11: The evolution of the average length of jams. $\langle n \rangle$ approaches a finite value n_∞ for $t \rightarrow \infty$. Model parameters: $a = \epsilon = 1$, $v_{\max} = 3$, $\rho = 0.25$, $L = 10000$.

phase transition. A similar result has recently been found in the discrete Nagel–Schreckenberg–model [17]. In that work, however, this result was derived from the behavior of a spatial correlation function during the jamming transition.

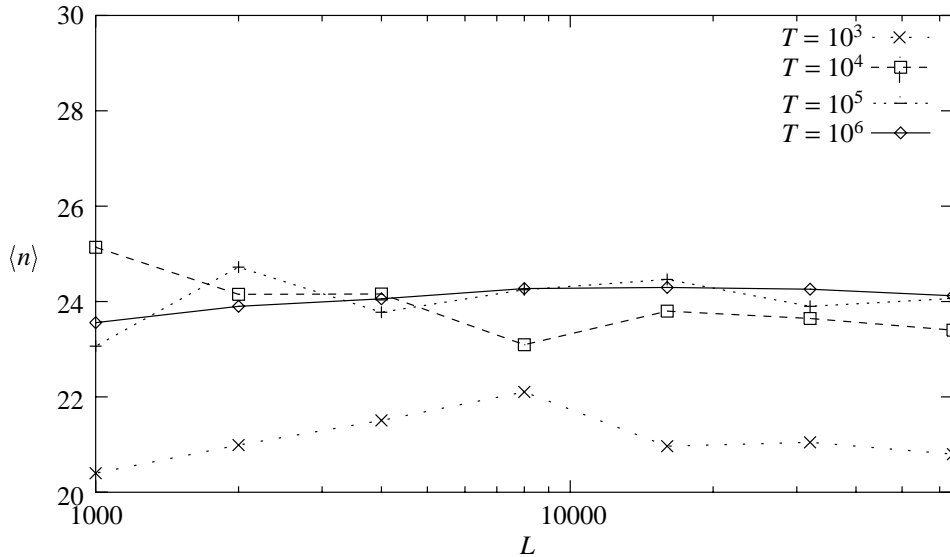


Figure 5.12: The average length of jams $\langle n \rangle$ as a function of the system length L for $v_{\max} = 3$, $a = \epsilon = 1$, $\rho = 0.25$. Averages were taken over T time steps after allowing the system to relax for T time steps.

5.4.3 The mechanism of microscopic jam formation

The mechanism of jam formation will now be explained in two steps. First, a semi-quantitative analysis of the formation of small jams will be proposed and secondly, the dynamics and growth of existing jams will be explained.

The first point that has to be made is the fact that slowing down of vehicles to a complete stop due to interactions is a purely stochastic phenomenon in this model. An interacting car with the gap $g(t)$ in front of it, following a leader with velocity $v_l(t)$ has a velocity \hat{v}_f before the randomization step given by

$$\hat{v}_f(t+1) = g(t) \geq v_l(t) . \quad (5.25)$$

So without the randomization step no car slows down to velocities lower than that of the leader. Consequently the maximum loss of velocity (with respect to the vehicle in front) in each interaction is given by the maximum random perturbation. If the randomization step slows the vehicles down by an amount equally distributed between 0 and ϵa , the number of interactions needed to obtain a stopped car in flowing traffic is roughly given by $v_{\max}/(\epsilon a)$.

Fig. (5.13) displays an event, where this slowing down to a complete stop takes place. For ease of understanding the road has been discretized in cells of length one and velocities have been assumed to have only integer values like in a cellular automaton. In that case the random noise slows down vehicles by the amount one with a certain probability. A situation is shown, where in a queue of vehicles that move at a gap equal to

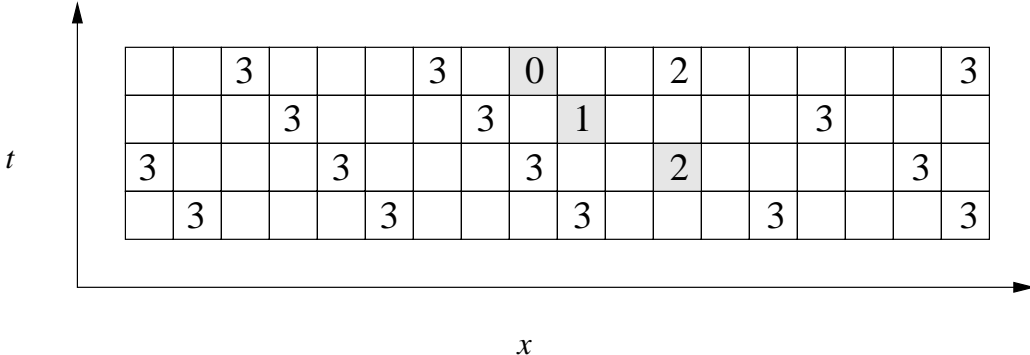


Figure 5.13: An example of how interaction can lead to a standstill.

their maximum velocity $v_{\max} = 3$, one car slows down to velocity zero due to a combination of interactions and deliberate braking as a consequence of random fluctuations. The cells where a car slowed down due to noise are shaded grey.

The kind of interaction shown in Fig. (5.13) can take place at any global density, no matter how low it is. So we should expect to find stopped vehicles at arbitrarily low densities. However, the probability of interactions decreases rapidly if the density becomes low.

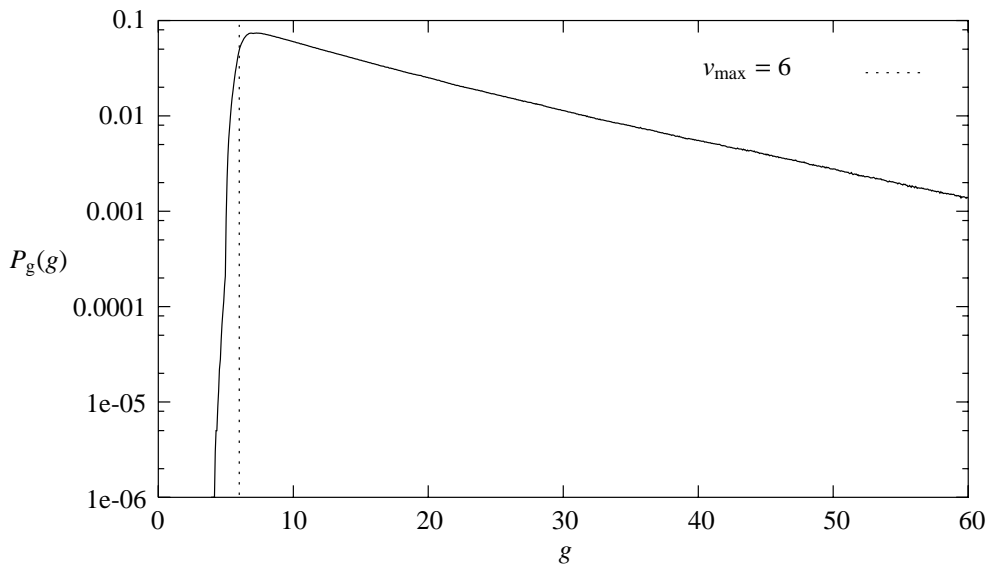


Figure 5.14: The gap distribution for almost free flow ($v_{\max} = 6$, $\rho = 0.05$, $\epsilon = a = 1$).

Assume now that the density is low enough that the motion of vehicles is almost free and interactions are rare. Fig. (5.14) shows the typical shape of the probability distribution of the gaps for that case. It can be seen that this distribution is almost strictly exponential with a cutoff at a gap g_0 which is near the maximum velocity v_{\max} . In a

situation like that only the small fraction of cars that is found near the edge g_0 can participate in interactions. So in a system with the mean gap $\langle g \rangle$ the probability P_{int} of a car to interact is to a good approximation inversely proportional to $\langle g \rangle - g_0$:

$$P_{\text{int}} \propto \frac{1}{\langle g \rangle - g_0}. \quad (5.26)$$

To estimate the number of stopped cars, the following mechanism will be assumed: A car can slow down to a velocity $v - \Delta v$ considerably lower than the mean velocity in the free flow by first interacting with a car that moves at velocity v and then being slowed down by Δv in the randomization step. So for the probability $P(v)$ to find a car at velocity v the relation

$$P(v - \Delta v) \propto P(v)P_{\text{int}} \quad (5.27)$$

holds. Using the first order Taylor series expansion of the left hand side and inserting the expression for P_{int} yields a first order differential equation for $P(v)$, which is solved to give

$$P(v) \propto e^{\left(1 - \frac{\alpha}{\langle g \rangle - g_0}\right) \frac{v}{\Delta v}}, \quad (5.28)$$

where α is some unknown parameter. The assumptions made here only hold for a small fraction of the vehicles, namely those that interact, so $P(v)$ in the form (5.28) certainly cannot be normalized. However, for velocities close to the mean free velocity the probability to find a car should become independent of g because the great majority of the noninteracting cars stay close to the mean free velocity and serve as a reservoir for the interacting cars. So instead of a normalization condition we have a boundary condition for $P(v)$ as v approaches the mean velocity in the free flow.

From this it can be concluded directly that the gap dependence of the probability $P(0)$ to find a stopped car has to be of the form

$$P(0) \propto e^{\frac{\hat{\alpha}}{\langle g \rangle - g_0}}, \quad (5.29)$$

where $\hat{\alpha}$ cannot be calculated from this simple analysis. It can be seen that the proportion of stopped cars grows rapidly and finally diverges, as the mean gap $\langle g \rangle$ approaches g_0 . Of course there is no divergence in reality, because the assumption that only few cars interact, made for the derivation of this formula, breaks down before.

Fig. (5.15) displays $P(0)$ on a logarithmic scale as a function of $1/(\langle g \rangle - g_0)$, where g_0 was measured from a gap distribution at low densities. The functional dependence of $P(0)$ estimated from the simple argumentation is reproduced remarkably well for about five orders of magnitude. For gaps close to g_0 deviations are found, as expected.

Just looking at Fig. (5.15) one may underestimate, how rapid the change of P_0 as a function of the density takes place when the “critical” density $\rho_0 = 1/(g_0 + 1)$ is approached. The simulation results displayed in the figure correspond to a change of P_0

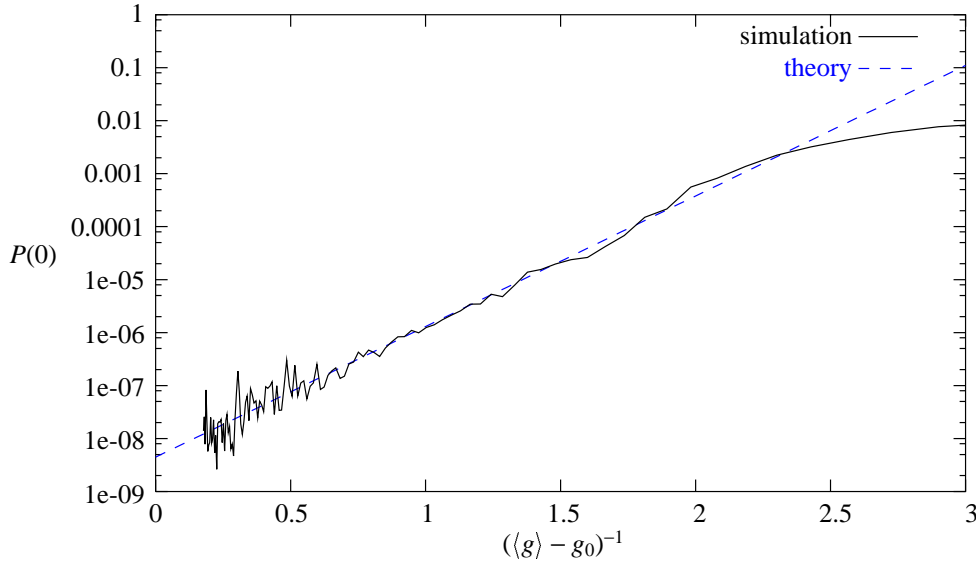


Figure 5.15: The proportion of stopped vehicles for $a = 1$, $\epsilon = 0.8$ as a function of $1/(\langle g \rangle - g_0)$.

by three orders of magnitude within a density interval of only about 0.02. This rapid change may easily be misinterpreted as indicating a phase transition. But first, as noted before, different types of investigations have shown that there is no phase transition at that point and secondly it has been shown here that the rapid change can be explained within the picture of almost free vehicle motion.

5.4.4 Evolution of jams

Intuitively a structure found in traffic would be considered a traffic jam, if two properties are found. First there have to be stopped cars in this structure. Secondly the structure has to be large in the sense that a sufficient number of vehicles are involved. If structures with these properties are found in the model, they at least look like traffic jams.

In the last section it has been shown that interaction always makes a small fraction of cars stop spontaneously. So all that remains to do is to show how these “microscopic” jams that are continuously injected into the system can evolve into macroscopic structures. This can be seen using a simple argument, following Paczuski [57].

Consider a single jam. The probability distribution $P(n, t)$ for the number n of cars involved in the jam is determined by the balance of vehicles entering and leaving the jam:

$$P(n, t + 1) = (1 - r_{\text{in}} - r_{\text{out}})P(n, t) + r_{\text{in}}P(n - 1, t) + r_{\text{out}}P(n + 1, t). \quad (5.30)$$

Here r_{in} and r_{out} are the rates, at which cars enter and leave the jam, respectively. The parameter r_{in} is mainly determined by the density upstream of the jam, while r_{out} is an intrinsic property of the jam.

If n is sufficiently large, this can be expanded to first order, yielding

$$\frac{\partial P}{\partial t} = (r_{\text{out}} - r_{\text{in}}) \frac{\partial P}{\partial n} + \frac{r_{\text{in}} + r_{\text{out}}}{2} \frac{\partial^2 P}{\partial n^2}. \quad (5.31)$$

If the global density is low enough so $r_{\text{out}} > r_{\text{in}}$, microscopic jams dissolve immediately. This is exactly the case, where the approximation made in the last section, that cars move almost freely, holds. When the density is high enough, the system will reach an equilibrium state in which the inflow into any jam is simply the outflow from some other jam upstream. In this state the first term on the right hand side of equation (5.31) vanishes and the probability distribution $P(n, t)$ is described by a diffusion process. Note that the norm of this distribution is not conserved if only $n > 0$ is considered, because jams cannot only change size, but also dissolve.

However, from the fact that the equation is invariant under the scale transformation ($n \rightarrow \alpha n, \tau \rightarrow \alpha^2 \tau$), it can be seen immediately that the average number of cars in surviving jams $\langle n \rangle(t)$ evolves like

$$\langle n \rangle \propto \sqrt{t}. \quad (5.32)$$

So if we look at an ensemble of jams, after a short while only large jams will remain. If no new jams are created, even the large jams will finally dissolve. However, if there is a mechanism to inject microscopic jams into the system, like in this model, the equilibrium state will contain large structures.

The important conclusion that has to be drawn from this simple theory is that the existence of large structures of very slow cars does not depend on the actual traffic flow dynamics, as long as there is some mechanism that injects stopped cars into the system. So the fact that these structures can be found in the model considered here does not necessarily mean that a model of real traffic jams has been found.

Still one question has to be answered. The above calculations have shown that the typical size of the jams does not grow like \sqrt{t} for large t as proposed from the random walk argument, but instead approaches a finite limit. The reason for this is that in the random walk argument the process of the branching of jams has been neglected. The branching of a jam becomes the more likely the larger the jam is. This fact limits the growth of the jams. Obviously the branching of jams and the stochastic dissolution of small jams in favor of the large ones are competing effects that reach a dynamical equilibrium for $t \rightarrow \infty$.

5.4.5 The outflow from jams

The evolution of jams is governed by the rates r_{in} and r_{out} at which vehicles enter and leave the jams respectively. The random walk that the length of a jam performs is biased, if these rates are different, it is unbiased, if they are equal. The case $r_{\text{in}} < r_{\text{out}}$, where a jam dissolves, has been noted. Still the question remains, whether the case $r_{\text{in}} > r_{\text{out}}$ is possible. This case would result in a positive bias, leading to an almost deterministic growth of jams.

The answer can be given easily by looking at the fundamental diagram of the model. Assume that the system can be described approximately by jammed regions displaying a mean flow q_j and free regions displaying a mean flow q_f . In that case the global flow in the system is given by

$$q(\rho) = \frac{(\rho - \rho_f) q_j + (\rho_j - \rho) q_f}{\rho_j - \rho_f}. \quad (5.33)$$

So the fundamental diagram $q(\rho)$ is a linear function of the density, that assumes the value q_f for $\rho = \rho_f$ and q_j for $\rho = \rho_j$. On the other hand we know that vehicles move almost freely in the free flow, so $q_f \approx \rho_f(v_{\max} - \epsilon a/2)$. Consequently the point (ρ_f, q_f) is found where the straight lines describing free and jammed flow intersect.

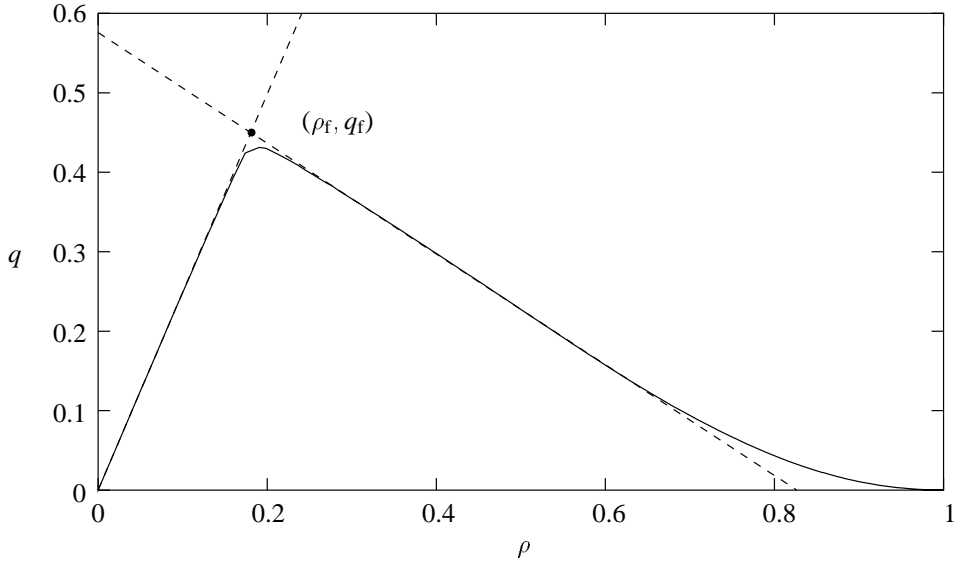


Figure 5.16: The outflow from jams is higher than the maximal globally attainable flow.

Fig. (5.16) displays this point. We see that the model does not reproduce the capacity drop of real traffic, because the outflow from jams is not lower than the maximum flow. In fact, it is even higher than the maximum flow attainable in global averages taken over long time intervals. This property may appear quite peculiar at first, but it simply expresses the fact that the outflow from jams is unstable and always breaks down to

form new jams. If a system is prepared at the global density ρ_f , it therefore contains small jams. However, these small jams have properties that are different from those of large jams. For example, they obviously have an outflow density lower than ρ_f .

The important point for the evolution of jams is the fact that a deterministic growth of jams is impossible in this model because the average inflow into a jam can never be larger than the average outflow from that jam. Consequently the only mechanism allowing the effective growth of jams is the stochastic dissolution of small jams described before.

5.4.6 Finite size effects

At this point some remarks on effects of very small system size should be made, because it is important to distinguish these effects from effects in infinite systems that look similar and will be reported later.

It has been shown that the slowing down of vehicles to a complete stop always involves a minimum number of interactions that is determined by the maximum velocity v_{\max} and the maximum deceleration due to the randomization step ϵa . Namely the minimum number of interactions is an integer near $v_{\max}/(\epsilon a)$. It is very obvious that the mechanism of bringing cars to a stop cannot work any more, if there are too few cars in the system to provide a sufficient number of interactions.

This can lead to the phenomenon that the shape of the fundamental diagram changes for very small systems. Fig (5.17) shows a sequence of fundamental diagrams for a system with $v_{\max}/(\epsilon a) = 6$ for different system sizes. The shape that the fundamental diagram exhibits looks similar to that of models that exhibit metastable states of high flow. Such models display a branched fundamental diagram and will be discussed in the next section. The effect shown here can be distinguished clearly from the effects in these models, because no second branch exists in the fundamental diagram and no discontinuity is found. This has to be kept in mind, when metastability is discussed later.

The finite size effect for a system containing N vehicles can be quantified looking at the difference $\Delta q(N)$ between the maximum flow of that system and the maximum flow for an infinite system. Fig. (5.17) displays the scaling of Δq with the system size N . A similar analysis has already been performed in [70].

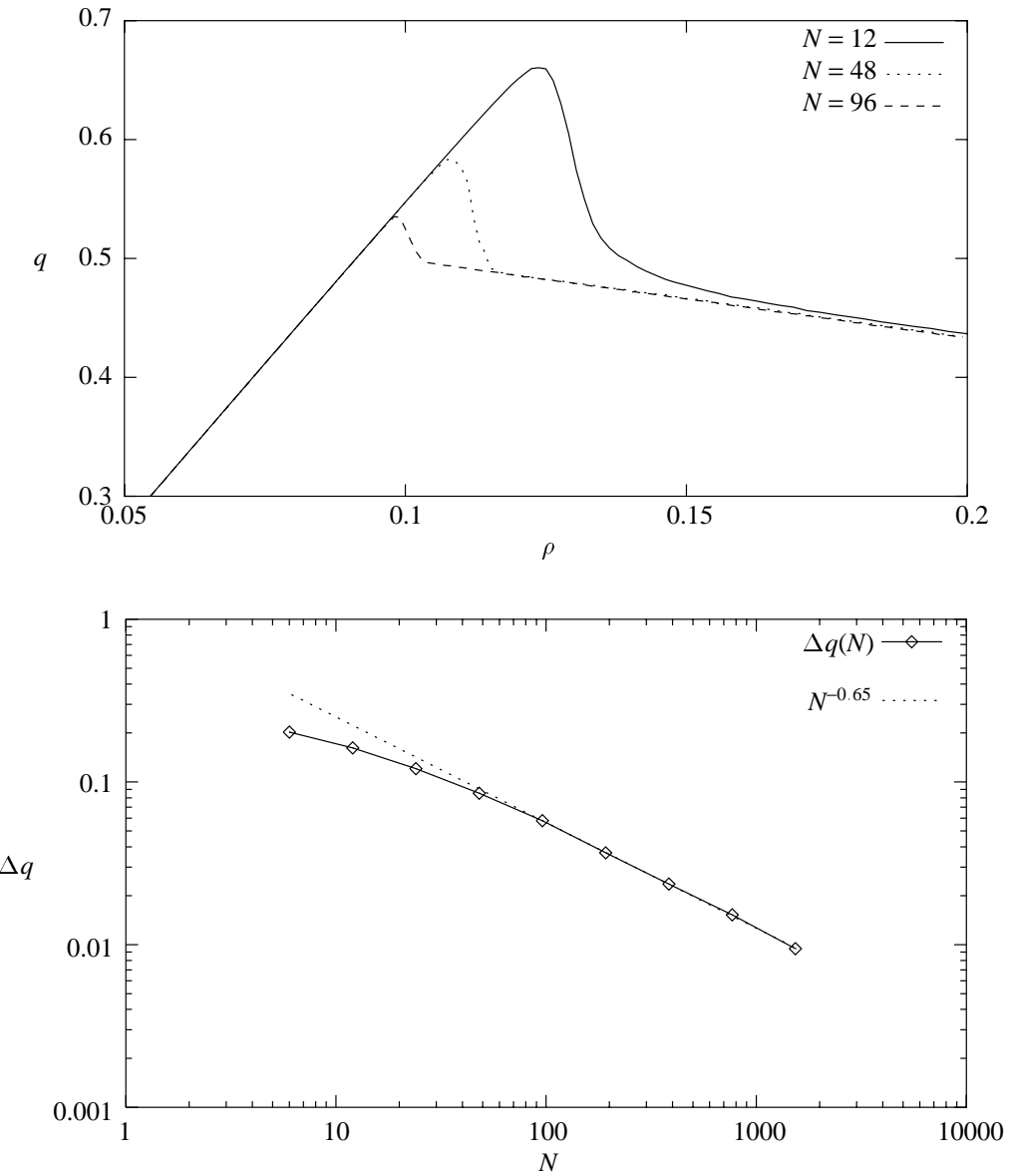


Figure 5.17: Shifting of the jamming point to higher densities in small systems containing N cars. The quantity $\Delta q(N)$ is defined as the difference between the maximum flow for a system of size N and the maximum flow for an infinite system.

5.5 Low-acceleration-low-deceleration-models

5.5.1 Phase separation

The next case that will be looked at is the case of low acceleration and low deceleration. We will now consider models for which the parameter b is small. The parameter a will be chosen to be small enough so the approximations of the high acceleration limit do not hold. Typical values of a and b considered in this section will be about of the order of magnitude as the values estimated to be realistic at the beginning of the model formulation ($a = 0.2$ and $b = 0.6$ for the following calculations). Since a is sufficiently small, it can be expected that jam formation takes place.

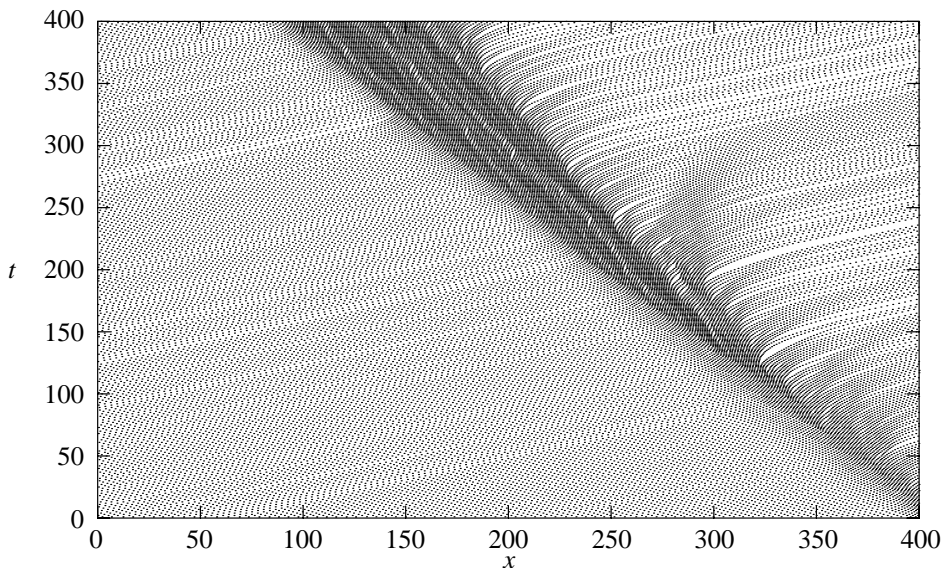


Figure 5.18: The early stage of a developing jam.

Indeed, taking a look at the space time plot in Fig. (5.18) shows that the system separates into free and jammed regions at intermediate densities. It can be seen immediately that the growth mechanism of the jam displayed here is fundamentally different from that of the models of the high deceleration limit. The jam seems to grow almost deterministically. Obviously the average inflow into the jam is larger than the outflow from it. Therefore such a jam can grow to an arbitrary size as long as the inflow is not lowered.

Fig. (5.19) displays the average length of jams for that density as a function of the system size after allowing the system to reach an equilibrium state. The average length of the jams rises linearly with the length L of the system, if L is sufficiently large. For that reason not $\langle n \rangle$ itself, but $\langle n \rangle/L$ is displayed in Fig. (5.19).

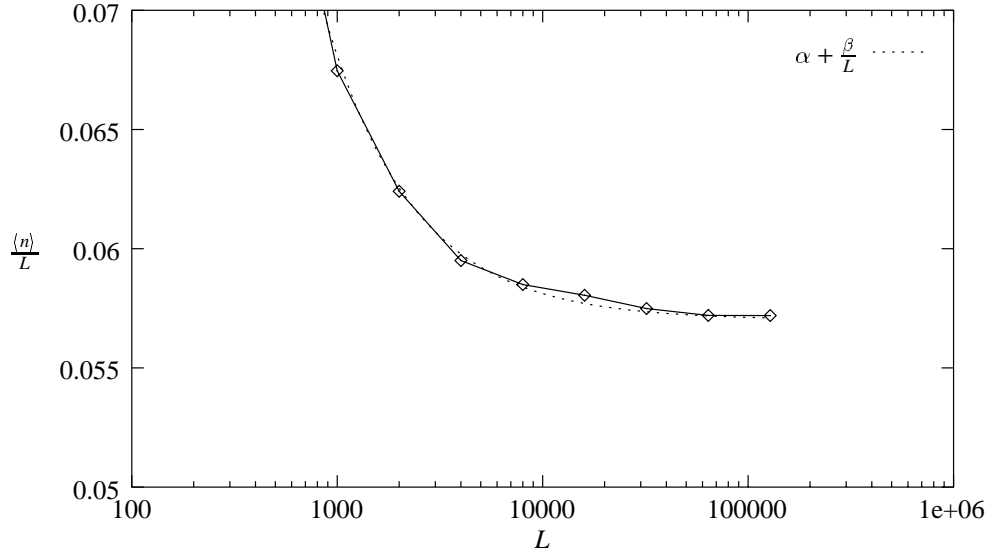


Figure 5.19: The ratio of average jam length and system size as a function of system size.

To create the figure a homogeneous state was prepared that will in the next section be identified as a metastable state. Then a single car was perturbed which created a single jam. No other jams developed, which explains the linear dependence of the jam length on the system size. Deviations from linearity for small systems originate from the transition region between jams and free flow. It can be seen easily that this leads to a behavior of the form $\langle n \rangle = \alpha + \beta/L$. A function of this form has been fitted to the data and included in the figure.

It is also possible to start the system at a density that is high enough so the homogeneous state is not metastable, but unstable. In that case a large number of jams develop simultaneously. Once these jams are in equilibrium (i.e. inflow equals outflow), the jams dissolve stochastically due to the random walk that their length performs, just like in the high deceleration limit. In contrast to that limit, however, no new jams are created, because the outflow from jams is stable, as will be shown later. So the number of jams decreases until only one jam is left. This last jam cannot dissolve any more, because its inflow and outflow are no longer independent, so the random walk picture is no longer valid. Fig. (5.20) displays the number of jams in a system that was started in a homogeneous state at a density of $\rho = 0.3$, where the homogeneous flow is unstable.

For models of this kind the jamming transition is obviously a phase transition in a rigorous sense and it is justified to denote the mechanism described here as phase separation.

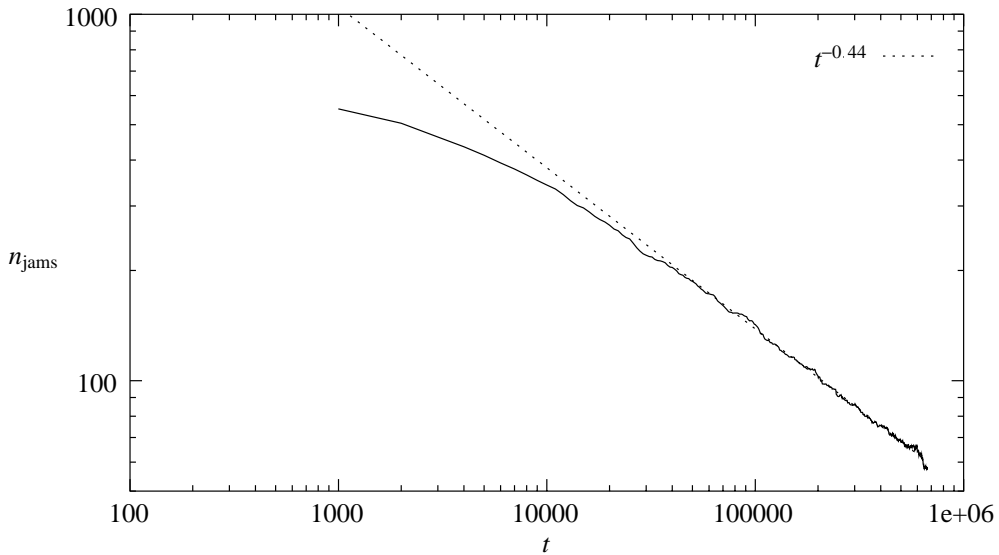


Figure 5.20: The number of jams in an initially homogeneous system as a function of time.

5.5.2 Metastability

Fig. (5.21) shows the fundamental diagram for a model of this kind in the vicinity of the point of maximum flow. The diagram has been calculated performing simulations in a system of length 10^5 , corresponding to about 750km of real road, averaging over 10^5 time steps, corresponding to roughly 28 hours of real time.

The striking property of this fundamental diagram is that it has got two branches. This means that in an intermediate range of densities the flow is no longer defined uniquely by the global density. Instead, the same global density can either lead to a homogeneous state of high flow or to a state containing macroscopic jams. The upper branch of the fundamental diagram was calculated starting the system in an initially perfectly homogeneous configuration. The lower one was calculated starting from an initially inhomogeneous configuration.

If the system were deterministic, the upper branch obviously would be metastable and the lower one stable, because in a state of the upper branch any small jam would inevitably grow. Due to the fact that the system is stochastic, however, there is also the stochastic dissolution process mentioned before that allows transitions from the lower branch to the upper branch. If the global density is close enough to ρ_f in a finite system, the rate, at which jams dissolve, finally becomes higher than the rate, at which jams are created, so in long time averages the upper branch will appear to be stable. In infinite systems this effect disappears, however, because the lifetime of the jams grows roughly quadratically with their size.

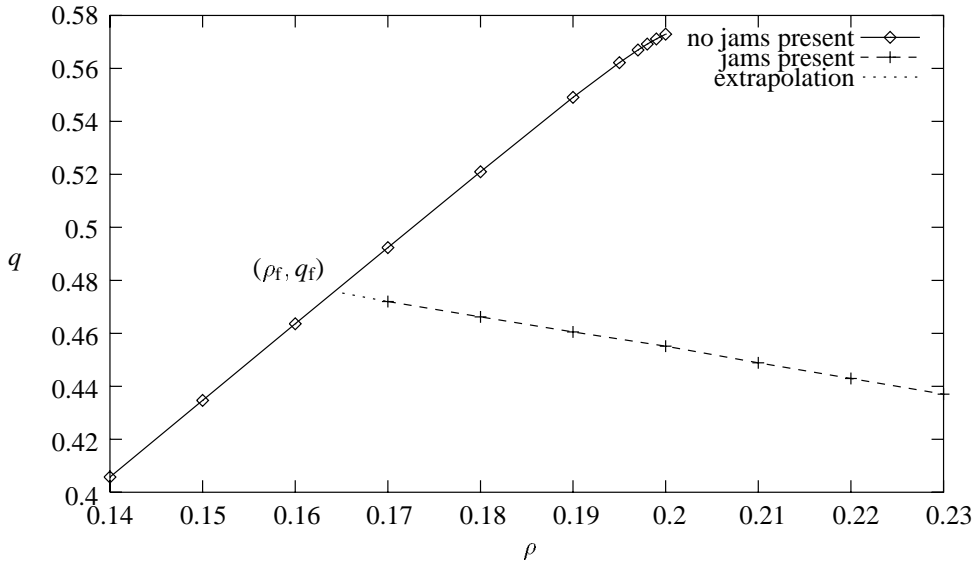


Figure 5.21: The branched fundamental diagram. The dotted line is an extrapolation of the calculated part of lower branch, intersecting the upper branch at ρ_f . Parameters $a = 0.2$, $b = 0.4$, $\epsilon = 1$.

When calculating the fundamental diagram, one can, instead of creating a new system for every density, just as well add vehicles to or remove vehicles from a system. If one keeps adding vehicles to a homogeneous state, the system remains on the upper branch of the fundamental diagram until it undergoes a transition to a jammed state, when the density leaves the range of metastable states and enters the region, where homogeneous states are unstable. After this transition the jams remain in the system, even if the vehicles just added are removed again. The jams only disappear, when the density reaches the point, where the two branches meet. In this way a hysteresis loop can be traced.

The point, where the upper and lower branch intersect, corresponds to the point where the last jam dissolves, i.e. when the global density becomes equal to the density of the free flow ρ_f , which in equilibrium is equal to the density of the outflow from the jams. We see that this density is considerably lower than the maximum density in the free flow. Obviously this finally models the capacity drop correctly. Note also that q_f is the boundary flux for the existence of jams, so the outflow from jams is stable.

5.5.3 The outflow from jams and jamming dynamics

The fact that the outflow from jams is not maximal alters the jamming dynamics considerably compared to the models of the high deceleration limit. In those models it has been shown that jamming can be described quite well by assuming that microscopic jams are injected into the system randomly, whose size n from that point on evolves

performing a random walk. The model considered now displays fundamentally different dynamics. Consider a system in a state corresponding to the metastable upper branch of the fundamental diagram. If a small jam occurs in this situation for whatever reason, the outflow from this jam is smaller than the inflow, and the jam will grow inevitably until an equilibrium situation is reached, where inflow and outflow are equal again.

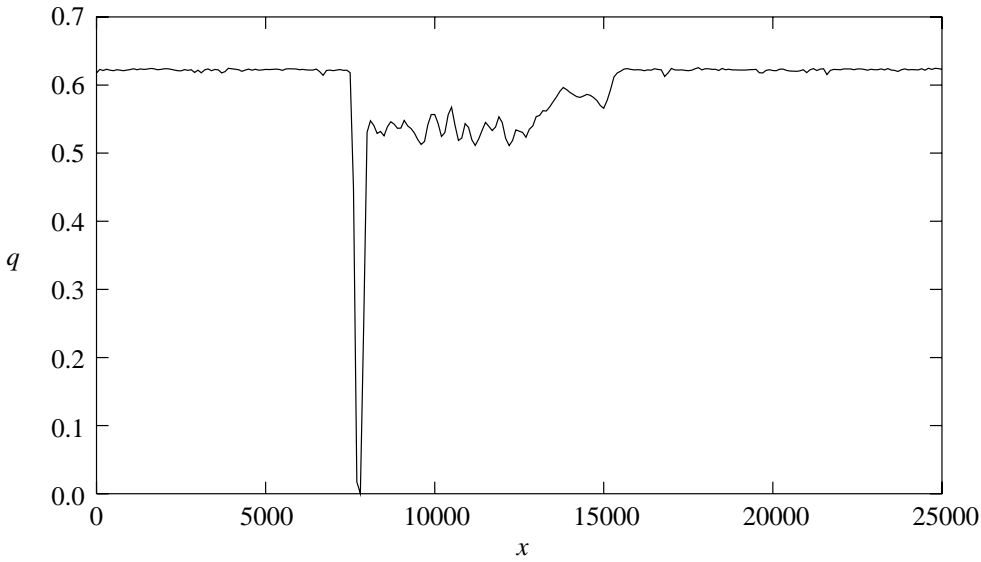


Figure 5.22: The reduced flux downstream of a jam.

Fig. (5.22) displays a situation of that kind. The flux is displayed as a function of the space coordinate x . A small developing jam can be seen. The outflow is significantly lower than the inflow, so the jam is growing. Due to the reduced density downstream of the jam, interactions between the cars are much weaker and the flow is stable as can be seen in Fig. (5.23).

It has been noted before that empirical traffic data show that there is no significant dependence of the outflow from jams on the inflow conditions in real traffic. To check, if this property is also found for the model proposed here, the following experiment is performed. A jam is prepared at the initial density 1. Then vehicles are fed into the jam at a prescribed inflow q_{in} . The position where the cars are fed into the jam is kept at a fixed distance from the upstream front of the jam. Downstream of the jam there is an open boundary. The system is allowed to equilibrate until the outflow q_{out} is stationary and the whole jam consists of vehicles that have been introduced into the jam at the prescribed inflow. Note that the state that is acquired in this way is not stationary in the sense that the length of the jam is time independent. In general, the jam will either increase or decrease due to the difference between inflow and outflow. In this setup q_{out} can only be, if at all, a function of the inflow q_{in} .

Fig. (5.24) displays the outflow as a function of the inflow. If a linear dependence be-

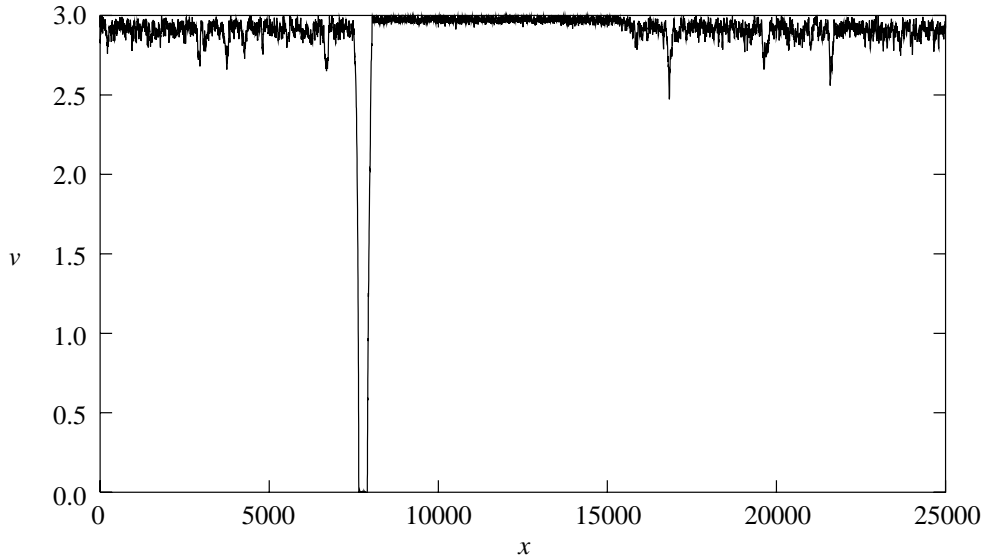


Figure 5.23: The reduced interactions downstream of a jam.

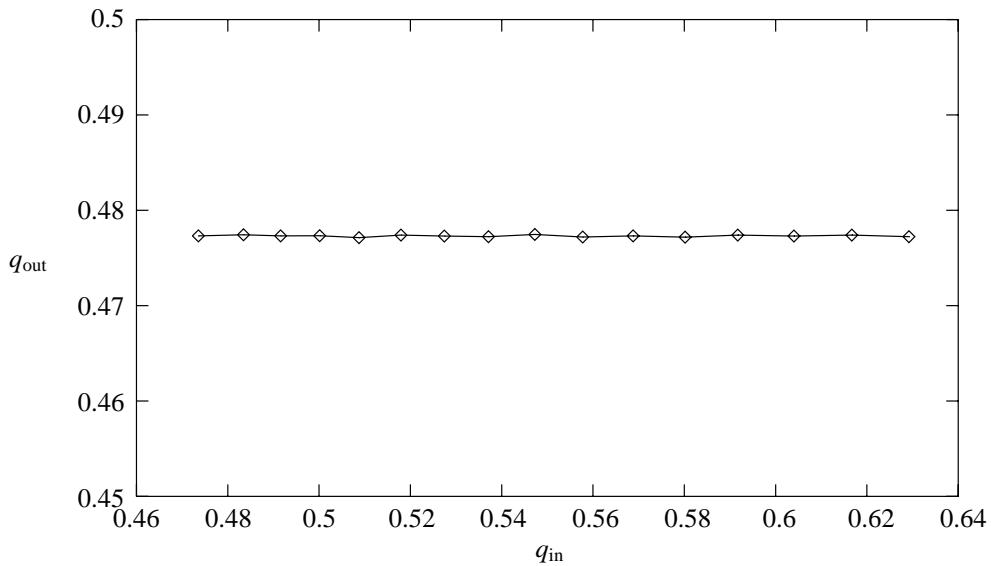


Figure 5.24: The dependence of the outflow from a jam on the inflow.

tween the quantities is assumed, the derivative dq_{out}/dq_{in} is numerically found to be $(2 \pm 5) \cdot 10^{-4}$. So there is no significant dependence between inflow and outflow in this model. At a first glance this may appear as a trivial result, but later a model will be discussed that lacks this important property.

5.6 The role of noise

5.6.1 Introduction

So far, it has been shown that there are two basic ingredients to a realistic model of jamming. Firstly, vehicles have to be able to slow down in an interaction to a velocity slower than that of the preceding car. That means there has to be some mechanism modeling overreactions. Secondly, the outflow from jams has to be lower than the maximum flow. In the model presented here it is the noise that is responsible for both of these features, which will be shown now. The considerations are restricted to the low-acceleration–low-deceleration–model, because this was the only case that displayed realistic jamming dynamics.

This section is to be understood as a preparation for section 5.7, where the phenomena found so far are interpreted in a unified, phenomenological framework.

5.6.2 The jamming point

First the mechanism of overreactions, that destabilizes dense traffic, is looked at. It has been noted before that the quantity $g - v_l$ is always nonnegative, so the maximum safe velocity is never lower than the velocity of the preceding car. The fact that drivers may “overreact” is modeled only in the randomization step, where drivers deliberately slow down to velocities lower than necessary. The probability that overreactions lead to a breakdown of traffic rises with increasing density. For a given noise parameter ϵ there is a density $\rho_c(\epsilon)$, where traffic flow typically breaks down due to overreactions. Again, this point cannot be defined rigorously, even if the breakdown is a true phase transition, it can only be stated that the lifetime of the homogeneous state changes rapidly at ρ_c . To calculate ρ_c approximately, a system is allowed to equilibrate for 10^6 time steps. After that it is checked, whether stopped vehicles are found.

It is quite obvious that ρ_c cannot become any larger than the jam density ρ_j , because jams contain stopped vehicles. Fig. (5.25) displays the quantity $\Delta\rho_c = \rho_j - \rho_c$ for the model that was considered in the last section, too. The quantity $\Delta\rho_c$ vanishes for small ϵ .

5.6.3 The outflow from jams

As noted before the second important ingredient of a model of jamming is the fact that the outflow from jams is not maximal.

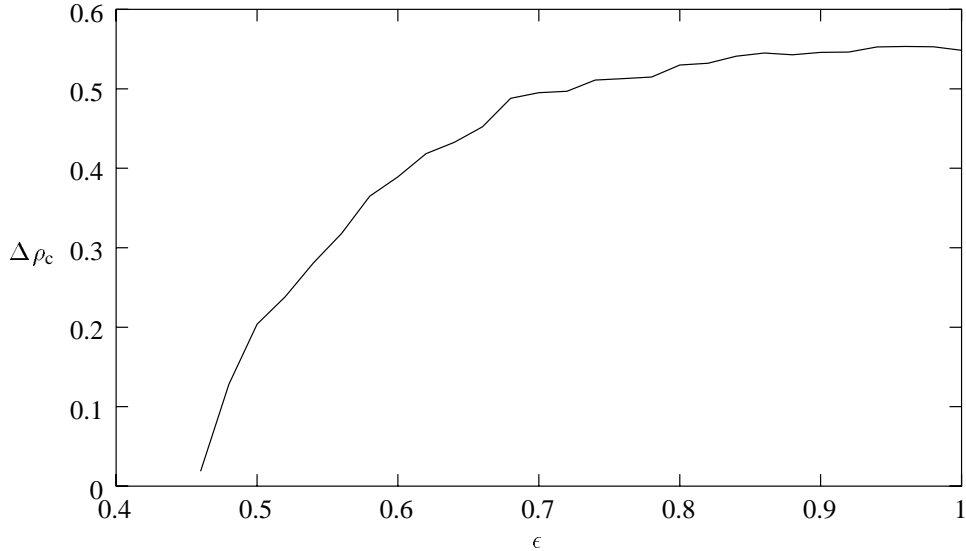


Figure 5.25: The difference between the density ρ_c , where the homogeneous flow becomes unstable, and the density of the jams ρ_j for $a = 0.2$, $b = 0.6$.

To show that the noise is also responsible for this, a single jam in equilibrium with free traffic is looked at and the flow in the free region is measured. It has been shown before that the outflow does not depend on the inflow, so this procedure determines the outflow uniquely. The outflow q_f can be compared to the maximum flow q_{\max} .

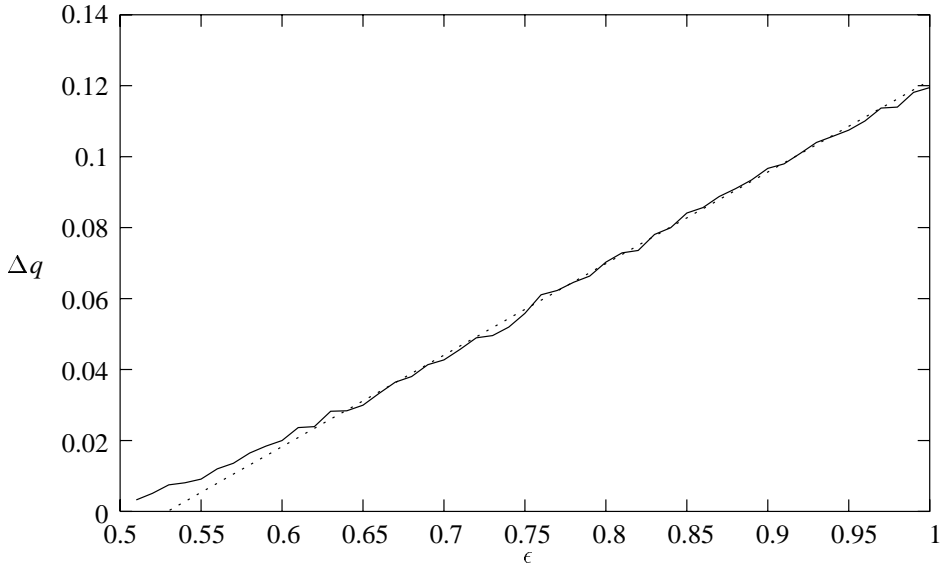


Figure 5.26: The difference between the maximum flow and the outflow from jams as a function of the noise parameter ϵ for $a = 0.2$, $b = 0.6$. The dashed line is a linear fit to the simulation result.

Fig. (5.26) displays $\Delta q = q_{\max} - q_f$ as a function of ϵ . To a good approximation a linear dependence is found. At the point, where Δq vanishes, the metastable branch of the fundamental diagram disappears and the type of jamming found in the empirical data is no longer possible.

5.6.4 The homogeneous flow

So far the effects of noise on the outflow from jams and the point where jams appear spontaneously have been discussed. Intuitively, it is quite obvious that noise also has an effect on car following, if drivers are not escaping from a jam or overreacting in dense traffic, but instead simply move in homogeneous traffic.

To describe these effects the concept of a (fictitious) perfectly homogeneous flow will be introduced, for which the equally fictitious density dependent velocity $V(\rho)$ is assumed. It is quite important to understand that this relation is indeed purely imaginary, because a perfectly homogeneous flow can never be realized in a stochastic system, especially in those regions where the homogeneous state is unstable. Switching the noise off to be able to measure $V(\rho)$, however, would change the properties of that function itself.

So $V(\rho)$ cannot be measured. Still it will be shown in the next section that it provides an extremely helpful conceptual basis for understanding all the phenomena found so far. In macroscopic models the concept of an equilibrium velocity $V(\rho)$ is a little simpler, because it represents a valid (although not necessarily stable) state there.

Although the relation $V(\rho)$ cannot really be measured, the density dependent average velocity $\langle v \rangle$ in a macroscopically homogeneous system with small fluctuations will be a good approximation to it. To get an idea of the effects of noise on this relation, we look at the mean field result of the high acceleration limit presented in eq. (5.11) as an example. Remember systems in that limit only evolved into macroscopically homogeneous states. For the deterministic case we would arrive at $\langle v \rangle = \langle g \rangle = 1/\rho - 1$. The leading effect of the fluctuations for $\langle g \rangle \gg \langle \eta \rangle$ is an increase of the time headway $\tau_h = \langle g \rangle / \langle v \rangle$ to

$$\tau_h \approx 1 + \frac{\langle \eta \rangle}{b} \quad (5.34)$$

So the drivers basically behave, as if their reaction time were greater than it actually is. Simulations show that an increase of the time headway is in fact the dominating effect of noise in the “homogeneous” flow, also if the mean field approximation does not hold.

5.7 Model classes in the Gipps–family

5.7.1 Introduction

In the preceding sections the phenomena that are found in the Gipps–family have been described. It has been shown that, depending on how the free parameters are chosen, the model either displays phase separation in a rigorous sense or formation of only finite structures or no structure formation at all.

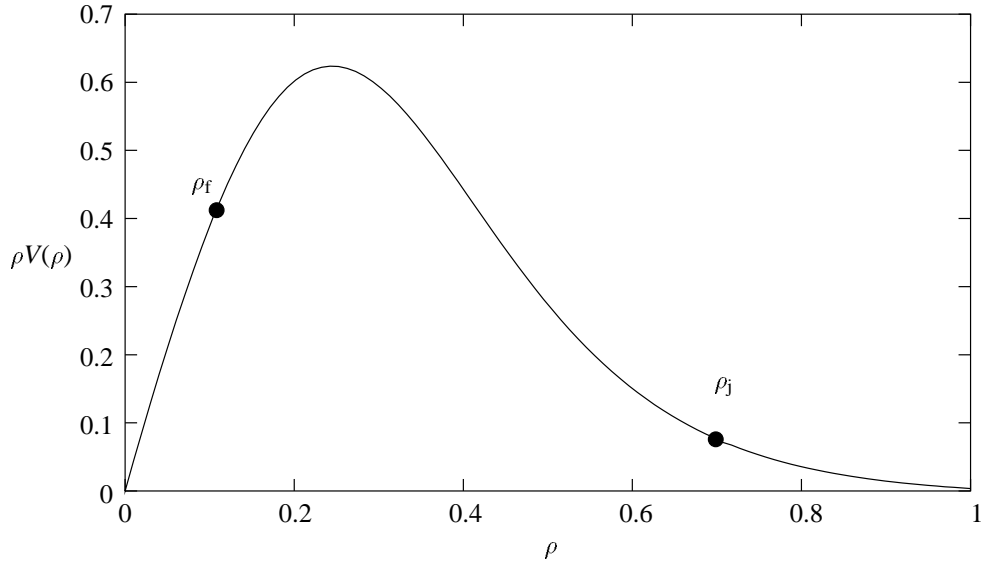


Figure 5.27: Schematic sketch of the characteristic quantities of a model.

Now the phenomena found so far are interpreted in a common framework. In this way an overview over the model family can be given. We start from the idea that the properties of each model are determined by the density dependence of the average velocity $V(\rho)$ in a fictitious homogeneous flow, as well as the densities ρ_j and ρ_f of jams and free regions, respectively, and the density ρ_c , where a homogeneous flow becomes unstable and displays a significant number of stopped cars. A similar approach has been presented in the analysis of macroscopic models [37].

Fig. (5.27) displays the characteristic quantities except ρ_c . Obviously the system can decompose into macroscopic regions of free flow and jammed flow only, if the density is in the interval $\rho_f < \rho < \rho_j$.

Whether or not it actually does decompose, depends on the position of the point ρ_c , where homogeneous traffic becomes unstable. Quite obviously ρ_c cannot become any larger than ρ_j . If these densities become equal, jams cannot be formed any longer. The two cases that have to be considered now are $\rho_c > \rho_f$ and $\rho_c < \rho_f$.

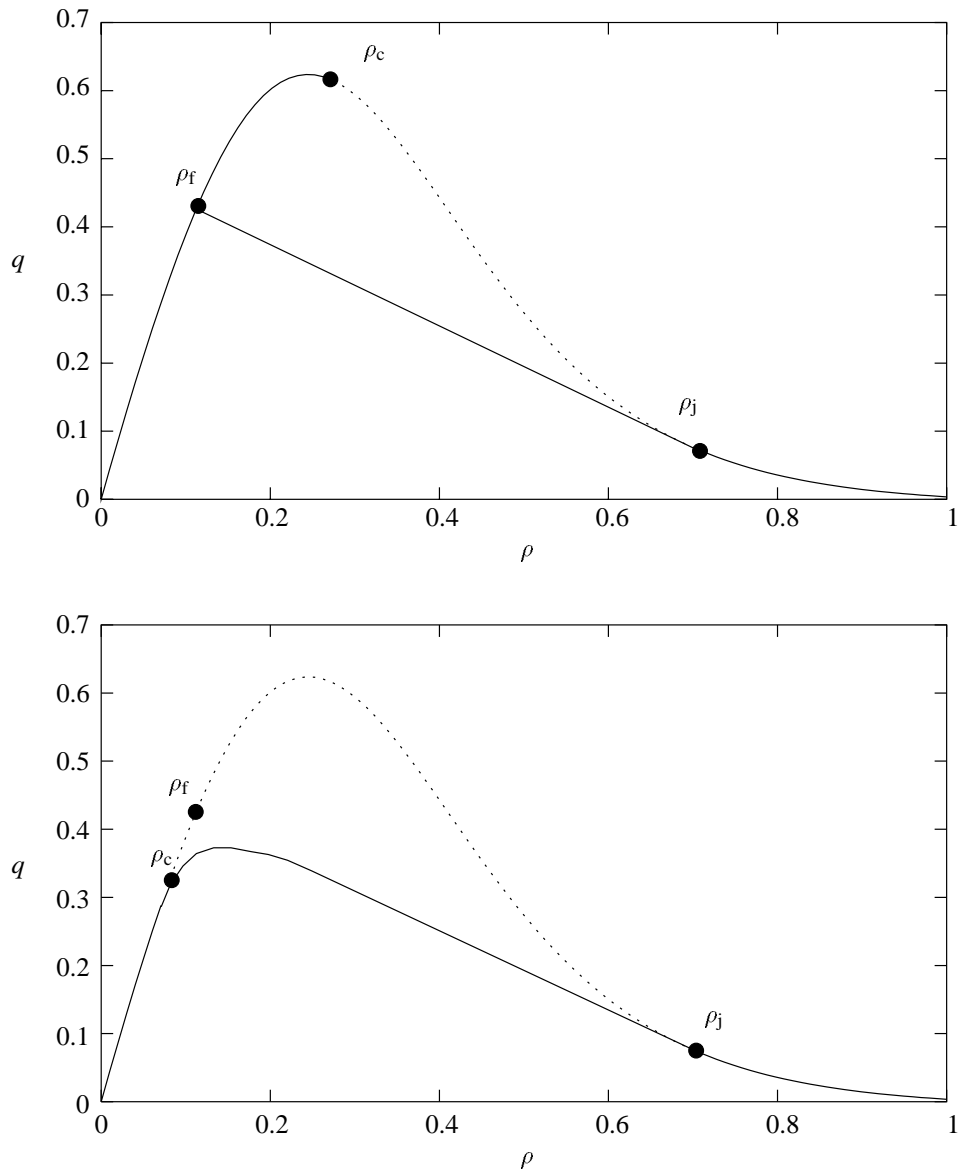


Figure 5.28: Schematic representation of the two basic types of behavior that are found. The dashed line corresponds to unstable homogeneous states.

If $\rho_c > \rho_f$, the outflow from jams is stable and the system decomposes into macroscopic regions of free and jammed flow. In this case the capacity drop and correspondingly metastable states are found. This is exactly the type of behavior found for the low–acceleration–low–deceleration models. Models of this kind will be denoted as models of type *I*. If, on the other hand $\rho_c < \rho_f$, the outflow from jams is unstable, so no large regions of free traffic can develop, in the presence of jams. The whole upper part of the fundamental diagram is missing in that case. This is exactly the type of behavior found for the high deceleration limit, which will be denoted as a model of type *II* from now on. Fig. (5.28) displays the two different types of fundamental diagrams that are obtained, if averages over the complete system are taken.

It has been noted before that the complexity in these models is mediated by the fluctuations introduced in the randomization step. If these fluctuations are made smaller the models degenerate. However, they do so in different ways depending on whether a model of type *I* or of type *II* is considered. For a model of type *I* ρ_c approaches ρ_j , whereas it approaches ρ_f for a model of type *II*. In both cases no more structure formation is possible. Models that do not display any structure formation (but are not necessarily deterministic) will be denoted as models of type *III*.

Now two things remain to be done. First it has to be found out, which models of the Gipps–family display structure formation and which models do not. Secondly it has to be checked, for which models $\rho_c < \rho_f$ and for which models $\rho_c > \rho_f$ holds.

5.7.2 The existence of jams

The analysis starts with the investigation of structure formation. To characterize, whether or not a flow is structured, a suitable order parameter has to be defined that indicates the existence of jams. In analogy to thermodynamics of critical points for fluids it seems reasonable, to use the difference of the densities in the jam and the free flow as an order parameter:

$$\Delta\rho = \rho_j - \rho_f \quad (5.35)$$

The main difficulty is the definition of these densities. We saw that even in cases where structures are found in traffic flow (like the high deceleration limit), there is not necessarily a unique way of defining what a jam actually is, because in general no real phase transition between free and jammed states takes place. This may be less problematic practically, if $\Delta\rho$ is large and the statistical properties of jammed and free cars can be distinguished clearly.

If, however, $\Delta\rho$ becomes small, the overlap of statistical distributions of jammed and free traffic becomes large. So from just looking at a single car it cannot be defined clearly, whether or not it is part of a jam.

It has been shown that the typical size of the structures that are found is much greater than one, so it will be tolerable to exclude very small structures from the definition of a jam. The criterion used here to decide whether or not a car is found in a jam, will be the vehicle's velocity. So a threshold velocity v_{thresh} is defined and a car is considered to be jammed, if more than half of the n nearest neighbors (including the car itself) have got a velocity below v_{thresh} . The threshold velocity has to be chosen in such a way that it is much higher than the average velocity in a jam and much lower than the average velocity in the free flow. For this reason it is taken to be $v_{\max}/2$. The density is chosen in such a way that half of the cars are attributed to jams. In this way it is ensured that the statistical weight of vehicles in jams and free vehicles is equal. The density of the jams and the free flow finally is determined by averaging over the gap in front of jammed and free vehicles, respectively.

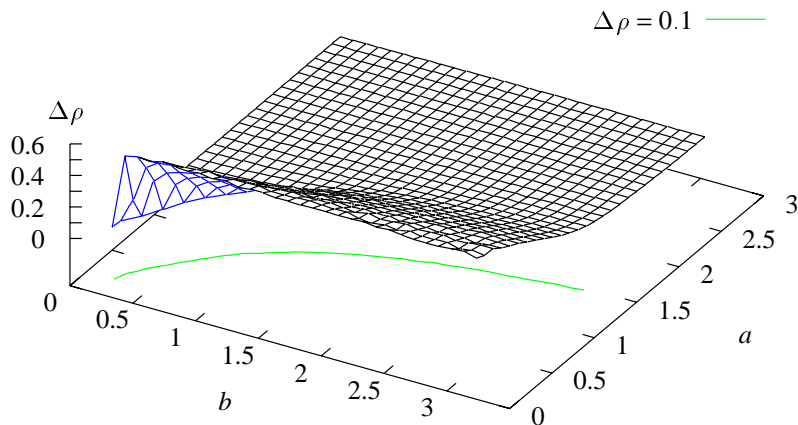


Figure 5.29: The density difference between jammed and free flow. System length $L = 2000$, $\epsilon = 1$, relaxation and measurement over 10^4 time steps, jams were identified considering $n=5$ nearest neighbors.

As it is not known a priori, what densities are found in jams and free flow, the condition that an equal number of vehicles be in jams and free flow leads to an iterative scheme for the calculation of the densities. Fig. (5.29) displays the quantity $\Delta\rho$ as a function of the parameters a and b . The contour line in the a - b -plane corresponds to the line where $\Delta\rho = 0.1$. In this case the noise parameter ϵ was held fixed, so the absolute amount of noise introduced into the system is proportional to a .

The quantity $\Delta\rho$ does not vanish exactly. This is a consequence of the fact that there is a correlation between the momentary velocity of the cars in the immediate vicinity of a vehicle and the gap in front of that vehicle, even in unstructured flow. So the criterion used here will have the tendency to attribute smaller gaps to jammed flow, even if there is no structure formation. This effect can be made arbitrarily small by letting the number n of nearest neighbors that are considered go to infinity. However, the larger n is, the more small jams are not captured. For this reason a tradeoff has to be made. For

the calculations presented here $n = 5$ has been chosen.

The calculations have shown that two different kinds of models can be distinguished clearly. The models with the ratio of a to b being large enough only exhibit macroscopically homogeneous flow as described for the high acceleration limit. If this ratio becomes small enough, spontaneous structure formation is found. Remember, however, that this does not necessarily mean that a true phase transition is found. It is worthwhile noting that it has been found for the discrete Nagel–Schreckenberg–model that for the case $v_{\max} = a = 1$ no structure formation is possible, whereas the classical choice $v_{\max} = 5, a = 1$ leads to spontaneous formation of jams. This result is in accordance with the results presented here.

5.7.3 Stability of the outflow from jams

It has been shown that the character of the jamming mechanism and the question, whether jamming corresponds to a phase transition, depends on the question, whether or not the outflow from large jams is stable, i.e. whether or not $\rho_f < \rho_c$. This property is checked easily for the model family by preparing systems at a global density equal to that of the free flow (i.e. the outflow from jams) and counting the number of stopped vehicles in that state.

We know that for the high deceleration limit there is a nonvanishing probability to find such cars in this kind of system. The proportion of stopped vehicles again will be denoted by P_0 .

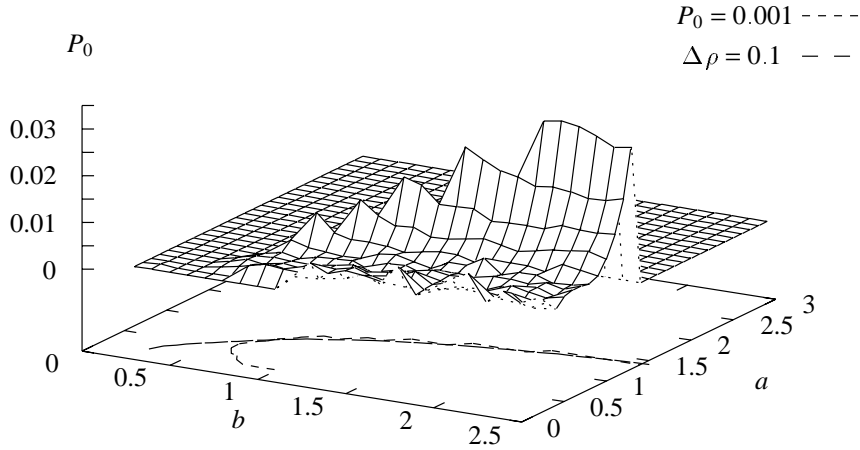


Figure 5.30: The proportion of stopped vehicles in the “free” flow

Fig. (5.30) displays P_0 as a function of a and b . Calculations have only been performed in the region, where structure formation has been found, because elsewhere ρ_f is not

well defined. To check structure formation, the criterion $\Delta\rho \geq 0.1$ has been used. The contour line $\Delta\rho = 0.1$ can be found in the diagram. It can be seen that P_0 is nonvanishing everywhere except in a small region where a and b are small. In this region the outflow from jams is stable.

5.7.4 Model classes

The results of the last sections can be summarized rather concisely by drawing a diagram that distinguishes the different types of models. The boundaries in this diagram are the contour lines, where the order parameters P_0 and $\Delta\rho$ acquire some small threshold value ($P_0 = 0.001$, $\Delta\rho = 0.1$). Fig. (5.31) shows such a diagram that was created combining the calculations presented above.

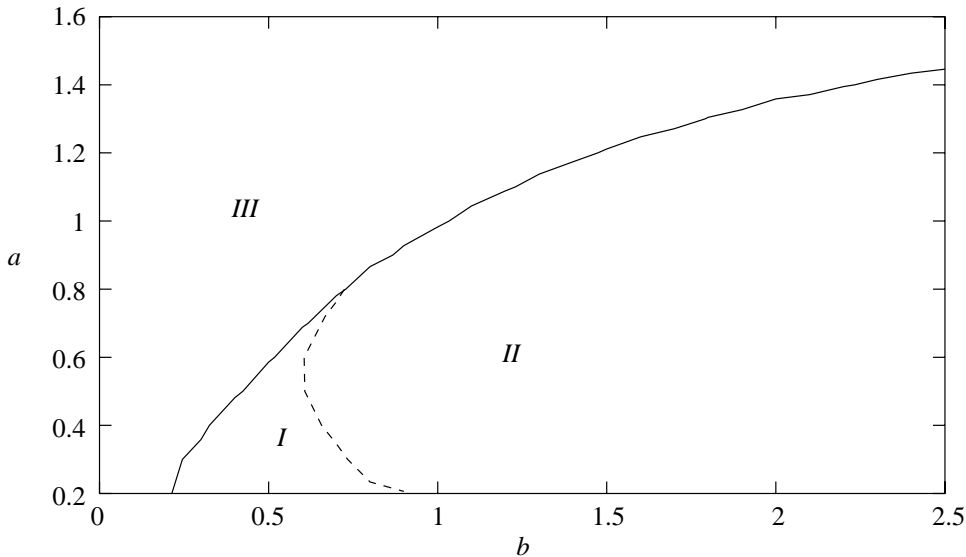


Figure 5.31: Model classes in the Gipps–family.

The diagram distinguishes three different types of models.

Models of class *III* (where the high acceleration limit is found) never display any structure formation. The equilibrium state of these models is always macroscopically homogeneous. Obviously real traffic cannot be described using models of this kind, because the important phenomenon of jamming cannot be described.

Models of class *II* (where the high deceleration/low acceleration limit is found) display spontaneous formation of structures. However, these structures do not grow arbitrarily and the jamming transition is no phase transition. The outflow from jams is unstable for these models.

This is different in models of class *I*. These models display jams with a stable outflow, and macroscopic phase separation is found. Models of this kind also show the important phenomenon of metastability. This means that the equilibrium state of the system is not determined uniquely by the global density in the system. Instead the same density can either lead to a partly congested state, where all vehicles are affected by interactions but remain in a macroscopically homogeneous state or to a state displaying jamming phenomena.

Thinking of the empirical properties described at the beginning of this work, it is rather clear that only models of class *I* describe traffic in a qualitatively correct way. Note that the set of parameters a and b that have been estimated at the very beginning of the analysis would indeed correspond to a model of class *I*.

5.8 Concluding remarks

It has been shown that a small part of the model family discussed in this chapter is able to model the qualitative properties of traffic jams quite well. This part corresponds to model parameters where accelerations and decelerations are bounded by values that represent realistic vehicle dynamics.

It has been shown that the model properties are not very robust. If accelerations or decelerations are allowed to become arbitrarily large, which of course is unrealistic on the level of vehicle dynamics, the macroscopic behavior of the model becomes unrealistic as well.

Furthermore it has been shown that the whole structure of the model behavior is mediated by the fluctuations introduced by the randomization step. Since the fluctuations are characterized only by a single parameter, it is quite difficult to isolate the different effects that the fluctuations have. Nevertheless, the effects can be interpreted in a phenomenological framework quite nicely, if the following effects are attributed to the fluctuations: The randomization step is responsible for

- the shape of the flow–density–relation in a (fictitious) homogeneous flow,
- disturbances of the homogeneous flow,
- overreactions of drivers, leading to instabilities,
- the density of jams and the outflow from jams,
- the stochastic dissolution of jams.

If the randomization is omitted or the noise parameter ϵ is made sufficiently small, the rich structure of the model dynamics degenerates and no significant property of traffic flow can be described any more. The way the model degenerates is different for the different model classes. For a model of class *I* ρ_c approaches ρ_j , for a model of class *II* it approaches ρ_f . Correspondingly, q_f approaches q_{\max} from below for models of class *I* and from above for models of class *II*.

One may feel uncomfortable with the fact that the whole structure of the model properties depends on artificial fluctuations that cannot be justified from real car following behavior (see car following experiment in Appendix (B)). The fluctuations also mask the fact that for the high-deceleration-limit no realistic jamming dynamics and no phase transition are found, because they produce some kind of structure formation by brute force. For this reason it will be tried to model certain parts of the effects of noise explicitly in order to obtain a deterministic model of jamming.

Before that, however, some remarks will be made on a cellular automaton version of the model proposed here.

Chapter 6

Discrete space coordinates

6.1 Spatial discretization of the model

Up to this point only models with continuous space coordinates have been considered. However, the Nagel–Schreckenberg– model, which is the best–known traffic flow model discrete in time and space, has been referred to, frequently. The discreteness of the space coordinate can bear significant computational advantages, because operations on integer numbers can in general be performed much more efficiently than floating point operations. The actual speedup in computational performance that can be acquired by discretizing the system, however, strongly depends on the architecture of the processor used.

Before a discretized version of our model can be used with confidence, the effects of discretization will have to be investigated thoroughly. This will now be done by proposing a series of models with discrete space coordinates that bears the continuous formulation as a limiting case. Up to now the space l that a car occupies in a dense jam has been used as the unit length, now it is assumed that there is some other unit length and l is an integer multiple of this unit length. The unit of time will remain unchanged. Each model will be characterized by the parameters l , v_{\max} , a , and b and a parameter describing the randomization step, as before.

The parameters l and v_{\max} , just like the space coordinate x and the velocity v , will be assumed to be integer numbers. The maximum deceleration due to the randomization step is now called Δv_r instead of ϵa and is an integer number between 0 and a .

The update rules of the model will be given by

$$\begin{aligned} v_{\text{des}} &\leftarrow \min[v_{\max}, v + a, v_{\text{safe}}] , \\ v &\leftarrow \max[0, \text{rand}[v_{\text{des}} - \Delta v_r, v_{\text{des}}]] , \\ x &\leftarrow x + v . \end{aligned} \tag{6.1}$$

Here only the case $\Delta v_r = a$ will be considered, corresponding to $\epsilon = 1$ in the continuous model. The safe velocity v_{safe} can now, instead of being calculated, be looked up in a table of moderate size. The safe velocity in the Gipps family was given by an expression of the form

$$\begin{aligned} v_{\text{safe}} &= v_l + \Delta v(g - v_l, v_l + v_s) , \\ \text{where} & \\ \Delta v(x, y) &= \frac{x}{\frac{y}{2b} + 1} . \end{aligned} \tag{6.2}$$

So a two-dimensional lookup table can be used. The largest distance, for which any interaction can take place is $g_{\text{range}} = v_{\max}(v_{\max}/(2b) + 1)$. So the size of the lookup table will have to be $g_{\text{range}} \times 2v_{\max}$. The entries of the table are calculated taking the nearest integer to the value for Δv that would be obtained for the continuous model. Due to the fact that Δv can be larger in the discrete than in the continuous case due to rounding, the safety condition $v_s < g$ can be violated and has to be checked explicitly.

It is obvious that the continuous case is recovered by letting v_{\max} , a , b , and l go to infinity with the ratios between l and the other parameters held fixed. If we set $l = a = 1$ and let $b \rightarrow \infty$, the Nagel–Schreckenberg–model is recovered.

The coarsest possible discretization is prescribed by the smallest length scale in the system. It has been shown that this is, at least for the models of interest, given by the maximum acceleration a (remember the time step was set to unity). So the coarsest discrete model corresponding to a continuous model with the parameters $a = 0.2$, $b = 0.8$, $v_{\max} = 6$, and $l = 1$ would have the parameters $a = 1$, $b = 4$, $v_{\max} = 30$, and $l = 5$. Different resolutions are obtained taking integer multiples of these parameters.

6.2 The effects of discretization

First the coarsest discretization $a = 1$ will be considered and be compared to the corresponding continuous model. Fig (6.1) shows the fundamental diagram of the continuous model described by the parameters $v_{\max} = 3$, $a_{\max} = 1/3$, and $b_{\max} = 1$. In addition, the fundamental diagram of the coarsest discrete model corresponding to this ($v_{\max} = 9$, $a_{\max} = 1$, $b_{\max} = 3$, $l = 3$) is displayed.

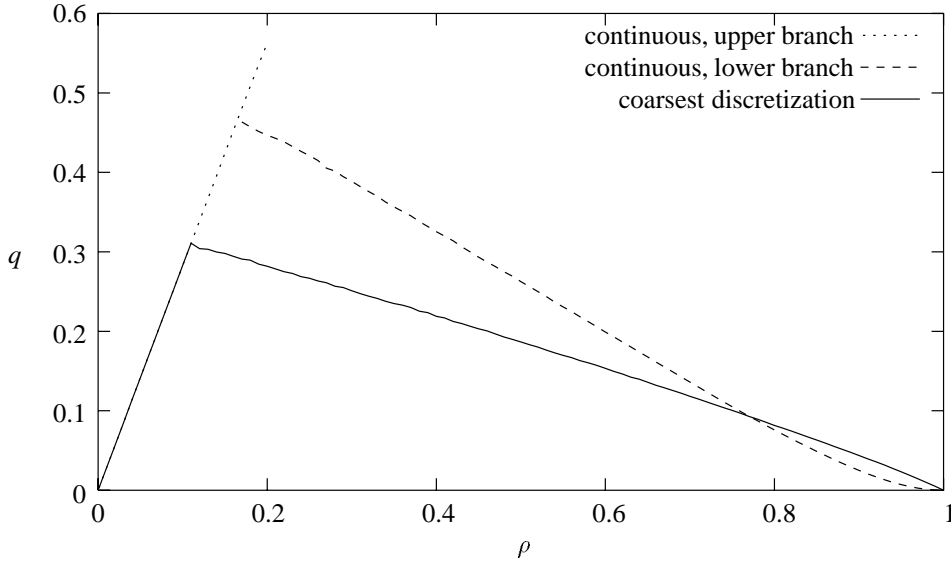


Figure 6.1: Comparison of the continuous model and the corresponding coarsest discretization.

Three significant differences between the models are found. First, no metastability is found for the discrete model, although the fundamental diagram for the continuous model is branched. Secondly, the behavior for high densities is different. For density $\rho \rightarrow 1$ the slope of the fundamental diagram vanishes in the continuous case, whereas it remains nonvanishing in the discrete model. Thirdly, the capacity in the discrete case is significantly lower than even the outflow from jams in the continuous model.

The latter can be understood considering the free flow statistics of both models. In [44] it has been pointed out that the outflow from jams is determined by the variance of the acceleration of a freely accelerating car. In the discrete case the variance is higher than in the continuous case, because in the discrete model the cars are slowed down by either zero or one in the randomization step, while the whole range between zero and one is covered uniformly in the continuous case. If the acceleration variance is adjusted to be equal in both cases, the outflows from jams become almost equal again in both models.

The next point of interest is the limit of high density. It has been shown before that in the continuous case the mean velocity becomes a quadratic function of the mean gap at very high densities. The same kind of argument used for the continuous model can now be used for the discrete model, as well. At very high densities the cars with gap g in front of them will have a velocity equal to g before the randomization step. If the density is high enough, only gaps of size zero and one will remain, so half of the cars having a nonvanishing gap in front of them will be slowed down and come to a stop in the randomization step, while the rest keeps velocity g . So the mean velocity of cars with gap g in front of them is $g/2$ after the randomization. Averaging over all vehicles

we arrive at the asymptotic behavior of the flow:

$$q_{\text{discr}} = \frac{1 - \rho}{2}. \quad (6.3)$$

For the continuous case it has been shown before that

$$q_{\text{cont}} = \frac{(1 - \rho)^2}{\rho}. \quad (6.4)$$

In the limit of high density the discrete and the continuous model are found in completely different states. In the discrete case the jams are dense except for ‘holes’ of size one that are passed from each vehicle to its successor. This leads to an efficient use of the holes, whereas in the continuous case holes of varying size are found, which are in the presence of noise used less efficiently. Since true roads are not discretized, the efficient use of the holes in the discrete case is rather unrealistic. Traffic flow data as well indicate that the slope of the fundamental diagram becomes smaller for high densities [43].

The high density behavior may not appear to be very important for the macroscopic properties of the model at a first glance. However, it obviously determines the behavior of cars in jams and therefore is of importance for the way cars escape from jams.

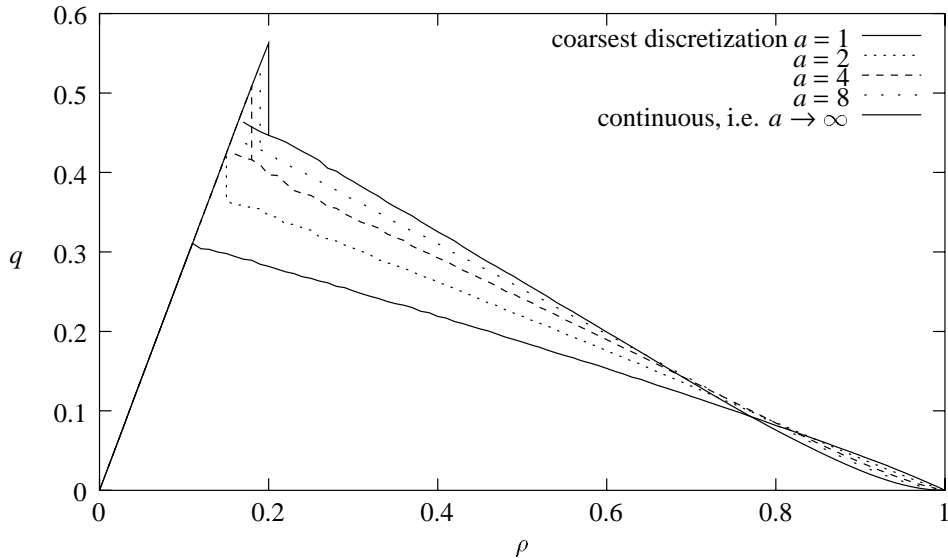


Figure 6.2: Sequence of discrete models converging towards the continuous limit.

Finally, to show that the discrete models proposed here actually bear the continuous model as a limiting case, Fig. (6.2) displays the fundamental diagrams of a series of models of increasing resolution, converging towards the continuous limit. It can be seen that the second branch in the fundamental diagram appears immediately as the resolution is doubled. So obviously the coarsest discretization is qualitatively different from all the other resolutions and the continuous case.

It has to be stressed again that the actual computational efficiency of the discrete model strongly depends on the architecture of the computer used and the minimum size of the lookup table prescribed by a . Remember that the size of the lookup table was approximately $g_{\text{range}} \times 2v_{\max}$, where g_{range} is quadratic in v_{\max} . So doubling the resolution of the automaton will lead to eight times as many entries in the table. The calculations presented here have been performed on a Sun Ultra Sparc Processor. On that processor the fully continuous model was running about ten percent slower than the coarsest discrete model, however significantly faster than the discrete model acquired after doubling the resolution.

Summing things up it can be said that it has been shown that discretizing the system may change the macroscopic properties of the model significantly. The coarsest discretization is fundamentally different from all other discretizations and the continuous limit. The reason for this is found in the way noise is introduced into the system. In the case that the maximum acceleration is set to one, the holes in dense traffic are used in the possibly most efficient way. This is the only case where no branched fundamental diagrams are found. The analysis presented in this chapter once more underlines the prominent role that noise plays in the models proposed so far. The model properties depend on the way noise is introduced in a most sensitive way.

Therefore, now a deterministic model will be proposed that allows the description of jamming and metastability without the introduction of a randomization step. In the framework of this model it will also be possible to understand qualitatively, why the coarsest cellular automaton models and the corresponding continuous models show different types of behavior and what role the car-following behavior at high densities plays for jamming dynamics.

Chapter 7

Deterministic jamming

7.1 Introduction

In the last chapters a family of stochastic models of traffic flow has been proposed. It has been shown that some models of that family display phenomena that look similar to jamming in real traffic flow. However, all models had in common that model performance depended crucially on the introduction of an unrealistically high noise term. This is a somewhat undesirable feature, because the noise cannot be attributed to anything in real traffic flow. It would be very desirable to find a model which has got the intrinsic ability to display jams and metastability independent of the noise introduced. In such a model noise would be responsible for the generation of microscopic “jam nuclei” that would then evolve into macroscopic jams independent of the noise, driven solely by the inner dynamics of the model.

The very obvious fact that a microscopic jam always evolves into a macroscopic one, if its outflow is smaller than its inflow, has been discussed before. If jams in a model display the property of a reduced outflow, the model should therefore show spontaneous jamming as well as metastability. This fact is independent of the question, whether or not any stochasticity is introduced into the system.

Now a deterministic model will be discussed that shows most of the phenomena known from the stochastic models of class *I* as defined in section 5.7.4 without the introduction of noise. The basic idea of the model formulation will be the following. Instead of describing the effects of imperfections in the way drivers react using a noise term, some of the effects of noise in the stochastic model will be captured introducing an “effective desired gap” \hat{g}_{des} , which is different from the optimal desired gap $v_l \Delta t$ used so far. In this way it will be possible to explain the phenomenon of jamming in a purely deterministic way.

7.2 The effective desired gap

When the model family discussed in this work was formulated, a velocity dependent “desired gap” g_{des} was introduced, which was in the Gipps family chosen to be $v_l \tau$, where v_l is the velocity of the leading car and τ is the reaction time. In the deterministic case the minimum time headway between successive vehicles in homogeneous traffic would be equal to τ , in stochastic models it is significantly larger.

It is not very far fetched to try to describe the effects of noise by introducing an effective desired gap \hat{g}_{d} . This quantity can be measured by averaging over the gaps that are found between pairs of vehicles for which $v_f(t + \Delta t) \approx v_l(t)$.

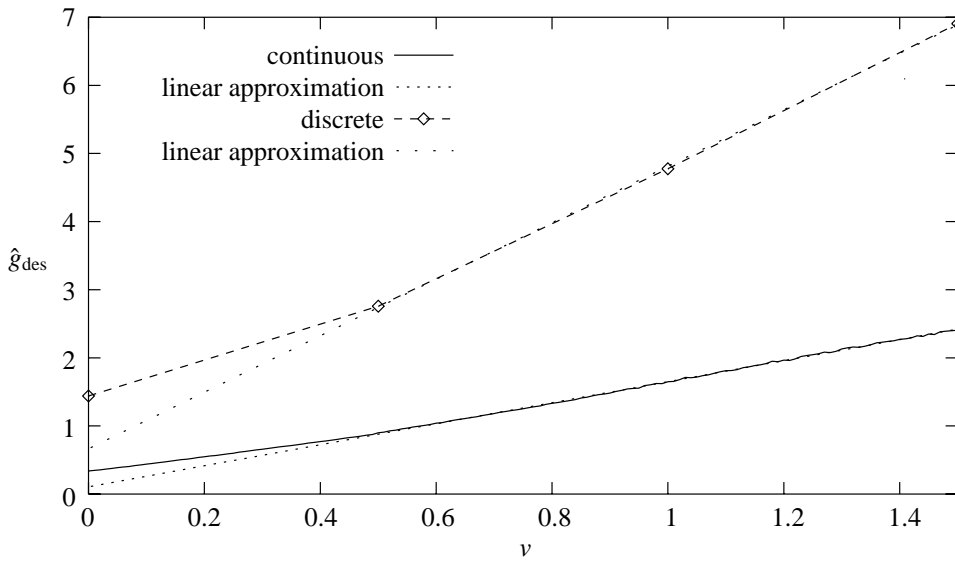


Figure 7.1: The effective desired gap for a continuous model and its coarsest discretization.

Fig. (7.1) displays the effective desired gap measured in this way, once for a continuous model with $a = 0.5$ and $b = 1$ and once for the corresponding coarsest discretization. The condition $v_f(t + \Delta t) \approx v_l(t)$ was checked before the randomization step for the following car. For the discrete model the velocities have been rescaled to the corresponding velocities of the continuous model to make it easier to compare the functions displayed.

The slopes of the curves (corresponding to the time headways) that are found for high velocities are different in the two cases due to the differences of the velocity variance as reported above. The functions are almost strictly linear for all but very low velocities. For velocities lower than a , however, the functions deviate from the linear velocity dependence substantially. Due to the fact that a prescribes the smallest length scale in the discrete model, this deviation is only significant for $v = 0$ in the discrete case.

This difference between the continuous model and its coarsest discretization is responsible for the fact that no metastable states can appear in the discrete model, as will be explained in the next section.

The deviation of the function $\hat{g}_{\text{des}}(v)$ from linearity for small values of v is not just a specific property of the model proposed here, but arises from the fact that gaps never become negative. At high velocities the gap for a given velocity may fluctuate symmetrically around its average. At lower velocities an asymmetry is imposed by the condition that gaps are nonnegative, which immediately leads to the effect of an increase of the effective desired gap.

For this reason the same behavior should also be found on real highways. Indeed, this behavior has been reported in the literature, see for example [54].

When a deterministic model is formulated, the deviation of the velocity dependent desired gap from linearity will have to be taken into account.

7.3 Deterministic car following and escaping from jams

To indicate, how jamming can occur within the framework of the modeling approach presented in this work, even in the deterministic case, a few remarks on deterministic car-following and escaping from jams have to be made.

Consider a pair of vehicles. In equilibrium the cars can follow each other safely at a time headway τ_h that is equal to the reaction time τ .

$$\tau_h = \tau \quad (7.1)$$

When cars escape from a jam, they can do this safely at a time headway equal to τ , too. In this case the outflow from the jam is equal to the maximum flow. However, there is no a priori reason why the delay time τ_{esc} in the process of escaping from jams should be exactly equal to τ . In fact it has been shown in the last section that the strict non-negativity of the gap imposes a boundary condition that leads to an effective increase of the gap at low velocities, thus increasing the escape time. Therefore τ_{esc} may be some time constant greater or equal to τ :

$$\tau_{\text{esc}} \geq \tau . \quad (7.2)$$

The ratio between the outflow from jams and the maximum flow is then given approximately by

$$\frac{q_{\text{out}}}{q_{\max}} \approx \frac{\tau}{\tau_{\text{esc}}} \leq 1 . \quad (7.3)$$

So the outflow is reduced, if the escape time is larger than the reaction time. This simple fact has been pointed out by Kerner [41].

Yet, how can the existence of two different time scales be modeled in the framework of the model proposed here? Consider two cars in the model, initially standing in a jam bumper to bumper ($g = 0$). As usual, the velocities of the cars are denoted by v_l and v_f . Assume that at time $t = 0$ both cars are still standing. After the time T , when the two cars have escaped from the jam and accelerated (in discrete time steps of length $\Delta t = 1$, as usual) to some final velocity $v(T)$, the gap between them is given by

$$\begin{aligned} g(T) &= \sum_{t=0}^T (v_l(t) - v_f(t)) \\ &= v_l(T) + \sum_{t=1}^T (v_l(t-1) - v_f(t)) \\ &\equiv v_l(T) + \Delta . \end{aligned} \quad (7.4)$$

From this, the approximate relation (7.3) can be resumed. However, we want to interpret this equation in a different way. A flow reduction in the outflow through a reduction of the density can only be achieved, if the second term Δ in the expression for the final gap (7.4) is positive.

Now consider the safety condition once more:

$$v_f(t+1) \leq v_l(t) + \frac{g(t) - g_{\text{des}}(t)}{\tau_r(t)} . \quad (7.5)$$

Obviously the safety condition forces Δ to become positive only if $g - g_{\text{des}}$ becomes negative. However, we saw that in the Gipps family this can never happen, so the deterministic outflow from jams in the Gipps family is always equal to the maximum flow.

The fact that the true gap never becomes smaller than the desired gap appears somewhat unrealistic, and in the beginning it has been mentioned that not all collision free models do possess this property. If g_{des} is assumed to be a function of the velocity of the car in front, for example, the gap g can become smaller than g_{des} during a phase of deceleration, if

$$\Delta t - \frac{g'_{\text{des}}(v_l)}{v_l} > 0 , \quad (7.6)$$

as shown in chapter 4. Note that in the Gipps family the left hand side of this inequality always vanished, so the inequality could not be fulfilled. However, if the slope of the desired gap as a function of the velocity of the vehicle in front becomes small enough, as is the case for the “effective” desired gap noted above, the inequality can be fulfilled and deterministic jamming can be expected.

7.4 A deterministic model of jamming

The model considered now only differs from the models of the Gipps family in the choice of $g_{\text{des}}(v_l)$ and the fact that the random perturbations have been eliminated. Again we set $\Delta t = \tau = 1$. So the model equations are given by

$$\begin{aligned} v(t+1) &= \min[v(t) + a, v_{\max}, v_l(t) + \frac{g(t)-g_{\text{des}}(v_l)}{\tau_b(t)+1}] , \\ x(t+1) &= x(t) + v(t+1) , \end{aligned} \quad (7.7)$$

where τ_b is defined as in the Gipps family and g_{des} is chosen to be the effective desired gap $\hat{g}_{\text{des}}(v)$ found for the stochastic model. For reasons of consistency with $\Delta t = \tau = 1$, however, $\hat{g}_{\text{des}}(v)$ has to be rescaled to yield slope 1 for high velocities.

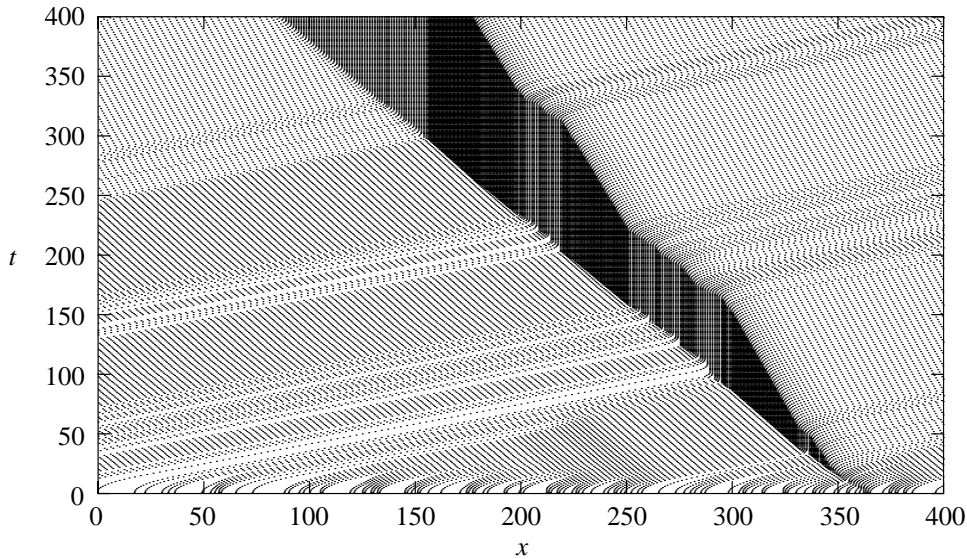


Figure 7.2: Space–time–plot of the deterministic model for a random initial configuration.

Fig. (7.2) displays a space–time plot of a model state of high density. The system was started in an initial configuration, where the position of every vehicle had been chosen randomly. Clearly phase separation is found, although no noise is present.

The velocity of the downstream front of the jam fluctuates due to the fact that the density within the jam is not constant. Quite in contrast to the stochastic model, this model appears to show a strong dependence of the outflow from a jam on the inflow conditions (this will be shown in the next section). This fact is quite remarkable and can be considered a major weakness of this model.

Next, the fundamental diagram is looked at. Fig. (7.3) shows the fundamental diagram in the interesting range of densities. The diagram was calculated starting the system

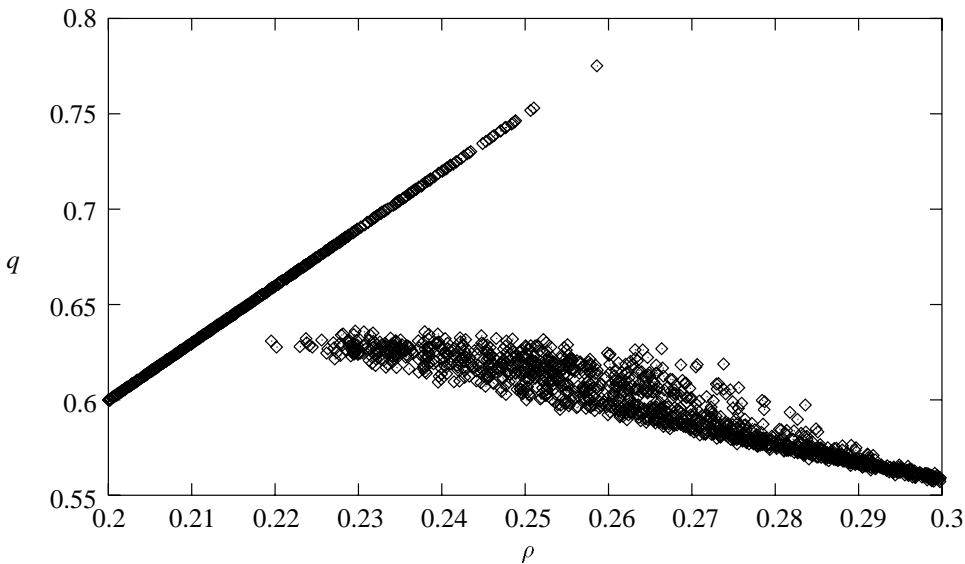


Figure 7.3: Fundamental diagram for the deterministic model of jamming.

from different random initial configurations and averaging over a time interval of 5000 time steps after a relaxation of 5000 time steps. We see the remarkable fact that the fundamental diagram again is branched. Due to the fact that the outflow from the jams is lower than the maximum flow, this result is not surprising.

Now it also becomes clear qualitatively, why the behavior of the coarsest discretization in the stochastic model was qualitatively different from discrete models of higher resolution and the continuous model. In the coarsest discretization a car never “sees” the deviations of the velocity dependence of \hat{g}_{des} from linearity as long as the predecessor moves ($v_l > 0$). If we used a corresponding discrete deterministic model of that kind, where g_{des} is derived from \hat{g}_{des} , the gap could never become smaller than the desired gap as long as the predecessor moves. Consequently the deviation of \hat{g}_{des} from the linear velocity dependence would have no effect on the way cars escape from jams and the escape time therefore would be equal to the time headway at high velocities. So no deterministic jamming would be possible in that case.

7.5 Outflow from jams

As already done for the stochastic model, the outflow from the jam q_{out} can be investigated as a function of the inflow q_{in} . Again, a homogeneous flow will be introduced into a jam at a prescribed distance from the upstream front of the jam.

Fig. (7.4) displays the results. This time a strong dependence between inflow and outflow is found. The outflow depends on the inflow in a quite peculiar way. This is even more surprising considering the fact that the density in the jam is a quantity that in-

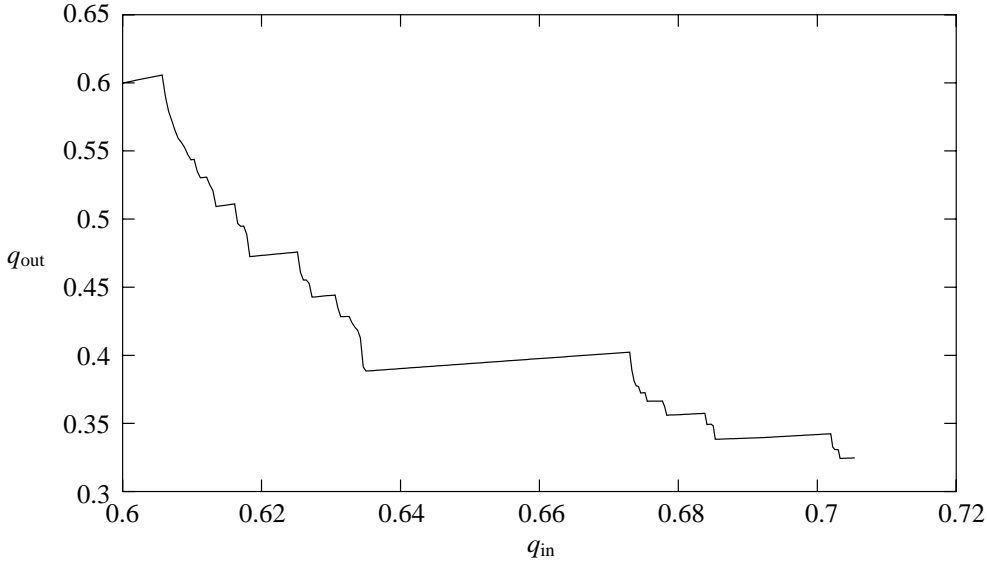


Figure 7.4: The flux out of the jam depends strongly on the inflow.

creases smoothly with increasing inflow (Fig. (7.5)).

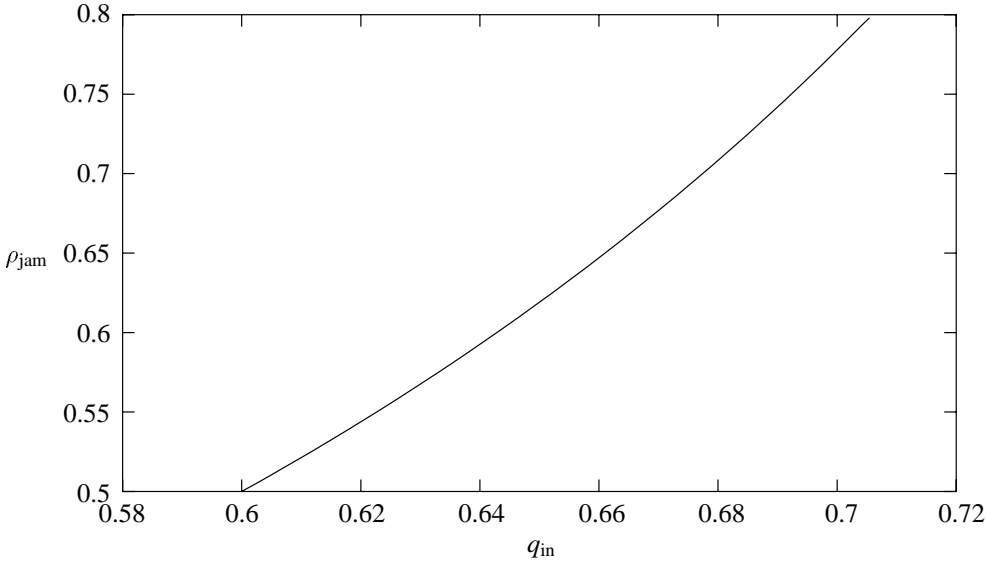


Figure 7.5: The density in the jam as a function of the inflow.

To understand the strange behavior of the outflow, we express the outflow as a function of the average escape time τ_{esc} and the density in the jam ρ_{jam} . For this end the velocity of the downstream front is written in two different ways:

$$\begin{aligned} v_{down} &= -\frac{1}{\tau_{esc}\rho_{jam}} \\ v_{down} &= -\frac{q_{out}-q_{jam}}{\rho_{jam}-\rho_{out}} \end{aligned} \tag{7.8}$$

The simulations show that q_{jam} vanishes in the deterministic model. Equating these ex-

pressions and taking into account that $\rho_{\text{out}} = q_{\text{out}} / v_{\text{max}}$ one arrives at

$$q_{\text{out}} = \frac{1}{\tau_{\text{esc}} + \frac{1}{\rho_{\text{jam}} v_{\text{max}}}} . \quad (7.9)$$

The decisive question is, what escape times are possible in a time discrete deterministic system. In the steady state the average downstream front of the jam will be some stationary moving profile. If the dynamics of escaping from jams within this stationary average profile are periodic with period p , that means, if the car with the index $n + p$ escapes from the jam in the same way as the car with index n , then the average escape time is given by

$$\tau_{\text{esc}} = \frac{1}{p} \sum_{i=1}^p \tau_i , \quad (7.10)$$

where τ_i are the individual escape times. Note that τ_i can only assume integer values due to the discreteness of the time step. So τ_{esc} is restricted to rational values as long as there is a finite period p .

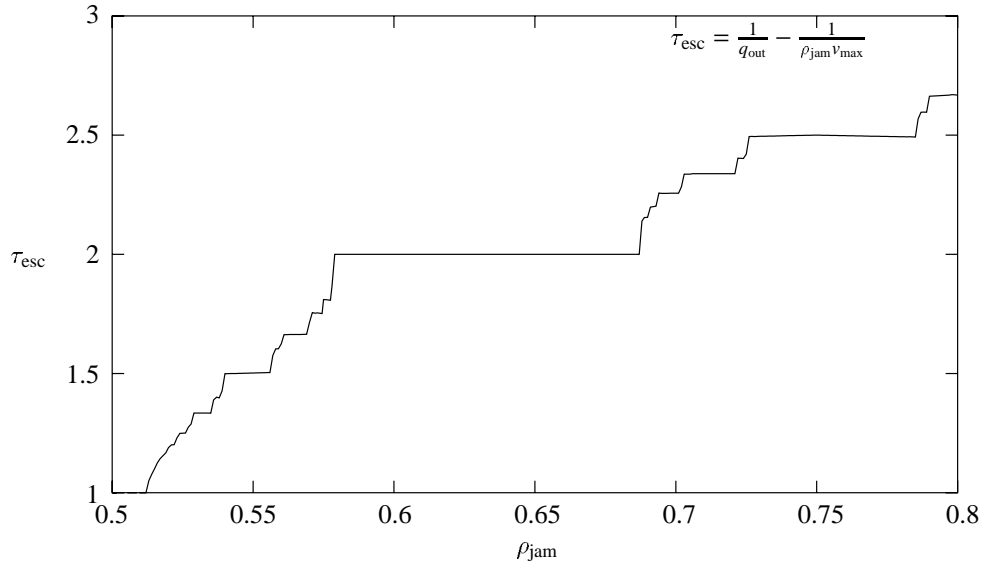


Figure 7.6: The measured escape time.

Fig. (7.6) displays the measured escape time as acquired by solving eq. (7.9) for τ_{esc} and inserting the measured outflow and jam density. Note that the fact that τ_{esc} takes the form of a “devil’s staircase” is not a specific property of the car following behavior, but arises from the discreteness of the model in time.

It could be shown in this chapter that jamming and the existence of metastable states can be explained within the framework of a purely deterministic model. The jamming transition this time again is a true phase transition. However, the model shows the great weakness that the outflow from jams strongly depends on the inflow conditions. For this reason the validity of the model is limited. Due to the fact that the stochastic model of jamming did not exhibit this weakness the deterministic model will not be considered any more in this work.

Chapter 8

Multilane traffic

8.1 The distribution of maximum velocities

Up to now only systems with a uniform maximum velocity of the vehicles have been considered. For single lane traffic it is indeed a reasonable assumption that all maximum velocities are approximately the same, because fast vehicles are trapped behind slow vehicles anyway, so drivers might adjust their maximum velocity to that of their predecessor. If a probability distribution for the maximum velocity is used that is different from a δ -function, the faster vehicles will build up queues behind the slower vehicles. These queues are usually referred to as platoons.

In multilane traffic this is substantially different. Here, there is a constant interplay between platooning due to the fact that the desired maximum velocities are different and the dissolution of platoons due to passing. If the maximum velocity is equal for all cars in multilane traffic, there is no point in passing. For this reason the question, whether or not quantities like the densities and flows on both lanes are modeled realistically, depends crucially on the correct choice of the maximum velocity distributions.

Consequently, for all calculations that will be performed in this section, distributions for the maximum velocity will be used that have been drawn from induction loop data under conditions of very light traffic. The probability distributions have been measured separately for trucks and cars, so effects that depend on the proportion of trucks in the system can be considered.

Fig. (8.1) shows the velocity distributions obtained from induction loops on the Autobahn A1 in Nordrhein-Westfalen, once for conditions of light traffic (density below 5 veh./km) and once for dense traffic (density above 30 veh./km). It can be seen that the probability distribution of the trucks resembles that of the cars under conditions

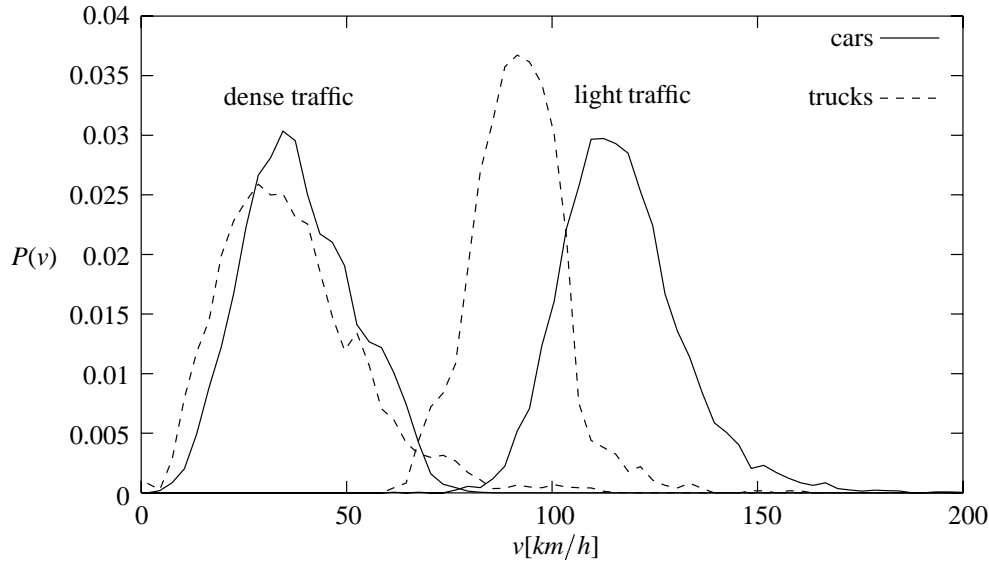


Figure 8.1: The velocity distributions as measured on the A1 under conditions of light and heavy traffic

of heavy traffic, because no vehicle can move at the desired speed. If traffic is light enough, however, so every vehicle can move almost freely, these distributions differ substantially. The distributions measured for light traffic are used as approximations for the distributions of maximum velocities in the simulations of this chapter.

8.2 Generalization of the model

So far only single lane traffic has been modeled. In reality, however, this situation is hardly ever found on highways. Instead, a road generally is made up of two or more lanes, which allow vehicles to pass. So the model will have to be generalized to multi-lane traffic.

After the generalization the time update will consist of three steps. In the first step lane changes are performed in the way specified below, in the second step the velocities are adjusted as specified in the single lane model, and in the third step the vehicles are moved according to their new velocity.

The generalization to multilane traffic is done in a straightforward way. To model multilane traffic, the car following model proposed so far will be used and be supplemented by lane changing rules. Remember that the whole car following model was developed on the basis of the assumption that velocity, acceleration, and deceleration are bounded and that the system is free of collisions. Now the same simple approach can be used to

describe lane changes. We will refer to the slow lane as the “right lane” and the passing lane as the “left lane”.

The model formulation is based on a few very simple assumptions:

- A lane change is performed, if it is favorable and safe.
- Passing on the right side is allowed only under congested conditions.
- There is a small probability p_{change} that a safe lane change is performed, even if it is not favorable.

Now the terms used in the above rules have to be specified. For this end the following notation will be adopted: The variables g , v_l and v_{safe} will keep their meaning, the superscript $\dots^{(o)}$ will denote these quantities taken with respect to the respective other lane.

For uncongested conditions the left lane is devoted to passing. In that case a lane change to the left is favorable, if a driver cannot go as fast as desired i.e. if $v_{\text{safe}} < v_{\max}$. A change to the right lane is favorable, if a driver is neither following a car on the left lane nor passing a car on the right lane, i.e. if $v_{\text{safe}} > v_{\max}$ and $v_{\text{safe}}^{(o)} > v_{\max}$.

Under congested conditions the situation of a driver cannot be improved significantly by changing lanes. Since passing on the right side is no longer prohibited then, both lanes are equally attractive for the drivers. Therefore a lane change is not favorable under congested conditions.

The simplest way to keep a vehicle on the right lane from passing a vehicle on the left lane is to treat the preceding car on the left lane in the same way, as if it were found on the right lane. That means, one demands $v(t+1) < v_{\text{safe}}^{(o)}(t)$ in the velocity update. However, it is certainly not desirable to have a car on the right lane brake hard due to the small gap $g^{(o)}$ that may arise if it has just been passed by another vehicle. This situation can be excluded quite easily. Remember that the car following rules always guaranteed that $g - v_l \geq 0$. So if the predecessor on the left lane is treated in the same way as the predecessor on the right lane, the situation $g^{(o)} - v_l^{(o)} < 0$ can only arise from being passed. Therefore we only demand $v(t+1) < v_{\text{safe}}^{(o)}(t)$, if $g^{(o)} - v_l^{(o)} \geq 0$.

Finally, a situation will be assumed to correspond to a congested state, if the safe velocities, taken with respect to both lanes, are found below some sufficiently low threshold v_{thresh} . The rules are summarized once more in a pseudo-code form (rand denotes a random number between 0 and 1):

- Lane changes:

$$\begin{aligned}\text{congested} &= (v_{\text{safe}} < v_{\text{thresh}}) \quad \text{and} \quad (v_{\text{safe}}^{(o)} < v_{\text{thresh}}) \\ \text{favorable(right} \rightarrow \text{left)} &= (v_{\text{safe}} < v_{\max}) \quad \text{and} \quad (\text{not congested}) \\ \text{favorable(left} \rightarrow \text{right)} &= (v_{\text{safe}} \geq v_{\max}) \quad \text{and} \quad (v_{\text{safe}}^{(o)} \geq v_{\max})\end{aligned}$$

if ((favorable($i \rightarrow j$) **or** ($\text{rand} < p_{\text{change}}$)) **and** safe($i \rightarrow j$))
then change($i \rightarrow j$).

- Passing on the right side: For vehicles on the right lane apply

if ($v > v_{\text{safe}}^{(o)}$) **and** (**not** congested)
then $v \leftarrow v_{\text{safe}}^{(o)}$.

To complete the model, it has to be defined, what a safe lane change is. In single lane traffic the system remains free of collisions if $g - v_l$ is fulfilled once in the whole system and the velocity $v(t+1)$ of each car is chosen in such a way that $v(t+1) < v_{\text{safe}}(t)$. The choice of v_{safe} was motivated by the intention that a driver can always avoid a collision using only limited braking capabilities b .

Now a lane change will be assumed to be safe, if after the lane change each vehicle is found in a situation that is compatible with safe car following in single lane traffic. That means we require that after the lane change the conditions

$$\begin{aligned}g - v_l &> 0 \\ \text{and} \\ v(t) - b &\leq v_{\text{safe}}(t)\end{aligned}\tag{8.1}$$

hold in the whole system.

Note that, if these conditions are used, drivers allow themselves to make the successive driver on the lane they are changing to brake as a direct consequence of the lane change. This is, of course, a quite aggressive driving strategy. At a first glance it might appear more appropriate to use a more cautious strategy by requiring, for example, that no one is hindered by the lane change. This would lead to the condition that $v(t) + a \leq v_{\text{safe}}(t)$ holds in the whole system after the lane change. If such a cautious safety rule is used, however, a problem arises that will be denoted as “desynchronization”. This means that systems of intermediate density decompose into almost free flow on the left and congested flow on the right lane, because the slow vehicles on the right lane, which are stuck in congested flow, do not dare change lanes, because they do not want to hinder the vehicles that are speeding by on the left lane. This state is never found in real traffic, so the aggressive lane changing rules seem to be more realistic.

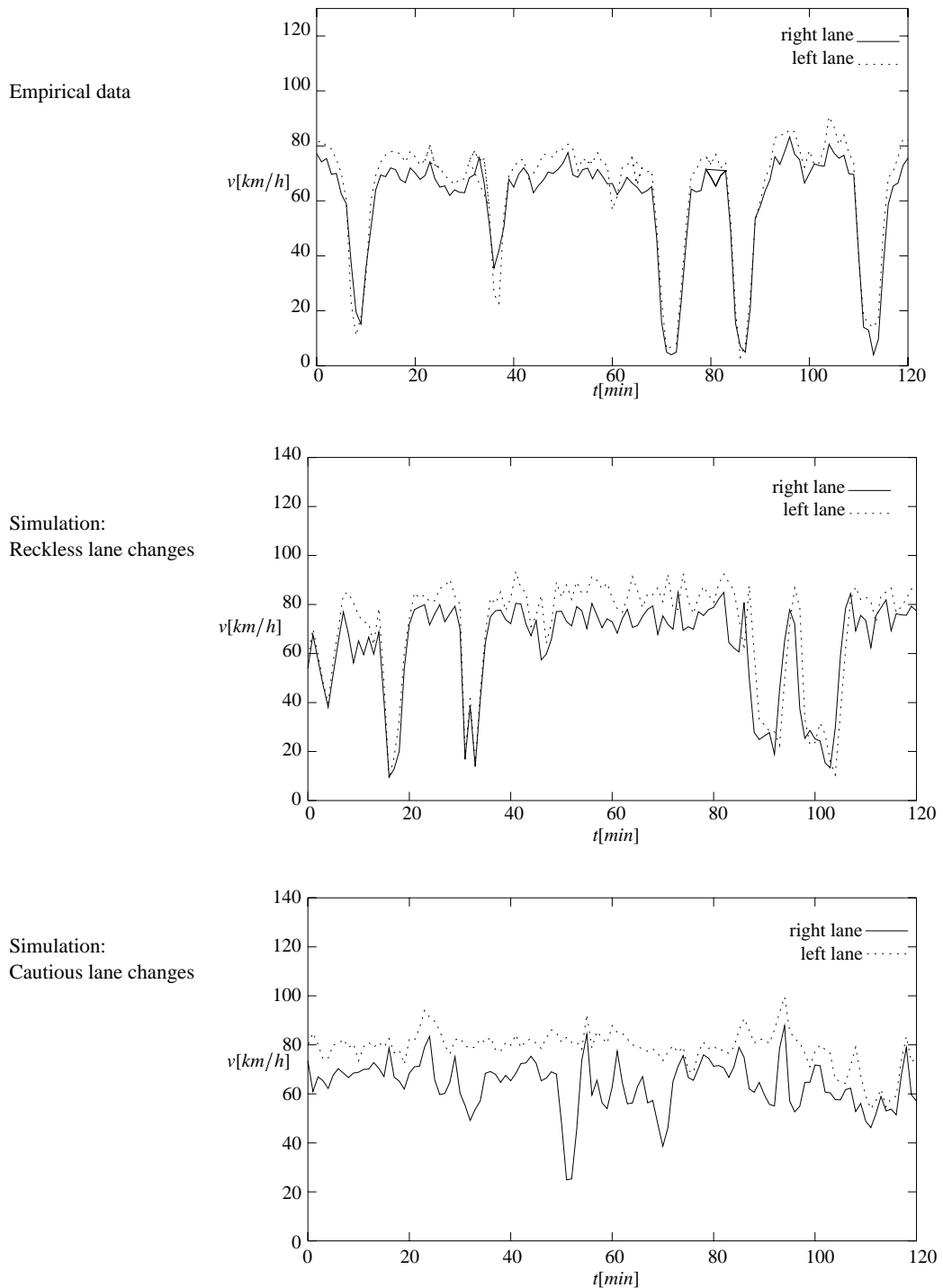


Figure 8.2: Small disturbances in dense traffic: If drivers are assumed to change lanes cautiously without hindering other drivers, the system desynchronizes at perturbations.

To illustrate desynchronization, Fig. (8.2) displays three different pictures of dense traffic at approximately the same density. The first displays induction loop data drawn from the Autobahn A43 near Bochum, the second corresponds to the model proposed here, using the “reckless” safety condition $v(t) - b \leq v_{\text{safe}}(t)$, the third displays the same model, where only the safety condition for lane changes has been changed to the more cautious condition $v(t) + a \leq v_{\text{safe}}$. It can be seen that the cautious strategy leads to wrong results, because the system desynchronizes at perturbations. This means that far too few vehicles use the left lane.

It has to be noted, however, that the effect of desynchronization becomes less pronounced, if a narrower distribution of maximum velocities is used. So the observation that less aggressive lane changing rules lead to desynchronization is not universal, but only applies for systems with sufficiently wide distributions of maximum velocities.

The lane changing rules are not symmetric for the two lanes, because one lane is devoted to passing. An important feature of the rules proposed here is the fact that a car stays on the left lane not only, if it is passing another car, but also, if it is following another car. This rule has first been proposed in [79] and will be responsible for the so called lane usage inversion, which means that for intermediate densities more cars are found on the left lane than on the right lane.

Note that the rules do not allow that a change to the right *and* a change to the left are favorable at the same time. For this reason the rules can readily be used not only for two lanes, but for any number of lanes. In that case the terms “right” and ”left” lane have a relative meaning.

8.3 Comparison to empirical data

8.3.1 Clustering

Before a quantitative comparison is performed, some qualitative properties of the model will be looked at. To make it possible to compare the dynamics of the model to that of real traffic, the data will be gathered in the same way in the simulation as in real traffic. That means, the data is collected at a fixed cross section, which corresponds to an induction loop, and averages over sixty seconds are taken. This experimental setup is exactly the same as that used in [38].

In all simulations again a measured distribution of maximum velocities is used. The following values for the free parameters are used: $a = 0.2$, $b = 0.6$, $\epsilon = 1$, $p_{\text{change}} = 0.01$, $v_{\text{thresh}} = 1.5$. The parameter values were drawn from a quantitative comparison to traffic flow data that will be described in the next section.

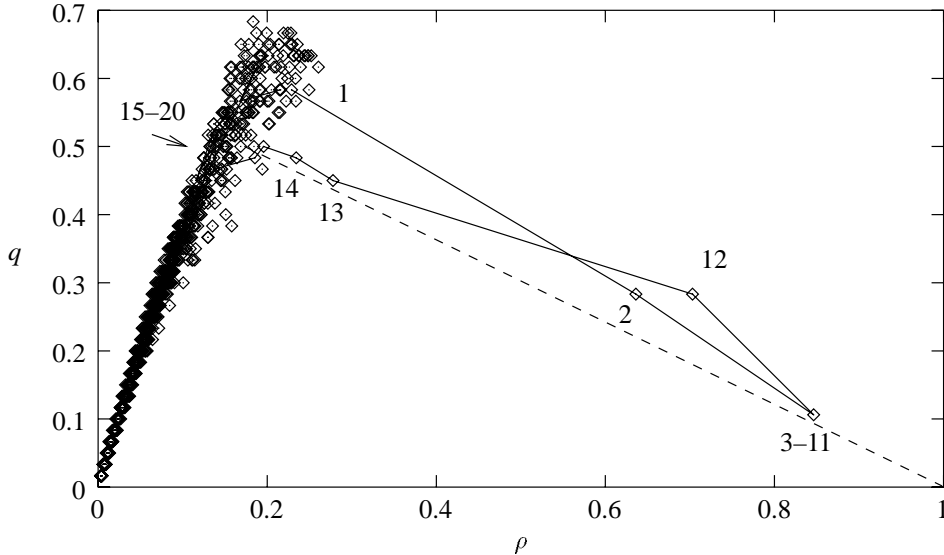


Figure 8.3: Free flow and a jam in the flow–density diagram. The numbers denote the time that each point in the jam corresponds to.

Fig. (8.3) displays free flow and a cluster in the flow–density plane. Successive points (in time) that correspond to the jam are connected by lines to display the time evolution of the system. The numbers in the figure denote the time (expressed in minutes) after the appearance of the jam that each point corresponds to. Note that within the jam, flow and density have been averaged over a few minutes to obtain a reliable estimate of the density.

The behavior of the jam is qualitatively exactly the same as described in [38, 39]. The outflow q_{out} from the jam is significantly lower than the maximum flow. The downstream front of the jam organizes approximately to the line between the points $(\rho_{\text{out}}, q_{\text{out}})$ and $(1, 0)$.

Quite obviously traffic jams are described well by this model. It has been noted before, however, that, besides free flow and jams, traffic can also be found in a state of synchronized flow. This state will be discussed in more detail later in this chapter. So far it has to be conceded that the model does not show a sign of synchronized flow. Since most congested situations correspond to synchronized flow rather than real traffic jams (as found by looking at data from highways in Nordrhein–Westfalen) this restricts the applicability of the model significantly. At the end of the chapter a further generalization of the model will be proposed that is able to model synchronized flow as well.

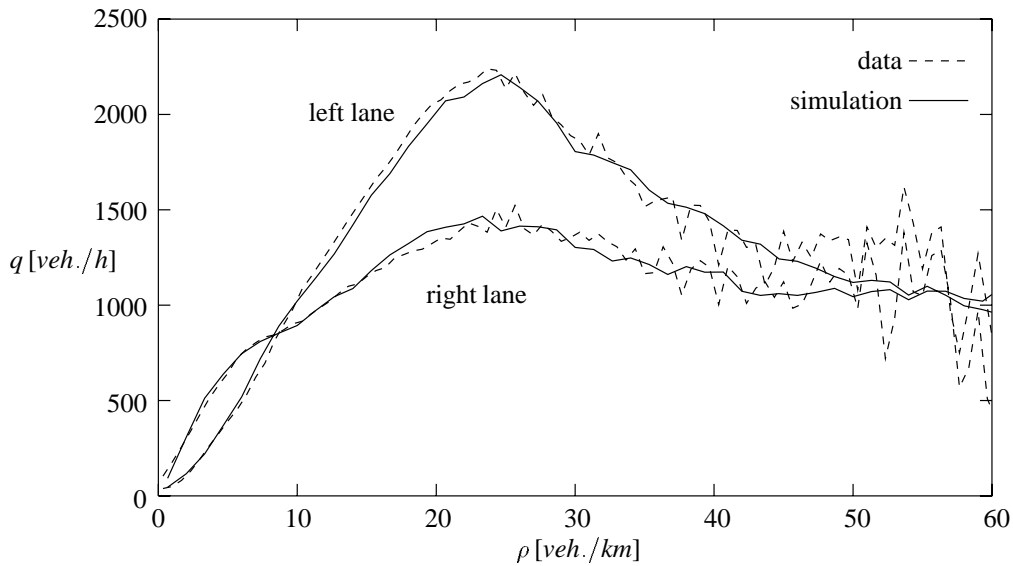


Figure 8.4: The flux on the right and the left lane on the Autobahn A43. Comparison between simulation and reality. Model parameters $a = 0.2$, $b = 0.6$, $v_{\text{thresh}} = 1.5$, $\epsilon = 1$, $p_{\text{change}} = 0.01$.

8.3.2 Quantitative comparison

For practical applications it is important that the model does not only reproduce the properties of traffic qualitatively, but also shows quantitative agreement. To show that this model does indeed reproduce traffic flow data in a quantitatively correct way, data from induction loops on the Autobahn A43 have been gathered. The A43 has two lanes for each direction. The quantities of interest for the model calibration are the fluxes q_{right} and q_{left} on the right and the left lane respectively, as well as the left lane usage P_{left} , which is defined as the proportion of vehicles found on the left lane.

The noise parameter ϵ is set to $\epsilon = 1$, the probability that an unfavorable lane change is performed is set to $p_{\text{change}} = 0.01$, because for this parameter value the models properties are relatively insensitive to changes of that parameter. The parameters v_{thresh} , a , and b are chosen in such a way that deviations between simulation and experiment are minimized.

The distribution of maximum velocities have been taken from measurements performed at night, when traffic volumes were low. The measured quantities q_{left} , q_{right} , and P_{left} have been averaged for every density separately. Due to averaging, all the information about the inner dynamics of jams is lost (that is why a qualitative discussion of the dynamics has been presented before), but a quantitative comparison becomes much easier.

The system is started at different global densities. To determine the proportion of trucks that has to be used in the simulations runs, we use the fact that longtime averages of the

density and the proportion of trucks are correlated. This phenomenon has to do with the fact that the proportion of trucks is typically higher at night, when low densities are found. So the proportion of trucks introduced into the system for a given global density will be chosen to be equal to the average value found for this density in the induction loop data.

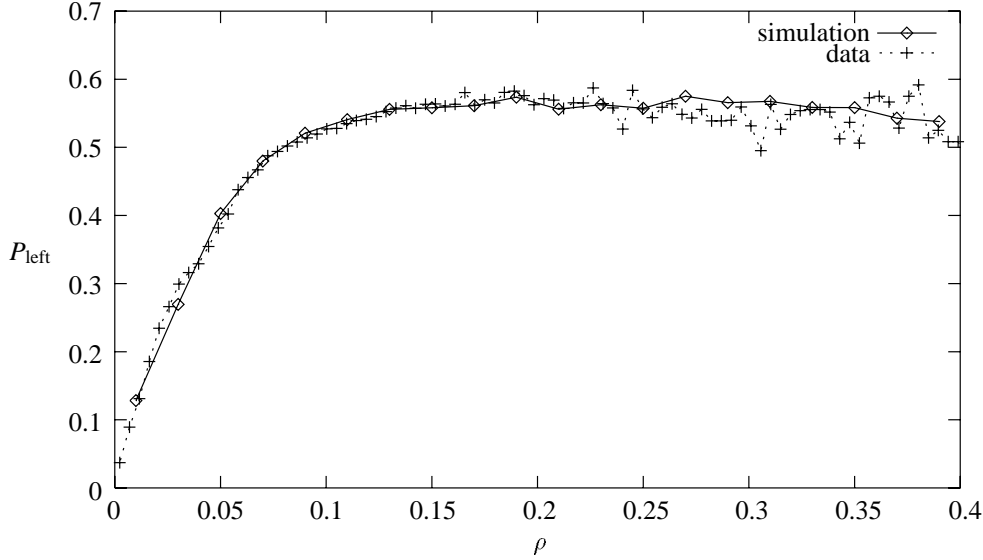


Figure 8.5: The left lane usage as a function of the density.

Fig. (8.4) displays the flux on the right and the left lane separately, once as drawn from induction loops on the A 43 and once as simulated. The agreement is excellent. The same holds for the proportion of vehicles P_{left} that are found on the left lane, as displayed in Fig. (8.5).

In Appendix B the quantitative performance of the model on a microscopic scale is discussed. The model performs surprisingly well, even in a car-following experiment. That experiment, however, refers to single lane traffic again.

8.4 Modeling of synchronized flow

The phenomenon of synchronized flow has been described shortly at the beginning of this work. The term “synchronized” flow may be a little misleading, because the fact that both lanes are approximately synchronized (i.e. average velocities are approximately the same on both lanes) is not the most important property of this state of traffic flow. Instead, what is most striking, is the fact that the system performs random translations in the flow–density plane. That means an increase of the density can be accompanied by an increase as well as a decrease of the flux. This is quite surprising at first,

because on the one hand synchronized traffic is quite dense, so the average velocity of the vehicles is very low due to interactions, and on the other hand the fact that an increase in density is sometimes accompanied by an increase of the flux indicates that vehicles move seemingly uninfluenced.

This kind of state appears in traffic flow, when traffic is dense enough, so vehicles almost cannot pass any more. In this kind of state there is no point in trying to move any faster than the average velocity, because fast vehicles are trapped behind the slower ones anyway. In this kind of situation one may suspect that drivers are more willing to give up some of their maximum safe velocity, because they can anytime make up easily for any loss in velocity. So the state of synchronized flow seems to be characterized by a complex interplay between interaction and free motion.

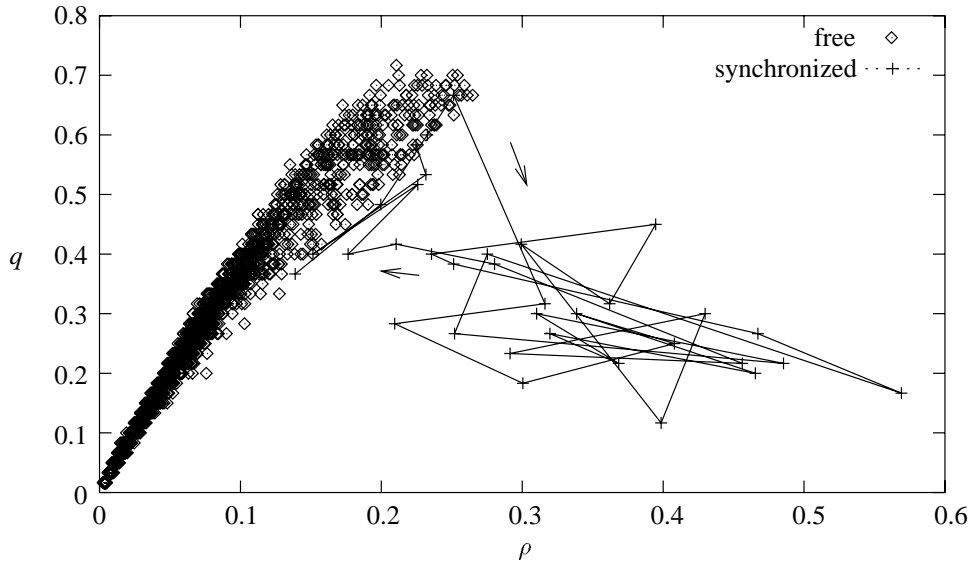


Figure 8.6: Free and synchronized flow in the generalized model.

With the above interpretation the model discussed so far can be generalized to show synchronized flow. The key point is that a way has to be found to make drivers who move in congested flow give up some space deliberately, so they appear to be uninfluenced for a while. A simple way to do this is to make drivers who have had to slow down due to an interaction resume their old driving strategy and acceleration capabilities not immediately, but only after a few seconds. Using the quantities a and v_{des} as defined before in this work an effective maximum acceleration a_{eff} can be defined as

$$a_{\text{eff}}(t+1) = \max[0, \alpha a + (1 - \alpha)(v_{\text{des}}(t) - v(t))] , \quad (8.2)$$

where α is a parameter between 0 and 1. For $\alpha = 1$ the ordinary model is restored.

In the model equations, that have been discussed before, the parameter a , which restricts accelerations, is then simply replaced by a_{eff} . Equation (8.2) has got the following meaning. For a freely accelerating vehicle obviously $v_{\text{des}}(t) - v(t) = a_{\text{eff}}(t)$ holds

after a has been replaced. If that vehicle continues to accelerate freely, the quantity a_{eff} relaxes towards a on the time scale $1/\alpha$, which may be a few seconds. If, however, a vehicle is hindered by some other vehicle, a_{eff} becomes small and it will take the vehicle approximately the time $1/\alpha$ to resume the maximum acceleration capabilities again. For this reason a vehicle that just had to slow down due to an interaction is likely to move uninfluenced for a while, even in dense traffic. Of course there are many ways to model the seemingly uninfluenced motion of a vehicle in dense traffic. For example it would be possible to modify the maximum velocity or to choose a different noise parameter ϵ in dense traffic.

Fig. (8.6) displays free and synchronized traffic in the resulting model, where α was set to 0.1. The figure displays two kinds of situations. First a large number of sample points from free traffic have been taken. Then a situation was prepared in such a way that traffic of density 0.4 was surrounded by free traffic. Then the system was allowed to run for 10^5 time steps. As found in empirical data [39] the region of synchronized flow showed no tendency to dissolve in the simulation. After 10^5 time steps the time evolution of the system in the flow–density plane was recorded. One transition from free to synchronized flow and one transition back to free flow can be seen clearly. As found in empirical data, traffic never recovers from congestion, i.e. the outflow from synchronized flow is significantly lower than the maximum flow.

It has to be stressed that this model of synchronized flow is far from being the final explanation for this very important phenomenon. It remains for future work to develop theories of similar quality, as those known for jams.

Chapter 9

Concluding remarks

9.1 Summary

Empirical observations [38, 39] have shown that traffic flow can assume three qualitatively different states, namely free flow, synchronized flow, and a jammed state. When traffic flow changes its state, it performs a transition that has been interpreted as a first order phase transition [40]. Instead of seeking to get quantitative agreement between reality and a traffic flow model for specific situations, the aim of any modeling effort should be to reproduce the qualitative properties of the phase transitions in traffic flow first.

The primary focus of this work was the description of jams. Empirically, jams have been found to have the following properties:

1. Traffic jams can develop and exist under “pure” conditions, i.e. in the absence of any obstacles.
2. The flux out of a jam is not maximal.
3. The outflow from jams is stable.
4. The outflow from jams and the velocity of the downstream front do not depend on the inflow conditions.
5. There are metastable states of high flow.

To describe jamming, a family of stochastic microscopic traffic flow models has been proposed, that has been derived from quite general and simple assumptions about traffic. Depending on how the free parameters characterizing acceleration and deceleration

capabilities are chosen, three qualitatively different classes of models are obtained. The model classes can be characterized by referring to the properties mentioned above as follows:

- Class *I*:

- Accelerations and decelerations realistic, i.e. long ranged interactions.
- All above properties of jams are modeled correctly,
- the jamming transition is a first order phase transition.

- Class *II*:

- Decelerations are unbounded, i.e. short ranged interactions.
- Properties 2,3, and 5 of jams are not reproduced,
- the jamming transition is no phase transition.

- Class *III*:

- Accelerations are unbounded.
- No jams exist.

From a phenomenological point of view also other models can be attributed to these classes. Phenomenologically the macroscopic Kerner–Konhäuser–model [37], the microscopic Bando–model [2], and some cellular automaton models using so called “slow-to-start–rules” [74, 4], that have recently been developed, are all models of class *I*, too. The Nagel–Schreckenberg–model [58], which is, apart from the discreteness of the space coordinate, identical to the high deceleration limit discussed here, is a model of class *II*. The stochastic version of the Fukui–Ishibashi model [22], which is apart from the discreteness of the space coordinate, identical to the high–acceleration–high–deceleration–limit of the model proposed in this work, is a model of class *III*.

A generalization of the model proposed in this work to multilane traffic has proven to show qualitative as well as quantitative agreement with empirical data.

Finally, the phenomenon of synchronized flow has been considered, using a model generalization that allows drivers to give up speed deliberately under congested conditions. In this way the fact that perturbations can travel in forward and in backward direction in synchronized flow could be modeled.

9.2 Conclusion and Outlook

The family of stochastic models proposed in this work incorporates effects of limited acceleration and deceleration capabilities of the vehicles. If realistic values of acceleration and deceleration are assigned to the vehicles, the model describes cluster formation very well. Unfortunately, not even the qualitative properties of the model are very robust. Every simplification discussed in this work (high acceleration, high deceleration, coarse spatial discretization) destroyed the ability of the model to describe jamming correctly.

The same happens if the stochastic component is removed from the model. In that case the model degenerates and the rich structure of the model dynamics disappears. The reason for this is that none of the properties that govern the qualitative appearance of traffic flow, like overreactions and reduced outflow from jams, has been modeled explicitly in the deterministic part of the car following rules. Instead, the structure of the model dynamics is mediated exclusively by the fluctuations that are introduced ad hoc through the randomization step. If these fluctuations are eliminated, none of the properties of traffic flow is modeled correctly any more.

Considering the fact, that none of the phenomena the model describes correctly proved to be of essentially stochastic nature, it seems doubtful that the exclusive role that stochasticity plays in the model is favorable. The fact that the large random fluctuations are not found in real traffic flow (see for instance car following experiment, discussed in the appendix) adds to this impression. The attempt presented in this work to develop a deterministic model of jamming was only partly successful, because escaping of the vehicles from jams was not modeled correctly. Therefore some future work should be devoted to the question, which phenomena actually do require a stochastic approach and which phenomena do not. It would be desirable to restrict the role of the stochastic parts of the model to those phenomena that actually are stochastic like the random generation of small jam “seeds”.

The second question that is still open is the description of synchronized flow. A large proportion of congestion phenomena in real-world traffic correspond to synchronized flow. Still there is, to the authors knowledge, no work that addresses this topic explicitly, so far. Existing work concentrates exclusively on traffic jams rather than synchronized flow. One reason for this might be that the qualitative differences between these two states of traffic were unknown before Kerner’s and Rehborn’s work [39] in 1996. The modification of the model discussed here leads to synchronized traffic, yet there are probably more natural mechanisms than the one assumed here to reach that state. Certainly one of the most important and challenging topics for future work will be the development of a unified theory of jams and synchronized flow.

In this work a first step towards a unified view of different traffic flow theories could

be performed by classifying model behavior in a qualitative, phenomenological framework. In this way models as diverse as the Kerner–Konhäuser–model, the Bando–model, the Nagel–Schreckenberg–model, and different models from the model family proposed here could be discussed and judged in a unified way. This work should be pursued in two ways. First some deeper analysis should be performed as for how far the model proposed here actually parallels the macroscopic Kerner–Konhäuser–theory and where significant differences are found. Secondly some work should be devoted to a phenomenological classification of other microscopic and macroscopic models, in order to obtain a better understanding for the relative merits of different approaches.

Appendix A

Remarks on the model

A.1 Update rules

To specify the model used in this work once more, the core part of two possible model implementations is presented.

A.1.1 Single lane traffic

The following program is a car-oriented implementation of the model in C. The variables $v[i]$ and $x[i]$ denote the velocity of and the gap in front of car i , respectively. The update scheme is due to Peter Wagner. It is assumed that other parts of the program supply the values for a , b , v_{\max} and $NCARS$.

```
inline float newV(float g, float vf, float vl)
{
    float vnext, vsafe;
    if (vf < vmax - a) vnext = vf + a;
    else vnext = vmax;
    vsafe = vl + (g-vl)/((vl+vf)/two_b + 1);
    if (vnext > vsafe) vnext = vsafe;
    vnext -= frandom()*epsilon_a;
    if (vnext < 0) vnext = 0;
    return vnext;
}

void update()
{
    int i, nCars1=NCARS-1;

    float v0 = v[0];
    v[0] = newV(x[0],v[0],v[1]);
    for (i=1; i<nCars1; i++)
```

```

    {
        v[i] = newV(x[i],v[i],v[i+1]);
        x[i-1] += (v[i] - v[i-1]);
    }
    v[nCars1] = newV(x[0],v[nCars1],v0);
    x[nCars1-1] += (v[nCars1] - v[nCars1-1]);
    x[nCars1] += (v[0] - v[nCars1]);
}

```

A.1.2 Twolane traffic

The following code provides an implementation of the twolane model in C++ (all methods that do not specify the model have been omitted). The code has not been optimized with respect to computational efficiency, but rather is supposed to be easily readable. For this reason it is different from the code used, when the actual calculations were performed.

The Classes *Simulator* and *Car* for a twolane model are defined as

```

class Simulator
{
protected:
    Car ***site;
    Car ***newsite;

    int length;
    int nLanes;

    float vThreshold;
    float pchange;
    int maxLook;
    ...
};

class Car
{
friend class Simulator;
protected:
    float x;
    float v;
    float vnext;
    float vmax;
    float amax;
    float bmax;
    float epsilon;
    ...
};

```

The methods that define the update rules are given as follows:

```

void Simulator::advance()
{

```

```

        laneChange();
        adjust();
        move();
    }

void Simulator::laneChange()
{
    Car *cptr, *pred[2], *succ[2];
    float gf[2], gb[2], vSafe[2];
    int fromLane, toLane;
    for (int lane=0; lane<=1; lane++)
        memset (newsite[lane], 0, length * sizeof (Car *));
    for(toLane=0, fromLane=1; toLane<=1; toLane++, fromLane--)
        for(int i=0; i<=length-1; i++)
        {
            cptr = site[fromLane] [i];
            if(cptr)
            {
                look(cptr, i, 1, pred, gf);
                getSafeVelocity(cptr, pred[fromLane], gf[fromLane], &vSafe[fromLane]);
                getSafeVelocity(cptr, pred[toLane], gf[toLane], &vSafe[toLane]);

                if (wishToChange(i, fromLane, toLane, vSafe))
                {
                    look(cptr, i, -1, succ, gb);
                    if ((changePossible(cptr, pred[toLane], succ[toLane],
                        gf[toLane], gb[toLane]))
                        && (!site[toLane] [i]))
                        newsite[toLane] [i] = cptr;
                    else
                        newsite[fromLane] [i] = cptr;
                }
                else
                    newsite[fromLane] [i] = cptr;
            }
        }
    Car ***help = site;
    site = newsite;
    newsite = help;
}

void Simulator::adjust()
{
    Car *pred[2];
    float gf[2], vSafe;

    for(int lane = 0; lane<=1; lane++)
        for(int i=0; i<=length-1; i++)
        {
            Car *cptr = site[lane] [i];
            if(cptr)
            {
                look(cptr, i, 1, pred, gf);
                getSafeVelocity(cptr, pred[lane], gf[lane], &vSafe);

                if (cptr->v < cptr->vmax - cptr->amax)
                    cptr->vnext = cptr->v + cptr->amax;
                else cptr->vnext = cptr->vmax;
                if (cptr->vnext > vSafe) cptr->vnext = vSafe;
                if ((lane == 0) && (pred[1]) &&(pred[1]->v<= gf[1]))
                {
                    float vSafe_o;
                    getSafeVelocity(cptr, pred[1], gf[1], &vSafe_o);

```

```

        int notCongested = ((vSafe >= vThreshold) || (vSafe_o >= vThreshold));
        if ((notCongested) && (vSafe_o < cptra->vnnext))
            cptra->vnnext = vSafe_o;
        }
        cptra->vnnext -= frandom()*cptra->amax*cptra->epsilon;
        if (cptra->vnnext<0) cptra->vnnext = 0;
    }
}

void Simulator::move()
{
    for (int lane=0; lane<=1; lane++) memset (newsite[lane], 0, length * sizeof (Car *));
}

for(int lane=0; lane<=nLanes-1; lane++)
    for(int i=0; i<=length-1; i++)
    {
        Car *cptra = site[lane] [i];
        if (cptra)
        {
            cptra->v = cptra->vnnext;
            cptra->x += cptra->vnnext;
            if (cptra->x >= length) cptra->x -= length;
            newsite[lane] [(int)(cptra->x)] = cptra;
        }
    }
    Car ***help;
    help = site;
    site = newsite;
    newsite = help;
}

int Simulator::changePossible(Car *cptra, Car *pred, Car *succ, float gf, float gb)
{
    float vSafe;
    int _changePossible = 1;
    if (succ)
    {
        getSafeVelocity(succ, cptra, gb, &vSafe);
        _changePossible = ((vSafe >= succ->v-succ->bmax) && (gb >= cptra->v));
    }
    if (_changePossible)
    {
        getSafeVelocity(cptra, pred, gf, &vSafe);
        if (pred)
            _changePossible = ((vSafe >= cptra->v-cptr->bmax) && (gf >= pred->v));
    }
    return _changePossible;
}

int Simulator::wishToChange(int i, int fromLane, int toLane, float *vSafe)
{
    int _wishToChange = 0;
    Car *cptra = site[fromLane] [i];

    if ((vSafe[fromLane] < vThreshold) && (vSafe[toLane] < vThreshold))
        return (frandom() < pchange);
    if (toLane == 1)
        _wishToChange = ((vSafe[fromLane] < cptra->vmax) || (frandom()<pchange));
    else
        _wishToChange = (((vSafe[1] > cptra->vmax) && (vSafe[0] > cptra->vmax))
                        || (frandom()<pchange));
    return _wishToChange;
}

```

```

}

void Simulator::getSafeVelocity(Car *cptr1, Car*cptr2, float gap, float *vSafe)
{
    if (cptr2 == NULL) *vSafe = cptr1->vmax + 1;
    else
        *vSafe = cptr2->v +
            (gap - cptr2->v)/(cptr1->v + cptr2->v)/cptr1->bmax + 1;
        /* constant 0.5 in 0.5*(cptr1->v + cptr2->v)/cptr1->bmax included in bmax*/
}

void Simulator::look(Car *cptr, int i, int direction, Car **succ, float *g)
{
    int counter = 0;
    for(int lane=0; lane<=nLanes-1; lane++)
    {
        int index = i + direction;
        if (index < 0) index += length;
        if (index > length-1) index -= length;

        while ((site[lane][index] == NULL) && (counter < maxLook))
        {
            counter++;
            index += direction;
            if (index < 0) index += length;
            if (index > length-1) index -= length;
        }
        succ[lane] = site[lane][index];
        if (succ[lane])
        {
            g[lane] = direction*(succ[lane]->x - cptr->x) - 1;
            if (g[lane] < -1) g[lane] += length;
        }
        else
            g[lane] = maxLook;
    }
}
}

```

The implementation displayed here performs about 1 Million Updates(site-oriented) per second on an Ultra Sparc Processor at a density of $\rho = 0.1$.

A.2 Computational performance

To get a good estimate of what the computational expense is that is necessary to run the different models discussed here, a car-oriented implementation of the model is considered for single lane traffic. This is done, because in a site-oriented implementation most of the computing time is wasted searching the system for vehicles. A thorough analysis of computational aspects of different models will be found in [33]. Here, only very few results of that work, which was done by S. Janz, are reported.

Three different models are compared here.

- Model 1: continuous model, using full safety condition (Gipps-family),

- Model 2: continuous model, using Nagel-Schreckenberg-condition (i.e. high deceleration limit),
- Model 3: discrete Nagel-Schreckenberg-Model.

The results have been obtained on one 167 MHz Sun Ultra-Sparc-processor. The performance is expressed in MUPS (Million Updates Per Second). Corresponding to the car oriented implementation, the updates of the vehicles, instead of sites are measured. Since a density of $\rho = 0.1$ was used, the corresponding site-oriented update rate is ten times higher. The results are:

- Model 1: 2.40 MUPS
- Model 2: 2.79 MUPS
- Model 3: 4.34 MUPS

It can be seen that the differences in computational costs are tolerable. If less optimized code is used, the differences between the models become even smaller. The same holds for different resolutions of discrete models. The actual computational expense of higher resolutions depends strongly on the parameter values of a and b , but generally it can be said that for reasonable parameter values any resolution higher than the coarsest has no computational advantages, compared to the corresponding continuous model.

Appendix B

A car-following experiment

Very often, car following experiments are used to calibrate and validate microscopic models of traffic flow. This method appears particularly appropriate for very detailed models of the driver's behavior, like the Wiedemann model. It has been noted before that the model proposed in this work cannot be considered a very precise model of actual drivers' behavior, so one cannot really expect it to perform well in a car following experiment. Anyway, such an experiment will be considered now.

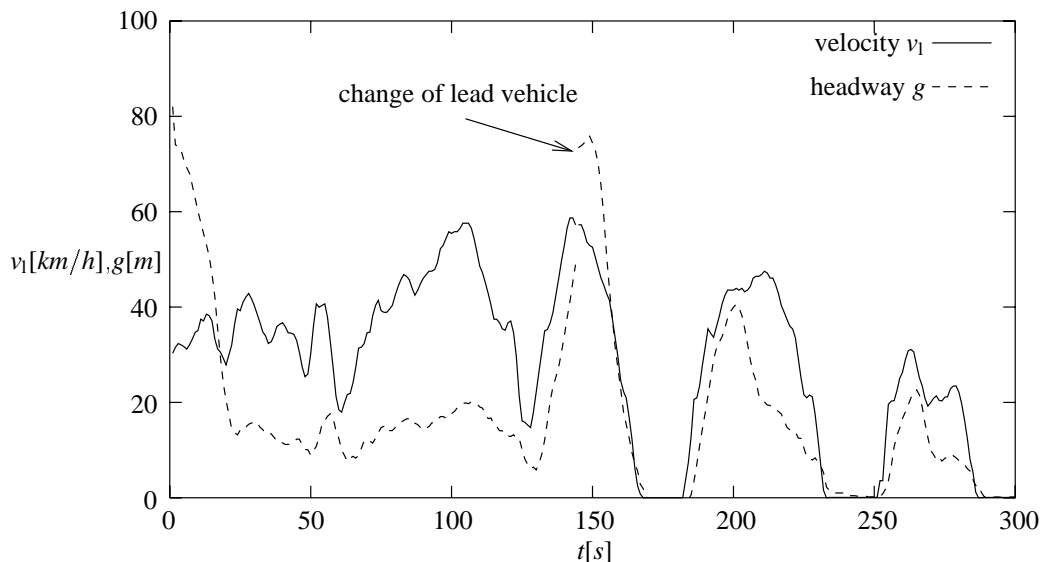


Figure B.1: Velocity of the lead vehicle and headway between the vehicles in the car following experiment as functions of time.

The experimental setup is as follows. Two cars are considered, that follow one another in an urban driving situation. The velocities of both vehicles, as well as the gap between the vehicles, are measured as functions of time. In the corresponding simulation

the velocity $v_l(t)$ of the leading vehicle is prescribed, and for every time step the velocity of the following vehicle is updated according to the rules 5.2. Fig. (B.1) displays the velocity of the leading vehicle and the distance between the two cars. It is important to note that the headway shows a discontinuity after roughly 150 seconds, where it performs a jump in upward direction. This means that the lead vehicle changed at that point of the experiment due to a lane change. This point is important, when model performances are judged.

To judge, how car following is captured in the model proposed here, the parameters that proved to be successful in the description of macroscopic properties of traffic flow $a = 0.2$, $b = 0.6$, and $\epsilon = 1$ are used. The way the model performs is compared to results obtained from a much more detailed model, based on the Wiedemann approach [53]. The quantity that is looked at is the deviation between the simulated and the measured headway $\Delta g = g_{\text{sim}} - g_{\text{exp}}$.

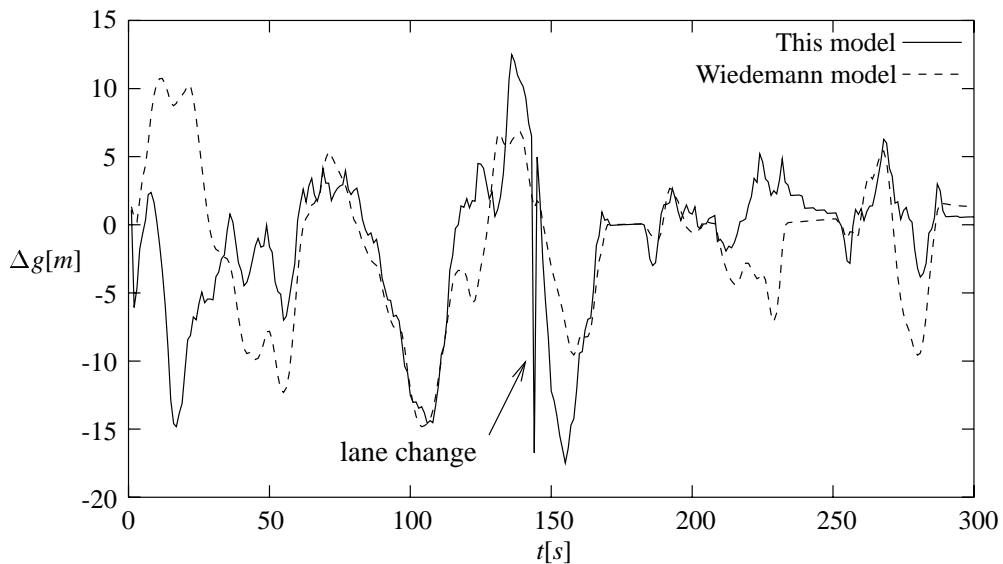


Figure B.2: The deviation of the simulated gap between the vehicles from the measured one in a Wiedemann-like model and the model proposed in this work.

Fig. (B.2) displays Δg once for the Wiedemann-type model and once for the model proposed here. It can be seen that the model proposed here performs about equally well as the much more complicated and computationally quite expensive model of the Wiedemann-type, which runs slower by roughly a factor of 1000. The only point, where the model proposed here performs much worse is in the vicinity of the lane change. Considering the fact that the average of the relative deviation of the gap is 43% and 37% for the model proposed here and the Wiedemann model respectively, one has to concede that none of the models really works satisfactorily.

Apart from this it is important to note that model performance on this microscopic level is not very meaningful with respect to the model properties on a macroscopic scale.

For example, the dynamics of jam formation in the Wiedemann model is, in contrast to that of the model proposed here, quite unrealistic, although it performs slightly better in the car following experiment. On this background the common practice to judge the validity of a model from car following experiments appears doubtful.

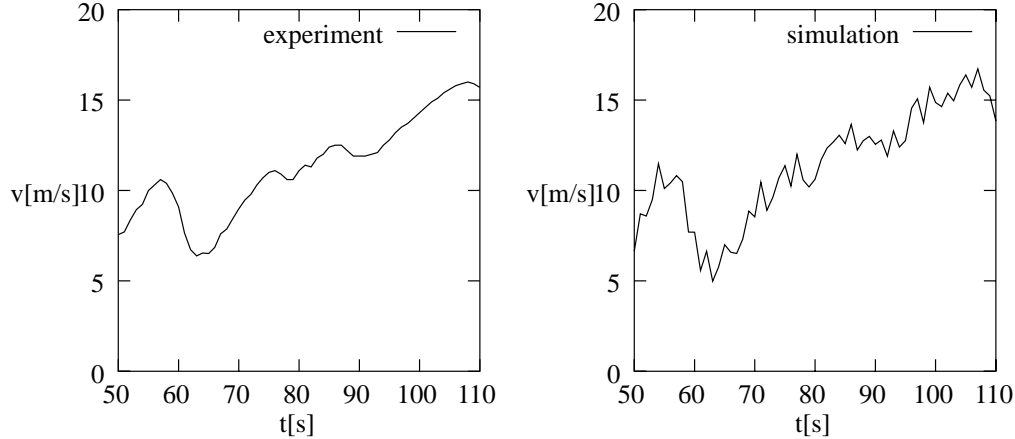


Figure B.3: Measured and simulated velocity profile of the follower vehicle. The fluctuations in the model are larger than those in reality.

Finally, one remark about the fluctuations originating from the randomization step should be made. Fig. (B.3) displays the measured velocity profile of the follower car together with the corresponding velocity profile obtained from the simulation for a range of sixty seconds. It is seen that the fluctuations in the model do not correspond to any fluctuations in reality. This is not of great importance for the model performance, however it shows clearly that the use of a randomization step cannot be motivated from observations in real driving situations, but is a purely theoretical concept.

Bibliography

- [1] A. Bachem, K. Nagel, M. Rickert, Ultraschnelle mikroskopische Verkehrssimulationen, *Parallele Datenverarbeitung aktuell TAT*, R. Flieger and R. Greb ed. (1994)
- [2] M. Bando, K. Hasebe, A. Nakayama, A. Shibata, and Y. Sugiyama, Structure Stability of Congestion in Traffic Dynamics, *Japan J. Indust. Appl. Math.* **11**(2), 203–223 (1994)
- [3] M. Bando, K. Hasebe, A. Nakayama, A. Shibata, and Y. Sugiyama, Dynamical model of traffic congestion and numerical simulation, *Phys. Rev. E* **51**(2), 1035–1042 (1995).
- [4] R. Barlovic, L. Santen, A. Schadschneider, M. Schreckenberg, Metastable States in CA models for Traffic Flow. *cond-mat/9711282* (1997)
- [5] Ch.L. Barret, S. Eubank, K. Nagel, S. Rasmussen, J. Riodan, and M. Wolinsky, Issues in the Representation of traffic using Multi–Resolution Cellular Automata, Los Alamos National Laboratory Technical Report: LA/UR 95–2658 (1995)
- [6] O. Biham, A. Middleton, D. Levine, Self Organisation and Dynamical Transition in Traffic Flow Models, *Phys. Rev. A* **46**, 10, R6124-27 (1992)
- [7] R.E. Chandler, R. Herman, and E.W. Montroll Traffic Dynamics: Studies in Car Following, *Opns. Res.* **6**, 165–184 (1958)
- [8] C.J. Leo, R.L. Pretty, Numerical Simulation of Macroscopic continuum traffic models, *Transpn. Res.* **B26 B** 207–220 (1992)
- [9] D. Chowdhury, D.E. Wolf, M. Schreckenberg, Particle Hopping Models for Two–Lane Traffic with Two kinds of Vehicles: Effects Of Lane–Changing–Rules, *Physica A* **235**, 417–435 (1997)
- [10] M. Cremer, Der Verkehrsfluß auf Schnellstraßen. Heidelberg, Germany: Springer Verlag (1979)

- [11] M. Cremer, J. Ludwig, A Fast Simulation Model for Traffic Flow on the Basis of Boolean Operations, *Mathematics and Computers in Simulation* **28**, 297–303 (1986)
- [12] C.F. Daganzo, The Cell Transmission Model: A dynamic Representation of Highway Traffic Consistent with the Hydrodynamic Theory, *Transpn. Res. B* **28B** 269–287 (1994)
- [13] C.F. Daganzo, The Cell Transmission Model, Part II Network Traffic *Transpn. Res. B* **29B** 79–93 (1995)
- [14] C.F. Daganzo, Requiem for second order fluid approximations of traffic flow, *Transpn. Res. B* **29B**, 277–286 (1995)
- [15] Deutsches Institut für Wirtschaftsforschung, Hrsg: Bundesminister für Verkehr, *Verkehr in Zahlen* (1996)
- [16] L.C. Edie, Car-Following and Steady State Theory for Non-Congested Traffic, *Opns. Res.* **9** (1), 66–76 (1961)
- [17] B. Eisenblätter, L. Santen, A. Schadschneider, M. Schreckenberg, Jamming Transition in a Cellular Automaton Model for Traffic Flow, to be published in *Phys. Rev. E* **57(2)** (1998)
- [18] H. Emmerich, E. Rank, Investigating traffic flow in the presence of hindrances by cellular automata, *Physica A* **216**, 435–444 (1995)
- [19] H. Emmerich, Simulation im Straßenverkehr, Dissertation, Universität Dortmund, Fakultät für Bauwesen (1997)
- [20] H. Emmerich, E. Rank, An improved cellular automaton model for traffic flow simulation, *Physica A* **234**, 676–686 (1997)
- [21] R.E. Franklin, On the flow–concentration relationship for traffic, in *Proc. 2nd Int. Symp. Theory Road Traffic Flow*, 120–128, London 1963
- [22] M. Fukui, Y. Ishibashi, Traffic Flow in 1D Cellular Automaton Model Including Cars Moving with High Speed. *J. Phys. Soc. Jp.* **65**(6) 1868 – 1870 (1996)
- [23] D.C. Gazis, R. Herman, R.W. Rothery, Nonlinear follow-the-leader models of traffic flow, *Opns. Res.* **9**, 545, 1961
- [24] D.C. Gazis, R. Herman, and R.B. Potts, Car Following Theory of Steady State Traffic Flow, *Opns. Res.* **7**(4), 499–505 (1959)
- [25] P.G. Gipps, A behavioural car following model for computer simulation, *Transpn. Res. B*, **15B**, 105–111 (1981)

- [26] P.G. Gipps, A model for the structure of lane changing decisions, *Transpn. Res. B* **20B**(5), 403–414 (1986)
- [27] H. Greenberg, An analysis of traffic flow. *Opsns. Res.* **7** 79–85 (1959)
- [28] B.D. Greenshields, A study of traffic capacity. in *Proc. Highw. Res. Bd***14**, Wahington, 448 (1935)
- [29] D. Helbing, Improved fluid-dynamic model for vehicular traffic, *Phys. Rev. E* **51**, 3164–3169 (1995).
- [30] R. Herman, I. Prigogine, A Two-Fluid Approach to Town Traffic *Science* **204** 148–151 (1979)
- [31] R. Herman, E.W. Montroll, R.B. Potts, and R.W. Rothery, Traffic Dynamics: Analysis of stability in Car Following *Opsns. Res.* **7**, 86–106 (1959)
- [32] M. Hilliges, Ein phänomenologisches Modell des dynamischen Verkehrsflusses in Schnellstraßennetzen, Dissertation, Universität Stuttgart (1995)
- [33] S. Janz, Minimalmodelle des Straßenverkehrs, in preparation
- [34] S. Janz, S. Krauß, P. Wagner, Dynamik von Verkehrsstaus und ihre mikroskopische Modellierung, to be presented at Frühjahrstagung Deutsche Physikalische Gesellschaft, 1998.
- [35] R. Kates, Mesoscopic simulation with ANIMAL: Optimal utilization of downstream traffic detector data and the propagation of information, paper presented at *Traffic and Granular Flow*, Duisburg, Germany (1997)
- [36] B.S. Kerner, and P. Konhäuser, Cluster effect in initially homogeneous traffic flow. *Phys. Rev. E* **48**(4), R 2335 (1993)
- [37] B.S. Kerner, and P. Konhäuser, Structures and parameters of clusters in traffic flow. *Phys. Rev. E* **50**, 54 (1994).
- [38] B.S. Kerner, and H. Rehborn, Experimental features and characteristics of traffic jams. *Phys. Rev. E* **53**, 1297–1300 , (1996)
- [39] B.S. Kerner, and H. Rehborn, Experimental properties of complexity in traffic flow. *Phys. Rev. E* **53**, 4275–4278 (1996)
- [40] B.S. Kerner, and Rehborn, H., Experimental Properties of Phase Transitions in Traffic Flow, *Phys. Rev. Lett.* **79**(20), 4030 (1997)
- [41] B.S. Kerner, Experimental characteristics of traffic flow for evaluation of traffic modeling. *Preprint of IFAC symposium on Transportation Systems*, 793–798 (1997)

- [42] B.S. Kerner, Traffic flow: Experiment and Theory, Paper presented at *Traffic and Granular Flow*, Duisburg, Germany (1997)
- [43] M. Koshi, M. Iwasaki, and I. Ohkura, *Proc. (th Intl. Symp. on Transp. and Traffic Theory*, ed. V.F. Hurdle, 403 (1983)
- [44] S. Krauß, P. Wagner, and C. Gawron Continuous Limit of the Nagel–Schreckenberg–Model, *Phys. Rev. E.*, **54**, 3707 (1996)
- [45] S. Krauß, P. Wagner and C. Gawron, Metastable states in a microscopic model of traffic flow. *Phys. Rev. E* **55**, 5597 (1997)
- [46] S. Krauß, Towards a unified view of microscopic traffic flow theories, *Proc. IFAC Symposium 1997 Transportation Systems* (1997)
- [47] R.D. Kühne, in *Proceedings of the Ninth International Symposium on Transportation and Traffic Theory*, edited by I. Volmuller and R. Hamerslag (VNU Science, Utrecht, 1984)
- [48] R.D. Kühne, *Transp. Res. Rec.* **1320**, 251 (1991)
- [49] R.D. Kühne, Traffic Patterns in unstable traffic flow on freeways, *Highway Capacity an Level of Service, Brannolte (ed.)*, Balkema, Rotterdam (1991)
- [50] A. Latour, Simulation von Zellularautomatenmodellen für Mehrspurverkehr, Staatsexamensarbeit, University of Cologne (1993)
- [51] W. Leutzbach, F. Busch, Spurwechselvorgänge auf dreispurigen BAB–Richtungsfahrbahnen. Institut für Verkehrswesen, Universität Karlsruhe (1984)
- [52] M.J. Lighthill, G.B. Whitham, On kinematic waves II: A theory of traffic flow on long crowded roads, *Proc. R. Soc. London A* **229**, 317–345 (1955)
- [53] J. Ludmann, D. Neunzig, and M. Weilkes, Traffic Simulation with Consideration of Driver Models — Theory and Examples, *Proc. EUROMOTOR–Seminar 1996 Telematics / Vehicle and Environment*, Institut für Kraftfahrwesen, Aachen
- [54] A.D. May Traffic flow fundamentals, Prentice Hall Engelwood Cliffs, New Jersey, 1990
- [55] R.M. Michaels, and L.W. Cozan, Perceptual and field factors causing lateral displacement, *Highw. Res. Rec.* **25**, 1–13 (1962)
- [56] T. Musha, H. Higuchi, The 1/f fluctuation of a traffic current on an expressway *Jap. Jrn. Appl. Phys.* **15**(7), 1271–1275 (1976)
- [57] K. Nagel, and M. Paczuski. Emergent traffic jams *Phys. Rev. E*, **51**, 2909 (1995).

- [58] K. Nagel, and M. Schreckenberg. A cellular automaton model for freeway traffic. *J. Physique I*, 2:2221 (1992).
- [59] K. Nagel, P. Wagner, D.E. Wolf, Lane-changing-rules in two-lane traffic simulations using cellular automata. Part II: A systematic approach, in preparation
- [60] K. Nagel, Life times of simulated traffic jams, *Int. J. Mod. Phys. C* **5**(3), 567 (1994)
- [61] K. Nagel, Verkehr separiert in Stau und Fließverkehr. talk held at *Forschungstag Phasenübergänge und Phasentrennung*, University of Cologne (1994)
- [62] K. Nagel, High Speed Microsimulations of Traffic Flow, Doctoral dissertation, University of Cologne (1995)
- [63] G.F. Newell, A simplified theory of kinematic waves in highway traffic, Part I: General Theory *Transpn. Res. B.* **27B**(4), 281-287 (1993)
- [64] G.F. Newell, A simplified theory of kinematic waves in highway traffic, Part II: queueing at freeway bottlenecks *Transpn. Res. B.* **27B**(4), 289–303 (1993)
- [65] G.F. Newell, A simplified theory of kinematic waves in highway traffic, Part III: Multi-destination flows *Transpn. Res. B.* **27B**(4), 290–314 (1993)
- [66] L.A. Pipes, An operational analysis of traffic dynamics. *J. Appl. Phys.* **24**, 274 (1953)
- [67] I. Prigogine, R. Herman, Kinetic theory of vehicular traffic, *American Elsevier Publishing Comp. Inc., New York* (1971)
- [68] A. Rekersbrink, Verkehrsflußsimulation mit Hilfe der Fuzzy-Logic und einem Konzept potentieller Kollisionszeiten. Doctoral dissertation, University of Karlsruhe, Germany, 1994
- [69] M. Rickert, P. Wagner, Parallel real-time implementation of large-scale, route-plan-driven traffic simulation, *Int. Jrn. Mod. Phys. C* **7**(2), 133–153 (1996)
- [70] M. Rickert, *Simulation zweispurigen Verkehrsflusses auf der Basis zellulärer Automaten*, Diploma thesis, University of Cologne (1994)
- [71] M. Rickert, K. Nagel, M. Schreckenberg, and A. Latour, Two Lane Traffic Simulation using Cellular Automata, *Physica A* **231**, 543 (1996)
- [72] P. Ross, Traffic dynamics. *Transpn. Res.* **22B**, 421-436 (1988)
- [73] A. Schadschneider, and M. Schreckenberg. Cellular automaton models and traffic flow. *Journal of Physics A*, 26, L679 (1993).

- [74] A. Schadschneider, and M. Schreckenberg, Traffic flow models with 'slow-to-start' rules. *Ann. Physik* **6**, 541 (1997)
- [75] M. Schreckenberg, A. Schadschneider, K. Nagel, and N. Ito, Discrete stochastic models for traffic flow, *Phys. Rev. E* **51**, 2939 (1995).
- [76] H. Schütt, *Entwicklung und Erprobung eines sehr schnellen, bitorientierten Verkehrssimulationssystems für Straßennetze*, Schriftenreihe der AG Automatisierungstechnik, TU Hamburg Harburg (1991)
- [77] U. Sparmann, Spurwechselvorgänge auf zweispurigen BAB-Richtungsfahrbahnen. *Forschung Straßenbau und Straßenverkehrstechnik*, Heft 263 (1978)
- [78] E.P. Todosiev, and L.C. Barbosa, A proposed model for the driver–vehicle–system, *Traff. Eng.* **34**, 17–20, (1963/64)
- [79] P. Wagner, K. Nagel, D. Wolf, Realistic multi-lane traffic rules for cellular automata, *Physica A* **234**, 687–698 (1996)
- [80] R. Wiedemann, *Simulation des Straßenverkehrsflusses*, Schriftenreihe des Instituts für Verkehrswesen, Heft 8, Universität Karlsruhe
- [81] R. Wiedemann, T. Schwerdtfeger, *Makroskopisches Simulationsmodell für Schnellstraßennetze mit Berücksichtigung von Einzelfahrzeugen (DYNEMO)*, Schriftenreihe Forschung Straßenbau und Straßenverkehrstechnik, Heft 500 (1987)
- [82] S. Yukawa, M. Kikuchi, Coupled–Map Modeling of One–Dimensional Traffic Flow. *Jrn. Phys. Soc. Jap.* **64**(1) 33-38, (1995)
- [83] S. Yukawa, M. Kikuchi, Density Fluctuations in Traffic Flow, *Jrn. Phys. Soc. Jap.* **65**(4) 916-919, (1996)

Acknowledgments

This work could only be performed with the support of many different people, some of which I would like to mention here.

First of all I would like to thank Professor Dietrich Stauffer and Professor Rainer Schrader for putting much time and effort in reading this thesis, and giving valuable advice. Also I would like to thank Professor Achim Bachem, who introduced me to the subject of traffic simulation and gave me the opportunity to work at the Center for Parallel Computing and the German Aerospace Center.

I thank the people working in the traffic simulation group at the Center for Parallel Computing (ZPR) and the German Aerospace Center, Rolf Böning, Christian Gawron, Stephan Hasselberg, Stefan Janz, Peter Oertel, Marcus Rickert, Andrea Vildosola Engelmayer, and Peter Wagner as well as all the other colleagues at the ZPR. The unique atmosphere made working there truly enjoyable.

My special thanks go to Peter Wagner, who constantly supported me in the best possible way in many respects and never let me keep him from believing in what I was doing.

Particularly grateful I am for many long and inspiring discussions with Boris Kerner, who pointed me to some of the essentials of traffic flow modeling, and without whom this work would not have been possible.

Many valuable and helpful discussions I had with Jörg Esser, Kai Nagel, and Michael Schreckenberg.

Finally, I would like to thank my family, who supported me in every way that was necessary to allow me to carry out this work.

Deutsche Zusammenfassung

In der vorliegenden Arbeit werden verschiedene mikroskopische Modelle zur Beschreibung des Verkehrsflusses auf Straßen vorgeschlagen und diskutiert.

Ausgangspunkt der Betrachtungen sind empirische Untersuchungen zur Dynamik des Verkehrsflusses durch Kerner und Rehborn [38, 39]. Dort wurde nachgewiesen, daß Straßenverkehr in drei qualitativ verschiedenen Zuständen, nämlich dem Zustand des freien Verkehrs, des synchronisierten Verkehrs und des Staus vorgefunden werden kann. Die Übergänge zwischen verschiedenen Verkehrszuständen sind in [40] als Phasenübergänge erster Ordnung interpretiert worden.

Staus sind, abgesehen von Ihrer offensichtlichen Eigenschaft, einen Verkehrsfluß hoher Dichte und niedriger Geschwindigkeit zu besitzen, durch folgende Eigenschaften charakterisiert:

1. Staus können auch in Abwesenheit irgendwelcher Hindernisse entstehen und lange Zeit existieren.
2. Der Fluß aus dem Stau ist deutlich niedriger als der maximale Fluß.
3. Der Fluß aus dem Stau ist stabil.
4. Der Fluß aus dem Stau und die Geschwindigkeit der flußabwärtigen Staufront hängen nicht vom Fluß in den Stau ab.
5. Es gibt metastabile Zustände hohen Flusses.

Ziel dieser Arbeit ist die Abbildung der qualitativen und quantitativen Eigenschaften des Verkehrs, basierend auf einer Simulation der Dynamik einzelner Fahrzeuge. Bei der Modellierung der Einzelfahrzeugdynamik wird auf einen minimalen Satz von Regeln zurückgegriffen, der aus wenigen Grundannahmen über den Verkehrsfluß abgeleitet wird. Diese Grundannahmen sind: 1) Geschwindigkeit und Beschleunigung der Fahrzeuge sind begrenzt. 2) Die Wechselwirkung von Fahrzeugen führt zur kollisionsfreien Bewegung im Verkehr. 3) Jedes Fahrzeug bewegt sich (von stochastischen Fluktuationen abgesehen) mit der höchsten Geschwindigkeit, die mit obigen Restriktionen

kompatibel ist. Aus diesen Annahmen wird eine Familie von Modellen abgeleitet, die jeweils durch einen geschwindigkeitsabhängigen Wunschabstand und eine geschwindigkeitsabhängige Relaxationszeit der Fahrdynamik charakterisiert sind.

Eine Spezialisierung dieser Modellfamilie führt auf eine hier als Gipps–Familie bezeichnete Unterfamilie. Hierbei handelt es sich letztlich um ein einziges Modell, das durch die freien Parameter a und b , die typische Beschleunigungs– bzw. Verzögerungsfähigkeiten der Einzelfahrzeuge bezeichnen, charakterisiert wird. Je nach Wahl der freien Parameter a und b und der Maximalgeschwindigkeit der Fahrzeuge v_{\max} zeigt das Modell drei qualitativ unterschiedliche Verhaltensweisen, die durch eine Einteilung der “Modellfamilie” in drei Klassen phänomenologisch jeweils gleichartiger Modelle charakterisiert wird.

- Klasse I:

- a und b bezüglich empirisch bekannter Fahrdynamik realistisch, langreichweite Wechselwirkung.
- Alle o.g. Eigenschaften des Staus werden korrekt abgebildet.
- Der Übergang in den gestauten Zustand ist ein Phasenübergang.

- Klasse II:

- b groß, kurze Bremswege, kurzreichweite Wechselwirkung.
- Eigenschaften 2,3 und 5 der Staus werden nicht abgebildet.
- Der Übergang in den gestauten Zustand ist kein Phasenübergang.

- Klasse III:

- a groß, Beschleunigung begrenzt Fahrdynamik nicht wesentlich.
- System bildet keine Staus.

Phänomenologisch gesehen sind der Klasse I neben dem hier vorgeschlagenen Modell auch das makroskopische Kerner–Konhäuser–Modell [36, 37], neuere Zellularautomatenmodelle [74, 4] und (mit Einschränkungen bezüglich der Eigenschaft 4) auch das Optimal–Velocity–Model von Bando et al. [2] sowie ein ebenfalls in dieser Arbeit entwickeltes deterministisches Verkehrsflußmodell zuzuordnen. Klassische Zellularautomatenmodelle des Verkehrsflusses, wie das Nagel–Schreckenberg–Modell [58] sind den Klassen II und III zuzuordnen.

Für eine praktische Anwendung, beispielsweise im Bereich des Verkehrsmanagements auf Schnellstraßen, sind nur Modelle der Klasse I geeignet, weil die anderen beiden Klassen die Dynamik der Staumentwicklung falsch oder gar nicht abbilden.

Das in dieser Arbeit entwickelte Modell des Einspurverkehrs läßt sich in einfacher Weise unter Wahrung der qualitativen Modelleigenschaften auf Mehrspurverkehr verallgemeinern. Nach dieser Verallgemeinerung wird eine exzellente quantitative Übereinstimmung der Modelleigenschaften mit empirisch ermittelten Daten der Verkehrsdy namik erreicht.

Das wichtige Phänomen des synchronisierten Verkehrs läßt sich im Rahmen dieser Modellierung jedoch nicht beschreiben. Aus diesem Grund wird eine Modifikation des Modells vorgeschlagen, mit der synchronisierter Verkehr nachgebildet werden kann. Ausgangspunkt der Überlegungen ist die Tatsache, daß im synchronisierten Verkehr Überholvorgänge kaum möglich und zumindest nicht sinnvoll sind, so daß kein Fahrer damit rechnen kann, seine Wunschgeschwindigkeit zu erreichen. Wird angenommen, daß hieraus ein zeitweiliger Verzicht der Fahrer auf die maximal mögliche Geschwindigkeit folgt, so können die für den synchronisierten Verkehr charakteristischen zufälligen Translationen des Verkehrszustandes im Fluß–Dichte–Diagramm nachgebildet werden.

Erklärung

Ich versichere, daß ich die von mir vorgelegte Dissertation selbständig angefertigt, die benutzten Quellen und Hilfsmittel vollständig angegeben und die Stellen der Arbeit — einschließlich Tabellen, Karten und Abbildungen —, die anderen Werken im Wortlaut oder dem Sinn nach entnommen sind, in jedem Einzelfall als Entlehnung kenntlich gemacht habe; daß diese Dissertation noch keiner anderen Fakultät oder Universität zur Prüfung vorgelegen hat; daß sie — abgesehen von unten angegebenen Teilpublikationen — noch nicht veröffentlicht worden ist sowie, daß ich eine solche Veröffentlichung vor Abschluß des Promotionsverfahrens nicht vornehmen werde. Die Bestimmungen der Promotionsordnung sind mir bekannt. Die von mir vorgelegte Dissertation ist von Prof. Dr. Dietrich Stauffer und Prof. Dr. Rainer Schrader betreut worden.

Teilveröffentlichungen:

- S. Krauß, P. Wagner, and C. Gawron, Continuous Limit of the Nagel–Schreckenberg–Model, *Phys. Rev. E.*, **54**, 3707 (1996)
- S. Krauß, P. Wagner, and C. Gawron, Metastable states in a microscopic model of traffic flow. *Phys. Rev. E* **55**, 5597 (1997)
- S. Krauß, Towards a unified view of microscopic traffic flow theories, *Proc. IFAC Symposium 1997 Transportation Systems* (1997)
- S. Krauß, Microscopic Traffic Simulation: Robustness of a Simple Approach., presented at Traffic and Granular Flow, Duisburg, 1997.
- S. Krauß, The role of acceleration and deceleration in microscopic models of traffic flow, to be presented at annual meeting of the Transportation Research Board, Washington (1998)

Lebenslauf

Persönliche Daten

Name:	Stefan Krauß
Geburtsdatum:	15. März 1969
Geburtsort:	Recklinghausen
Eltern:	Erika Krauß, geb. Nückel, Dr. Hans-Jürgen Krauß
Staatsangehörigkeit:	deutsch
Familienstand:	ledig

Schulbildung/Wehrdienst/Studium

1975 – 1979:	Grundschule am Kohlkamp, Recklinghausen
1979 – 1988:	Gymnasium Petrinum, Recklinghausen
1988:	Abitur
1988 – 1989:	Wehrdienst
1989 – 1994:	Studium der Physik an der Rheinisch-Westfälischen Technischen Hochschule Aachen
Oktober 1991:	Vordiplom in Physik
September 1994:	Diplom in Physik

Berufstätigkeit

November 1994 – November 1995:	Wissenschaftlicher Mitarbeiter am Lehrstuhl für Strömungsmechanik der Universität Erlangen-Nürnberg (Prof. F. Durst)
Dezember 1995 – Juli 1996:	Wissenschaftlicher Mitarbeiter am Zentrum für Paralleles Rechnen der Universität zu Köln (Prof. A. Bachem, Prof. R. Schrader)
Seit August 1996:	Wissenschaftlicher Mitarbeiter am Deutschen Zentrum für Luft- und Raumfahrt (Prof. A. Bachem)